Chapter 6
Formulation Development

Chapter 6

6.1 Development of lipoplexes:

Liposomes were developed using cationic lipids such as i.e. DOTAP or stearyl amine, DSPE as neutral lipid and modified DSPE lipids and DOPE as fusogenic lipid. Along with cationic lipids, other supporting lipids were also used for development of stable liposomal formulations which can be used for further development of pDNA lipoplexes. Cationic lipids used for development of lipoplexes are described below.

6.1.1 Stearylamine

Stearylamine has been used as a gene delivery agent in several studies due to its high transfection potential. Stearylamine is a lipophilic alkylamine with log P of 5 and an amine headgroup with pKa of 10.21 which remains completely ionized at physiological pH giving a positive charge on the amine terminal. Due to its cationic character as well as lipophilic chain, it has been used for gene delivery through various vesicular delivery delivery systems like cationic nanoemulsions, microemulsions and liposomes. Stearylamine bears the high transfection potential due to its high cell penetration capability which makes it efficient in delivering genetic cargo inside the cells even in cell lines very hard to transfect i.e. HeLa cell line, muscle fibroblasts, etc.

Despite its high transfection potential, stearylamine bears demerit of its being immunogenic and cytotoxic. It has been demonstrated to be the inducer of apoptosis through generation of reactive oxygen species (ROS) and other mechanisms of apoptosis. This makes it a less preferred gene delivery agent and only few literatures have reported its potential as gene delivery vector as compared to other lipidic and polymeric vectors i.e. other cationic lipids (mainly phospholipids and cholesterol based cationic lipids), PEI, chitosan etc. In the present system we have used stearylamine for imparting cationic character to the formulation, so as to complex pDNA with it, which in effect will minimize the charge based toxicity of the lipid and further a fraction of the amine of this lipid will also be utilized for conjugation of ligand on the formed lipoplexes.

6.1.2 DOTAP

[1,2-bis(oleoyloxy)-3-(trimethylammonio)propane], or DOTAP, was first synthesized by Leventis and Silvius in 1990 (1). The molecule consists of a quaternary amine head group coupled to a glycerol backbone with two oleoyl chains. The only differences between this molecule and DOTMA are that ester bonds link the chains to the backbone rather than ether bonds. It was originally hypothesized that ester bonds, which are hydrolysable, could render the lipid biodegradable and reduce cytotoxicity. This study showed that the transfection activities and levels of cytotoxicity associated with DOTAP/DOPE formulations are not statistically different from those associated with DOTMA/DOPE composites. Notably, this type of monovalent lipids also showed little to no cytotoxic effect on near-confluent cell monolayers (1).

The use of 100% DOTAP for gene delivery is inefficient due to the density of positive charges on the liposome surface, which possibly prevents counter ion exchange (2). DOTAP is completely protonated at pH 7.4 (which is not the case for all other cationic lipids) (2), so it is possible that more energy is required to separate the DNA from the lipoplex for successful transfection (3). Thus, for DOTAP to be more effective in gene delivery, it should be combined with a helper lipid, as seems to be the case for most cationic lipid formulations.

High temperature and long incubation times have been used to create lipoplexes that exhibit resistance to serum interaction. Interestingly, this approach was only observed to affect monovalent cationic lipids such as DOTMA, DOTAP, or DC-Chol, as opposed to multivalent cationic lipids. The specific reasons for this phenomenon remain unclear. In fact, the specific mechanism behind serum inactivation of lipoplexes in general is as yet unexplained. Several hypotheses have been offered as to the mechanism, including the prevention of lipoplex binding to cell membranes by serum proteins, the prevention of structural complex maturation by serum proteins binding to cationic charges on the lipoplexes (4), and the disparity of endocytosis pathways-which have varying kinetics-that are used for lipoplex endocytosis, with the method of endocytosis being regulated by the size of the lipoplexes or aggregates of lipoplexes plus serum proteins.

6.1.3 Synthesized lipids

Lipids developed from modified DSPE were used for preparation of the liposomes and for development of lipoplexes of APOE pDNA.

Development was carried out in two stages

1. Development of blank cationic liposomes containing DSPE / modified DSPE.
2. Complexation of pDNA with preformed cationic liposomes

6.2 Preparation of liposomes

6.2.1 Preparation of Stearyl amine-DSPE based liposomes

Liposomes were prepared by thin film hydration method. Appropriate quantities of stearyl amine, HSPC, DSPE, DOPE, mPEG$_{2000}$-DSPE (optionally for PEGylation) and Chol were weighed and dissolved in chloroform:methanol (3:1 v/v) mixture in a 50 mL round bottom flask (RBF). Solvent was evaporated at -450 to -500 mmHg vacuum and 45°C temperature using rotary flask evaporator (IKA RV-10, USA) at 100 rpm rotation speed. Nitrogen purging was used to remove the residual organic solvent from the film. Thin film formed was hydrated with autoclaved double distilled water (DNAse free water-DFW) at 65°C temperature. After 1 hr of hydration, liposomes formed were collected from RBF in a USP Type I tubular glass vials (10 mL, Klasspack Pvt. Ltd., Maharashtra, India) and capped with rubber stoppers (Helvoet, Belgium). Liposomes were kept at 65°C temperature and were extruded through each of 1 μ, 0.8 μ, 0.4 μ, 0.2 μ, and 0.1 μ polycarbonate membranes (Whatman, USA) supported by polyethylene drain disk (Whatman, USA) using high pressure extruder (Avestin, USA) for 10 cycles. Size reduced liposomes were stored in USP type I vials at 2-8°C in a refrigerator till further use.

For formulation development, different molar ratios of lipids were arbitrarily tried based on previous experience to obtain desired particle size distribution. Optimized ratio was used for preparation of liposomes with other lipids synthesized from DSPE.

6.2.2 Preparation of lipoplexes:

Lipoplexes were prepared by incubating preformed cationic liposomes with pDNA based on the ratio of moles of stearyl amine (or modified stearyl amine lipids) to moles of phosphate of pDNA. Briefly, sufficient quantity of liposomes (diluted with DFW if

necessary) was taken and incubated with pDNA at 25°C±2°C temperature for a period of 30 min to 1.5 hr. Prepared lipoplexes were filled in USP- type I glass vials and lyophilized. Lipoplexes were prepared at pDNA concentration of 5 µg/mL.

6.2.3 Optimization of Parameters

Various process and formulation parameters involved in the preparation of liposomes and of lipoplexes were optimized to arrive at the best suitable formulation of pDNA lipoplexes. Process parameters characterized for the development of liposomes were solvent system for lipids, solvent evaporation temperature and time, vacuum condition and rotation speed while those for preparation of lipoplexes involved incubation time and temperature for maximum complexation of pDNA. Formulation parameters i.e. lipid types and content and L/P ratio (lipid:pDNA molar ratio) were optimized based on the desired particle size distribution characteristics of liposomes and lipoplexes.

6.2.4 Lyophilization of Lipoplexes

Lipoplexes prepared were lyophilized to endow the lipoplexes with the physical stability for long term storage. Various bulking-cum-cryoprotecting agents were tried at different concentrations to circumvent the detrimental effects of freezing on lipoplex integrity. Lipoplexes were prepared and diluted with cryoprotectant containing DFW to obtain desired concentration of cryoprotectant in the final lipoplex formulation. Lipoplexes, then, were filled in the 2 mL USP type 1 glass vials (Schott-Kaisha Pvt. Ltd., Maharashtra, India) having 20 mm diameter. Vials were stoppered partly with chlorobutyl rubber stoppers with notch (Helvoet, Belgium) to allow sublimation of ice during lyophilization. Vials were placed on the shelves inside the lyophilizer (Virtis Advantage-Plus, SP Scientific, USA). Two vials were inserted with temperature probes to monitor the temperature changes inside the product during the lyophilization. Lipoplexes were frozen to -40°C and dried under vacuum of 100 mTorr. Complete lyophilization cycle with freezing cycle, primary drying cycle and secondary drying cycle (with temperature treatments, ramp and hold periods, and vacuum levels) is given in **Figure 6.1 and Figure 6.2**. Lyophilized formulation was stoppered and sealed with 20 mm aluminum flip-off caps until further use and analysis.
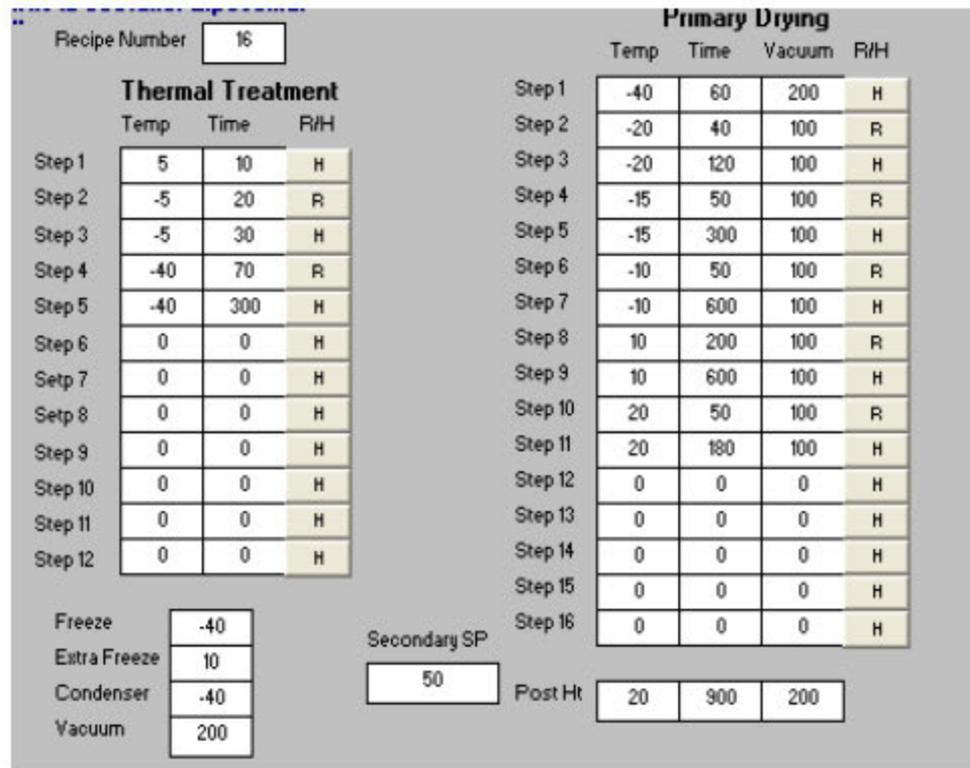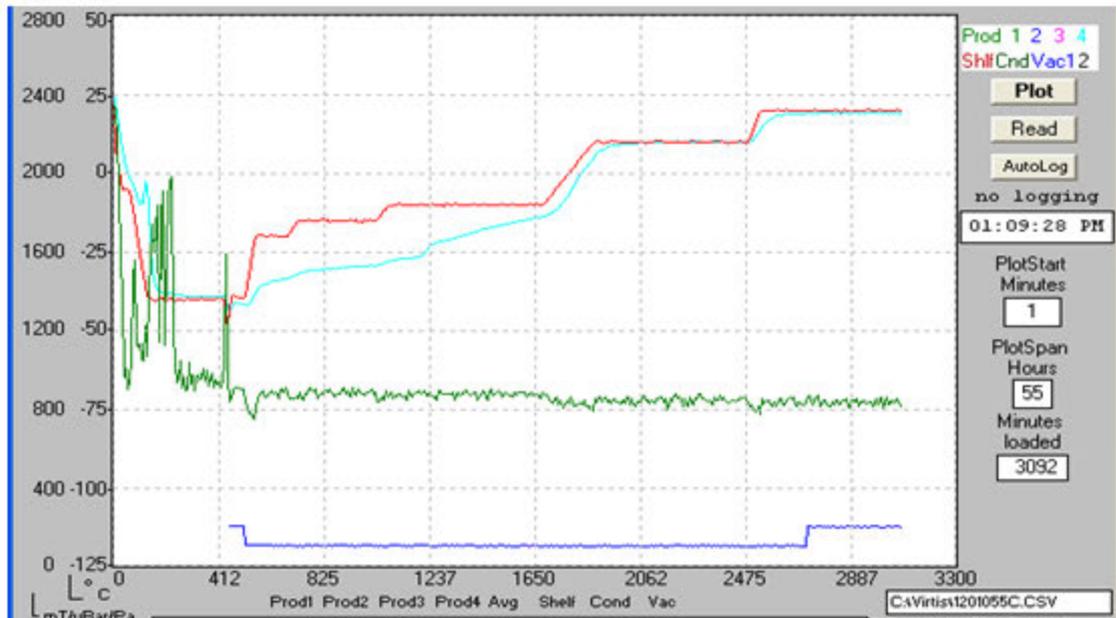
Recipe Number 16

Thermal Treatment

	Temp	Time	R/H
Step 1	5	10	H
Step 2	-5	20	R
Step 3	-5	30	H
Step 4	-40	70	R
Step 5	-40	300	H
Step 6	0	0	H
Setp 7	0	0	H
Setp 8	0	0	H
Step 9	0	0	H
Step 10	0	0	H
Step 11	0	0	H
Step 12	0	0	H

Freeze	-40
Extra Freeze	10
Condenser	-40
Vacuum	200

Secondary SP 50

Primary Drying

	Temp	Time	Vacuum	R/H
Step 1	-40	60	200	H
Step 2	-20	40	100	R
Step 3	-20	120	100	H
Step 4	-15	50	100	R
Step 5	-15	300	100	H
Step 6	-10	50	100	R
Step 7	-10	600	100	H
Step 8	10	200	100	R
Step 9	10	600	100	H
Step 10	20	50	100	R
Step 11	20	180	100	H
Step 12	0	0	0	H
Step 13	0	0	0	H
Step 14	0	0	0	H
Step 15	0	0	0	H
Step 16	0	0	0	H
Post Ht	20	900	200	

Figure 6.1 Lyophilization Cycle

Figure 6.2 Temperature Change during Lyophilization

6.2.5 Physicochemical characterization of liposomes and lipoplexes

6.2.5.1 Complexation Efficiency

i. EtBr intercalation assay using gel electrophoresis

Lipoplexes prepared by incubating pDNA with cationic liposomes were subjected for determination of complexation efficiency of cationic liposomes with negatively charged pDNA. Prepared lipoplexes, diluted if necessary, were loaded on to gel at level of 200 ng/well using gel loading buffer and electrophoresis was carried out at 5 V/cm for 45 min in 1X TAE buffer. Uncomplexed pDNA migrated on gel was visualized by UV transillumination on GelDoc ImageXR+ system (Bio-Rad Labs., USA). Amount of free pDNA was quantified using naked DNA band as reference and determining the band densities using ImageJ software ver. 1.50c (National Institute of Health, USA). Complexation efficiencies were calculated by following expression:

$$\% \text{ complexation efficiency} = (BD_{naked\,pDNA} - BD_{sample}) \times 100 / BD_{naked\,pDNA}$$

Where $BD_{naked\,pDNA}$ and BD_{sample} stands for band density obtained with naked pDNA used as reference band and band density obtained with pDNA complex.

ii. UV spectrophotometric determination after Centrifugation

pDNA lipoplexes were sampled in Beckman® ultracentrifugation tubes and centrifuged at 100,000g for 4 hr at 4°C (OptimaTM Max-xp Ultra Centrifuge; Beckman Coulter, USA). Supernatant was removed and pellet was dispersed by sonication in 100 µL of DFW. 200 µL of phenol/chloroform (1:1) mixture was added and vortexed for vigorous mixing to separate out lipids from pDNA. Aqueous layer was separated and washed again with chloroform by sonication and subsequent phase separation by centrifugation to remove any traces of phenol. Washed aqueous layer was separated and used for spectrophotometric analysis using NanoDrop 2000 instrument (NanoDrop, Germany). Lipoplexes prepared at L/P ratio of 0.50, 1.00 and 2.00 were evaluated for complexation efficiency using spectrophotometry. Complexation efficiency was determined by following expression.

$$\% \text{ complexation efficiency} = (Q_{pellet} / Q_{pDNA\,taken}) \times 100$$

ii. Spectrofluorometric determination after Centrifugation

Supernatant obtained after centrifugation of lipoplexes was used for QuantiFluor assay to quantitate pDNA in supernatant. Supernatant diluted with appropriate quantity of

DFW, if necessary, and treated with equal quantity of Quantifluour dye solution and fluorescence intensity was recorded. Concentration of pDNA in supernatant was determined by extrapolation of fluorescence units in calibration curve on concentration axis. Lipoplexes prepared at L/P ratio of 0.50, 1.00 and 2.00 were evaluated for complexation efficiency using spectrofluorometry. Complexation efficiency were determined by using following expression:

$$\% \text{ complexation efficiency} = (Q_{pDNA\,taken} - Q_{Supernatant}) \times 100 / Q_{pDNA\,taken}$$

6.2.5.2 Particle size and zeta potential analysis.

Liposomes before and after pDNA complexation were analyzed for particle size and zeta potential. For particle size analysis two methods were employed namely dynamic light scattering and cryo-transmission electron microscopy (described later).

Briefly, in dynamic light scattering method, particle size analyses were performed in a clear sizing cuvette at 25°C temperature using 633 nm laser as a light source and 90° back-scatter photon detector using ZetaSizer Nano ZS (Malvern Instruments Ltd., UK) Sample for analysis were prepared by 10 times dilution of liposomes/lipoplexes in DFW. Intensity based particle size distribution curves were generated and z-averaged diameter were determined using Stokes-Einstein equation using the Zetasizer software Ver. 7.11 (Malvern Instruments Ltd., UK). Polydispersity of formulation was reported as polydispersity index (PDI). PDI and z-average particle size were considered for the optimization of the formulation as this is the most robust measurement of the software that allows proper comparison of the formulations.

Zeta potential analysis were performed on 10 times dilute samples at 25°C temperature using a zeta cuvette at 633 nm wavelength from laser light source and 173° back-scatter detector under externally applied voltage. Electrophoretic mobility was determined and was converted to zeta-potential using Smoluchovski equation by Zetasizer software Ver. 7.11 (Malvern Instruments Ltd., UK).

6.2.5.3 Cryo-Transmission Electron Microscopy (Cryo-TEM)

Cryo-TEM was performed for the liposomes and lipoplexes in order to determine the particle size and lamellarity. Formulations (liposomes and lipoplexes) were diluted 10 times before analyses and cryo-TEM was performed on cryo-transmission electron microscope (TECNAI G2 Spirit Bio TWIN, FEI-Netherlands). Glow discharge was performed prior to

analysis for transition of the copper grid from hydrophobic to hydrophilic. Transitioned grid was then covered uniformly with liposomal dispersion/lipoplex dispersion which was followed by freezing in the liquid ethane at -180°C. Frozen copper grid was taken into a liquid nitrogen storage box for transferring to the cryo-holder of the microscope maintained at -175°C. Cryo-holder was placed inside the microscope and imaging was carried out at 0.27 nm resolution and 750,000X magnification level. TEM images were obtained and observed for lamellarity. Images were also analysed by ImageJ software ver. 1.50c (National Institute of Health, USA) in order to determine the lamellar thickness and liposome diameter. For comparing the particle size data with those obtained with TEM analyses, z-average diameter was considered.

6.2.5.4 Assay

Total amount of pDNA in the formulation was determined by assay of the formulation for pDNA content. Assay of the formulation gives the idea of integrity of pDNA during processing and identifies any loss of DNA due to degradation. Further, assay would help in determining the potency calculations for *in vitro* and *in vivo* studies. pDNA content of the formulation was determined before and after the lyophilization of the lipoplexes. Assay was carried out by following methods:

Lipoplexes (equivalent to 1 µg of pDNA) were sampled and diluted if necessary with DFW to give final volume of 100 µL. 200 µL of phenol/chloroform (1:1 v/v) mixture was added to the lipoplex samples. Vigorous mixing is done to break lipoplexes and to partition the pDNA in water and lipids into phenol:chloroform layer. Samples were then phase separated by centrifugation (Remi Compufuge, Remi, India) at 14000 rpm at 4°C temperature. Separated aqueous layer is removed and treated separately with chloroform (200 µL) and vigorously vortexed and phase separated by centrifugation similarly to remove any traces of phenol in chloroform. Aqueous layer is used for determination of pDNA content using following methods:

1. Gel electrophoresis: Aqueous layer (equivalent to 200 ng of pDNA) was directly loaded on the agarose gel at along with naked pDNA samples as reference to determine the assay. Gel was run at 5 V/cm for 45 min in tank buffer using gel loading dye. Gel was visualized using UV transilluminator assembled with gel documentation system (GelDoc ImagingXR+ system, Bio-Rad, USA) and images

were captured on ImageLab software as described earlier. Band densities were analyzed by ImageJ software ver. 1.50c (National Institute of Health, USA).

2. UV spectrophotometry: Aqueous layer (diluted if necessary with DFW) was measured for absorbance using NanoDrop 2000 (NanoDrop, USA) for determination of pDNA content. Content of DNA was calculated by correcting for turbidity by 320 nm absorbance reading i.e. A260-A320 and multiplying the reading by dilution factor and using the relationship that A_{260} of $1.0 = 50$ μg of dsDNA.

Concentration of pDNA (μg/mL) = (A260-A320) x dilution factor x 50 μg/mL

3. QuantiFluor assay: Quantifluor assay was performed for assay using QuantiFlour dye which specifically binds to dsDNA. Aqueous layer was diluted with appropriate quantity of DFW and treated with equal quantity of dye solution and fluorescence units were extrapolated to concentration of pDNA using calibration curve obtained using APOE pDNA.

6.2.5.5 Residual Water content:

Residual water content of the lyophilized liposomal cake was determined by Karl-Fisher titration method using commercially available pyridine free reagent (5). Commercially available pyridine free reagent was used for analysis. Reagent was calibrated using sodium tartrate dehydrate as a standard which contains 15.66%±0.3% w/w of water content. Briefly, 20 mL of anhydrous methanol was taken and titrated with KF reagent to remove any traces of residual water in methanol. Weighed quantity of the sample was added in the methanol and dissolved. Sample solution was titrated with KF reagent to determine the residual water content of lyophilized powder. End point was detected using amperometric end point.

6.2.5.6 Statistical Analysis

Experiments were conducted in triplicate and data reported are as mean±standard deviation. Statistical analysis of data was performed using a Student-t test and ANOVA. GraphPad Prism (version 6, USA) was used for all analyses and p values < 0.05 were considered statistically significant.

6.3 Results and Discussion

6.3.1 Preparation of stearyl amine-DSPE based liposomes

6.3.1.1 Optimization of process parameters

Different process parameters involved in the preparation of liposomes were optimized initially. These process parameters included solvent evaporation time, hydration time and rotation speed of RBF during hydration were optimized for desired results. While keeping other factors constant, effect of one variable was observed on desired output parameters. Results observed with the drug are shown in **Table 6.1**.

Table 6.1 Effect of process parameters for lipid films

Solvent system	
Solvent system	**Observation**
Chlorofom:Methanol (3:1 v/v)	Suitable for different lipids having dipeptide/amino acid headgroups Solvent system was kept the same to keep the processing same for all formulations
Solvent evaporation temperature	
Temperature (°C)	**Observation**
48°C	Suitable for evaporation of solvent mixture under reduced pressure based on the Tg of the lipids
Solvent evaporation time (at 48°C, 100 rpm, 400 mmHg)	
Time (min)	**Observation**
30	Efficient drying
60	Efficient drying
90	No further improvement
Vacuum condition (30 minute at 48°C and 100 rpm)	
Vacuum (mmHg)	**Observation**
200	Inefficient drying (higher rotation times required)
300	Inefficient drying (higher rotation times required)
400	Thin uniform film
450	Thin uniform film

Rotation speed (for 30 minutes at 48°C and 450 mmHg)	
Rotation speed (rpm)	**Observation**
50	Localized deposits on the wall with uneven film thickness
80	Thin uniform film
100	Thin uniform film
120	Uniform to noncontiguous films with gaps in between
150	Noncontiguous films with gaps in between

*Experiments were performed in triplicate.

Initially, process parameters for thin film formation were optimized (**Table 6.1**). chloroform:methanol (3:1 v/v) mixture was chosen as an organic solvent system for film formation. Selection of solvent was based on the solubility of the lipids used for liposomes. i.e. some modified lipids with dipeptide/amino acid head groups were soluble in methanol also, solubility of mPEG$_{2000}$-DSPE required presence of methanol for solubilization in chloroform. Based on the solvent system, 48°C temperature which is highest efficient temperature for solvent evaporation but well below the Tg of highest Tg lipid was chosen.

Vacuum conditions were optimized at 48°C temperature, 100 rpm rotation speed for 30 min period. -400 to -500 mmHg vacuum were efficient to produce film without any solvent detected on smelling. Effective solvent evaporation was considered when no solvent was detected in RBF on smelling. Low vacuum did not produce complete evaporation within 30 min, rather it required longer time periods for complete evaporation of solvent. For further process optimization -450 mmHg vacuum was considered optimum.

At vacuum of -450 mmHg and temperature of 48°C, solvent was evaporated from lipid solution in organic solvent (chloroform:methanol 3:1 v/v). Appropriate lipid film was considered when even distribution of lipids was observed on the wall of the RBF. Lipid film of desired quality was observed for solvent evaporation time of 30-60 min at rotation speed of 80-100 rpm. Higher rotation speed led to freckles in the film i.e. gaps in the film due to rapid movement of solvent on the wall under vacuum leading to blank spaces on the RBF wall without any lipid deposits. RBF rotation speeds below the optimum range caused localized deposits on the wall with uneven film formation i.e. areas with thick and thin films. Time required for complete drying were higher at lower rotation speeds i.e. >1 hr and sometimes led to formation of dried film areas covering the undried deposits below the film hindering the complete evaporation of solvent from the film even after 1-2 hr. Values

158

between the optimum range for proper film formation i.e. 45 min at 100 rpm were considered suitable for thin, uniform and evenly dried film formation and was further used for preparation of liposomes. Removal of solvent from the films was further ensured by nitrogen purging of the RBFs. Residual solvent analysis was performed by gas chromatography and the spectra are provided in supplementary material at end of the thesis. The residual solvent amount was found well below the limit (for methanol: below 30 mg/day or 3000 ppm and for chloroform: below 0.6 mg/day or 60 ppm → As per ICH).

After optimization of process parameters for lipid film formation, process parameters were optimized for hydration (**Table 6.2**) Hydration temperature was chosen based on the Tg of the highest Tg lipid among the lipid mixture used. Lipids were hydrated with DFW for 30 min to 120 minutes at a temperature of 75°C temperature. Complete hydration was considered when lipid films were completely dislodged from the glass surface during hydration forming a liposomal dispersion with translucent appearance. Hydration time of 1 hr-1.5 hr was required for complete hydration of thin films. Lower hydration times were inefficient for complete hydration leaving unhydrated spots on the glass surface. Higher hydration times were of no further advantage, hence, hydration of 1-1.5 hr was considered optimum for development of liposomes.

Table 6.2 Effect of process parameters on hydration of lipid films

Hydration Temperature*	
Hydration Temperature (°C)	**Observation**
75°C	Suitable for hydration based on Tg of highest Tg lipid in lipid mixture used for liposome preparation
Hydration Time*	
Hydration Time (min)	**Observation**
30	Non-hydrated spots were observed in the RBF
60	Complete hydration of film
90	Complete hydration of film
120	No further improvement

*Experiments were performed in triplicate.

6.3.1.2 Optimization of formulation components

Stearyl amine liposomes containing DSPE were initially developed using different other lipids i.e. HSPC, DSPC, DMPC, DPPC, Egg PC, DOPE and Cholesterol. Different molar ratios of lipids were tried to develop stearyl amine liposomes. Fraction of DSPE was replaced using 3 mole% of mPEG$_{2000}$-DSPE to develop PEGylated liposomes. DOPE was involved in all formulations due to its fusogenic potential which eases the cytosolic release of pDNA. Liposomes comprising of different lipid compositions were prepared using thin film hydration. Optimization was done by randomly varying the lipids and their compositions based on the literature and past experience. Two output parameters considered for optimization were particle size and particle size distribution characteristics. Other parameters such as hydration of film and precipitation were also noted for feasibility of a few batches. Lipid compositions tried for development of liposomes are detailed with their particle size distribution in **Table 6.3**.

Table 6.3 Optimization of SA based liposomes: Trial batches

Batch Code	Lipid composition	Ratio in mole%	Particle size z-averaged diameter (nm)	PDI	Size distribution characteristic and remarks
B1	SA:HSPC:DOPE:Chol	20:20:30:40	95.44±12.48	0.303±0.042	Bimodal Film not hydrated properly, unhydrated precipitates on wall observed
B2	SA:HSPC:DOPE:Chol	22:36:21:20	121.6±15.45	0.302±0.041	Bimodal
B3	SA:HSPC:DOPE:Chol	26:28:28:18	139.6±11.66	0.323±0.068	Bimodal
B4	SA:HSPC:DOPE:Chol	36:16:15:33	1009-1310	0.594±0.036	Bimodal Thin uniform film but complete hydration didn't take place
B5	SA:DOPE:Chol	25:35:40	239.6±15.70	0.421±0.032	Trimodal Thin uniform film but complete hydration didn't take place
B6	SA:HSPC:DOPE:Chol	12:30:28:30	161.25±7.89	0.278±0.065	Bimodal
B7	SA:HSPC:DOPE:Chol	9:31:25:35	115.8±13.21	0.295±0.056	Unimodal to bimodal

| Batch Code	Lipid composition	Ratio in mole%	Particle size z-averaged diameter (nm)	PDI	Size distribution characteristic and remarks
B9	SA:HSPC:DOPE:Chol	12:30:38:20	421.6±13.23	0.602±0.038	Bimodal
B10	SA:HSPC:EPC:DOPE:Chol	5:20:20:30:25	93.68±9.59	0.466±0.075	Bimodal
B11	SA:DSPC:EPC:DOPE:Chol	10:40:24:12:13	81.11±6.59	0.529±0.027	Bimodal
B12	**SA:HSPC:EPC:DOPE:Chol**	**10:20:30:10:24**	**96.74±11.74**	**0.239±0.068**	**Monomodal**
B13	SA:HSPC:DOPE:Chol	14:32:24:30	95.31±9.49	0.526±0.072	Trimodal
B14	**SA:HSPC:EPC:DOPE:Chol: mPEG$_{2000}$-DSPE**	**10:27:20:20:20:3**	**104.49±8.89**	**0.209±0.047**	**Monomodal**
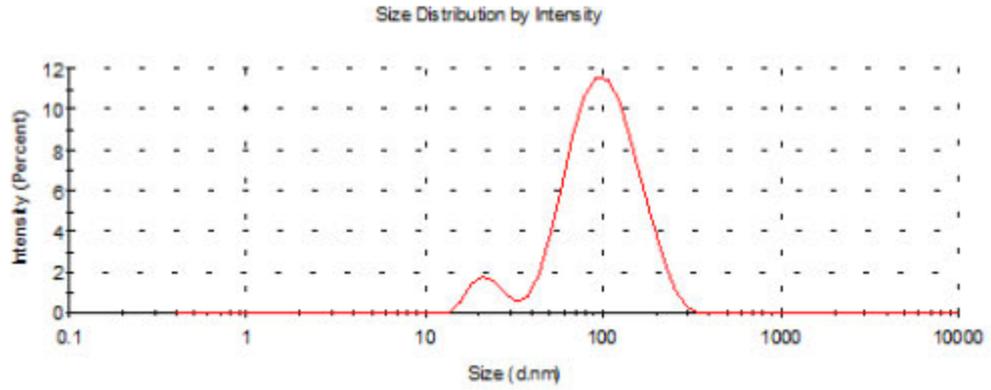
Figure 6.3 Intensity-weighted particle size distribution of Batch B1
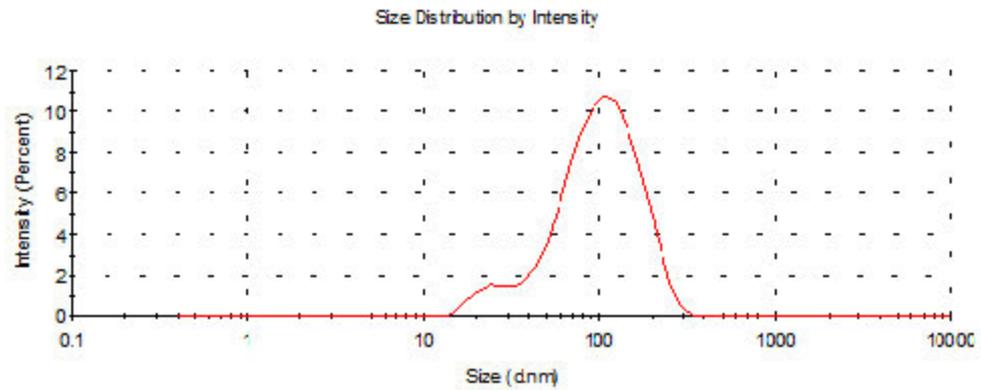
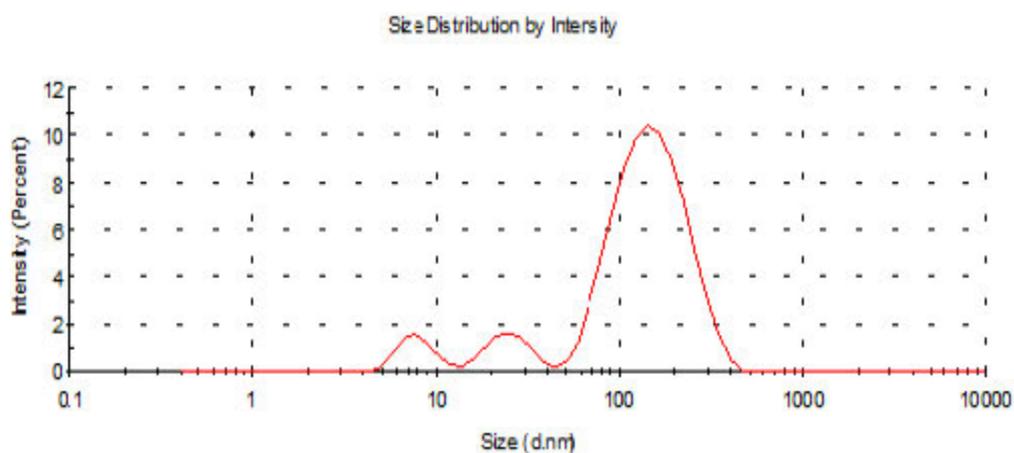**Figure 6.4 Intensity-weighted particle size distribution of Batch B2**
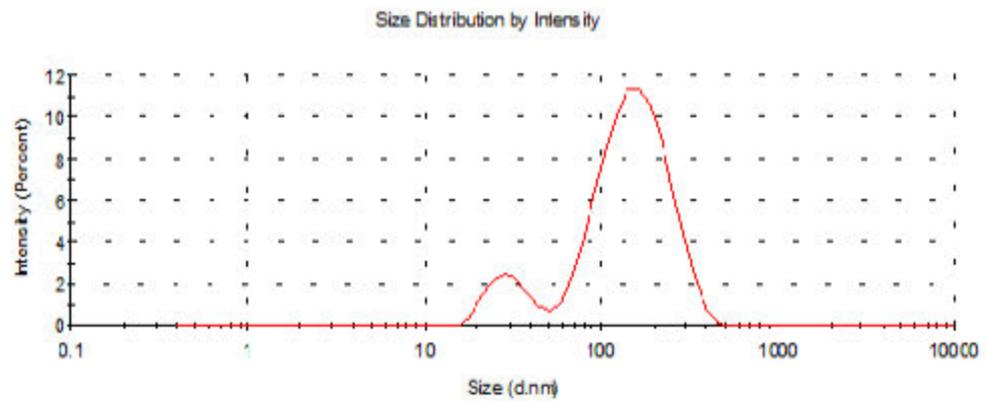
Figure 6.5 Intensity-weighted particle size distribution of Batch B3
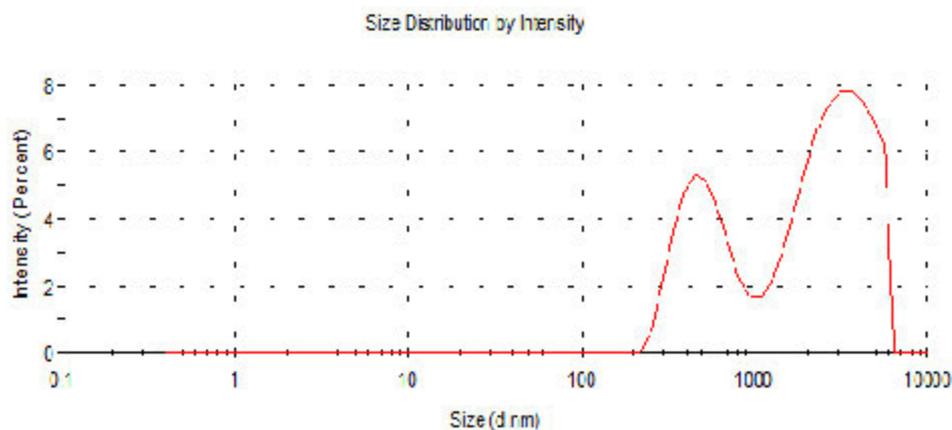
Figure 6.6 Intensity-weighted particle size distribution of Batch B4
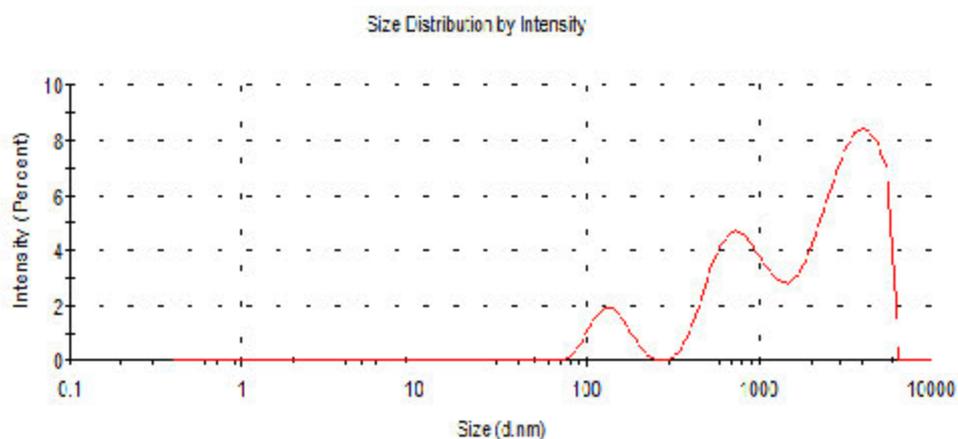
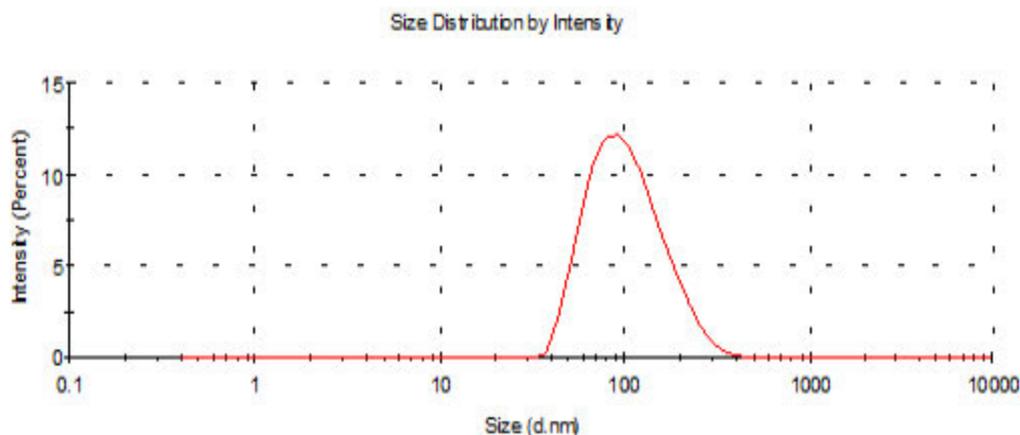**Figure 6.7 Intensity-weighted particle size distribution of Batch B5**
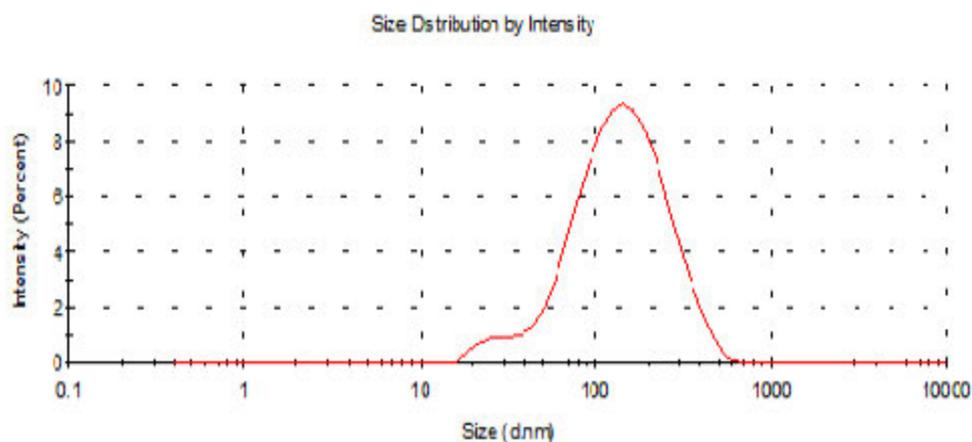
Figure 6.8 Intensity-weighted particle size distribution of Batch B6
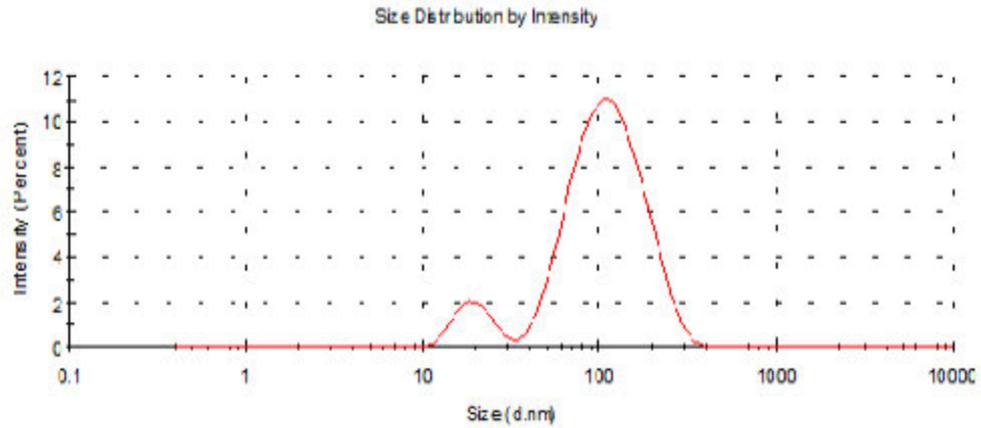
Figure 6.9 Intensity-weighted particle size distribution of Batch B7
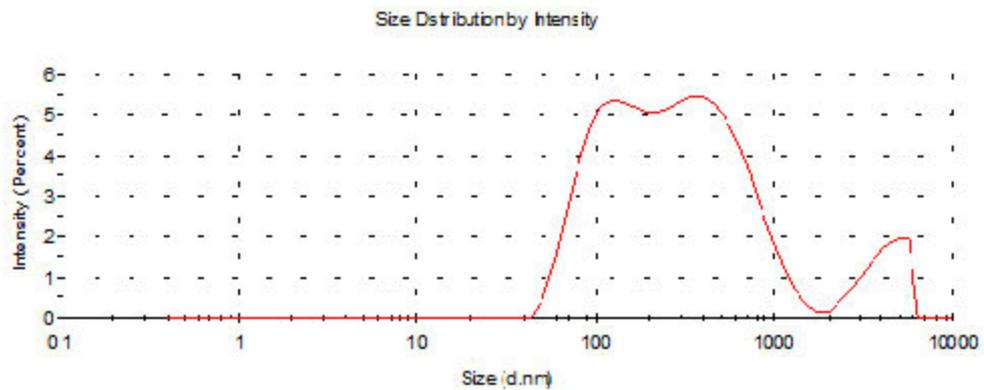
Figure 6.10 Intensity-weighted particle size distribution of Batch B8
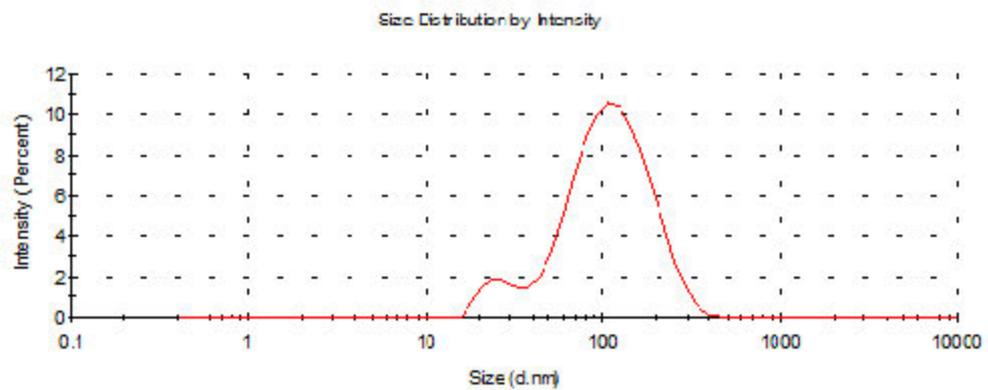
Figure 6.11 Intensity-weighted particle size distribution of Batch B9
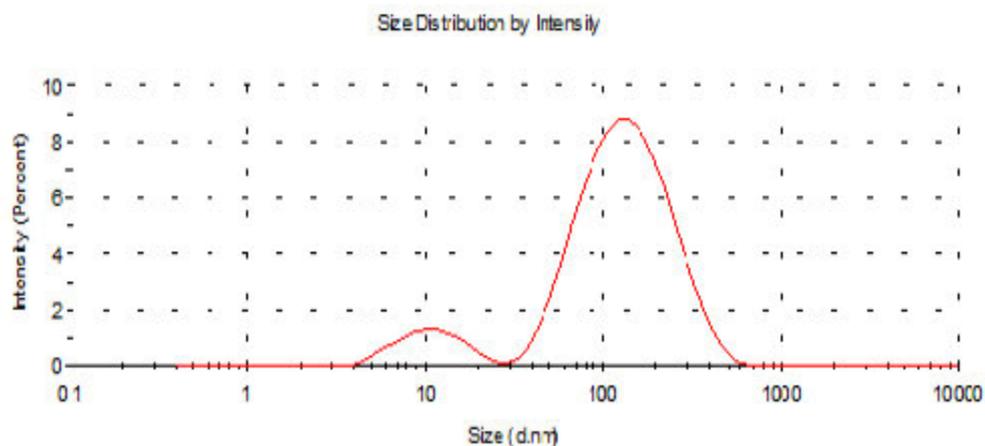
Figure 6.12 Intensity-weighted particle size distribution of Batch B10
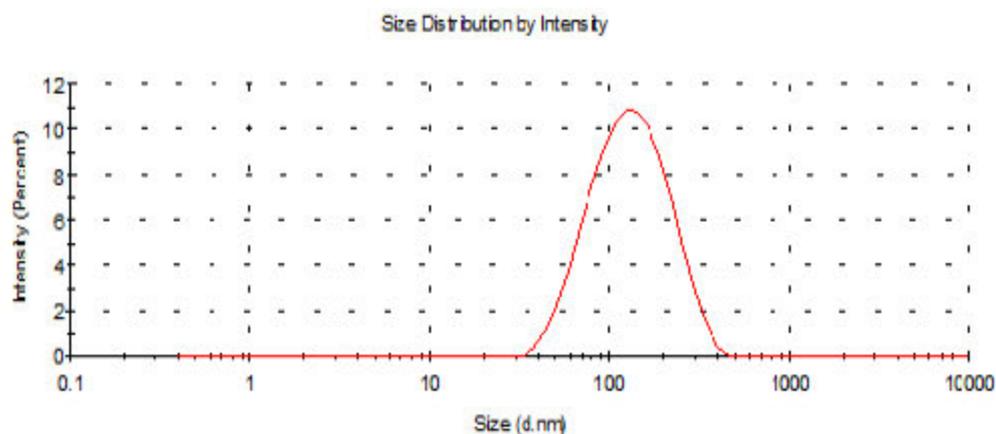
Figure 6.13 Intensity-weighted particle size distribution of Batch B11

Figure 6.14 Intensity-weighted particle size distribution of Batch B12

Size Distribution by Intensity

Figure 6.15 Intensity-weighted particle size distribution of Batch B13

Aim of the optimization of the formulation components was to develop liposomal formulation with unimodal distribution of particles with desired size and size range such that the formulation can be extrapolated to lipids synthesized from DSPE at same molar ratio. Phospholipids with saturated fatty chains (HSPC and DSPC), unsaturated chains (DOPE) and mixed short chain and long chain fatty chains (EPC) were used as bilayer forming lipids. Cholesterol was included as a fluidity buffer in the bilayer to promote formation of and stabilize bilayers. Particle size and particle size distribution characteristics of different batches evaluated are shown in **Figure 6.3** to **Figure 6.15**.

It was observed that incorporation of EggPC promoted formation of micelles which was evident by the peaks observed between ~10 nm-30 nm in the size distribution curves observed in DLS particle size analyses. Similar results were observed on incorporation of high levels of DOPE in the bilayers which promoted formation of micellar phases with amine lipid as indicated by multimodal particle size distribution curves.

Incorporation of HSPC was tried at lower to higher molar levels in the liposomes i.e. 10-40 mole%. At all levels, multimodal particle size distribution was observed. Even though the mean particle sizes were below 100 nm, PDI of formulations exceeded the value of 0.45. Particle size distribution curves indicated presence of different liposomal phases in the formulation i.e. of particles of different particle sizes. However, due to presence of DSPC and DPPC in HSPC, at lower levels in bilayers depending on the presence of high molar levels of cholesterol produced liposomes with uniform particle size distribution.

167

Monomodal particle size distribution with <18 mole% SA in optimized liposome composition is supported by previous report showing the solubility of stearyl amine in the phospholipid bilayers which is ~18.6 mole% (6). Above this level, formation of micelles has been reported. The presence of micellar phases in the liposomal dispersion is due to the critical packing parameter ($P=V/a_0 l$ where V = volume of chain, a_0 = equilibrium head-group cross-sectional area and l = chain length) of stearyl amine being less than 0.5 indicating its cone shaped structure which makes it more of a surfactant molecule able to form micelles than to form bilayer structures when present alone in water (7).

Based on the zeta potential determination results, it was observed that increasing amount of SA led to increase in zeta potential as expected due to its cationic head group. In case of other lipids the effect on zeta potential was different. Incorporation of HSPC, DSPC and EPC did not alter the zeta potential to a great extent indicating that their insignificant effect on zeta potential. However, incorporation of DOPE has exhibited a noticeable effect on zeta potential. It was observed that addition of DOPE led to reduction of zeta potential of liposomes. This might be attributed to the pKa of the amine group and phosphate group of DOPE which show differential ionization in aqueous dispersions as compared to zwitterionic PC molecules and further, placing of these molecules in the bilayer could affect the surface potential of the liposomes which would turn out to be the change in the zeta potential (8). Such effect has been spotted in the literature with cationic liposomes made of DOTAP, DOSPA and DMRIE which supports the results obtained herein (8). The combined effect of SA and DOPE would produce zeta potential observed in the prepared liposomes.

Based on particle sizes of the liposomes prepared with different compositions, the batch with SA:HSPC:DOPE:EPC:Chol:mPEG2000-DSPE with %mole ratio of 10:27:20:20:20:3 were found to be giving the best results in terms of monomodal distribution and z-averaged particle size less than 120 nm. Formulation containing DOPE was chosen because DOPE has known characteristic of imparting fusogenicity to liposomes which promotes the cytosolic release of liposomes. PEGylated liposomes were evaluated for particle size and zeta potential in comparison non-PEGylated liposomes. The mean particle size of the PEGylated and non-PEGylated liposomes showed only marginal increase which was of amplitude of less than 5 nm indicating no significant change in the particle size on incorporation of mPEG2000-DSPE. Additionally, as it can be seen from

168

the particle size distribution curves (Figure), characteristic of monomodal distribution of particle size of non-PEGylated liposomes was not lost on incorporation of PEGylated lipid in the lipid composition. However, the zeta potential liposomes was changed on PEGylation. This might be attributed to the PEG chains that extend over the surface of liposomes masking the surface charge of liposomes which in turn leads to less accumulation of charges in the stern layer around liposomes ultimately affecting the stern layer potential i.e. zeta potential.

A preliminary evaluation of the hemolytic potential and cytotoxicity of this optimized formulation containing stearlyamine was carried out in HEPG2 cell line (details in chapter 8). It was observed that the formulation was highly hemolytic and having high cytotoxicity (with % cell viability <40% @ 0.5 mM concentration of cationic lipid) for non-PEGylated formulation. PEGylation was observed to confer some level of protection from the direct damage to cell with % cell viability around 70%. It was thus rationalized, that increasing the bulk around the liposomes surface may further mask the direct deleterious impact of stearylamine on the cells. Hence, DSPE was incorporated in the liposomes and modification of the head group by boc-protected/deprotected amino acids was done, which will confer the needed masking characteristic. Further, as these amino acids are short residues, they do not confer an increase in the bulk to the liposomal system which may hinder the transfection potential. Further, these amino acids due to their aromatic head groups/ guanidine residue will get ionized at physiological condition, imparting buffering characteristic to the liposomes which is a favorable property for developing an efficacious delivery system that will protect the payload from harsh endosomal environment and subsequent degradation. With this background, DSPE containing liposomes were formulated and optimized containing 10 mole% SA that were optimized in above formulation approach.

6.3.2 Preparation of DSPE based liposomes

6.3.2.1 Preliminary Screening of Formulations: DSPE lipid incorporated

Preliminary studies were carried out using same process parameters as that of SA based liposomes. Herein, 10 mole% of SA was taken forward for screening the batches. Results of the preliminary liposomes prepared with DSPE tried are shown in **Table 6.4**. Representative particle size distribution plots (intensity weighted) are depicted **Figure 6.16** to **Figure 6.30**.

Table 6.4 Optimization of DSPE based liposomes: Composition of trial batches with their particle size and its distribution characteristics (SA: 10 mole%)

| Batch Code.	Lipid composition	Ratio of mole%	Particle size (nm)	PDI	Distribution
C1	HSPC:DSPE:DOPE:Chol	30:21:20:20	171.6±8.1	0.212±0.021	Monomodal
C2	DSPC:DOPE:Chol	31:34:25	830.5±40.6	0.782±0.019	Multimodal
C3	HSPC:DOPE:Chol	35:34:22	93.89±11.6	0.281±0.081	Bimodal to monomodal
C4	DSPC:DOPE:Chol	40:17:33	132.1±5.4	0.238±0.038	Monomodal
C5	DSPC:DSPE:EPC:DOPE:Chol	20:10:20:22:18	91.21±8.1	0.314±0.042	Monomodal with tailing
C6	DSPC:EPC:DOPE:Chol	27:10:40:13	ND (not determined)	ND	Sonicated formulation rapidly changed to hazy suspension
C7	DSPC:DSPE:EPC:DOPE:Chol	11:25:10:32:12	299.2±17.8	0.449±0.053	Trimodal
C8	DSPC:DSPE:DOPE:Chol	10:40:30:10	86.59±10.2	0.491±0.082	Bimodal
C9	DSPC:EPC:DOPE:Chol	20:20:40:10	77.95±8.7	0.371±0.091	Bimodal
C10	HSPC:EPC:DOPE:Chol	24:20:28:18	166.34±10.6	0.266±0.081	Monomodal
C11	DSPE:HSPC:DOPE:Chol	10:40:30:11	228.5±10.6	0.236±0.039	Monomodal
C12	HSPC:EPC:DOPE:Chol	30:11:30:19	>1 μ	1.000	Size not suitable, precipitated
C13	**DSPE:DOPE:HSPC:EPC:Chol**	**10:10:35:24:12**	**108.5±6.4**	**0.175±0.031**	**Monomodal**
C14	DSPE:HSPC:EPC:DOPE:Chol	16:30:8:26:10	84.21±4.9	0.282±0.051	Monomodal to bimodal
C15	HSPC:DOPE:Chol	38:36:16	160.5±5.3	0.263±0.056	Monomodal
C16	HSPC:EPC:DOPE:Chol	30:20:20:20	81.42±4.2	0.392±0.062	Monomodal to bimodal
C17	**DSPE:DOPE:HSPC:EPC:Chol :mPEG$_{2000}$-DSPE**	**10:10:32:25:10:3**	**109.2±8.5**	**0.180±0.0045**	**Monomodal**
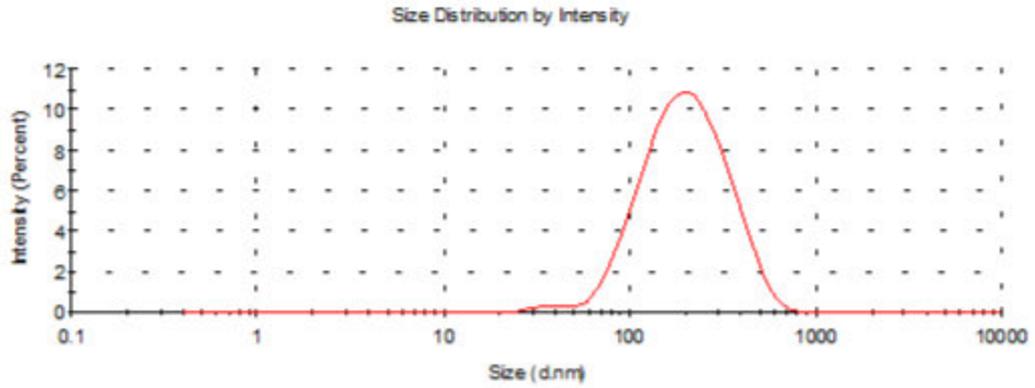
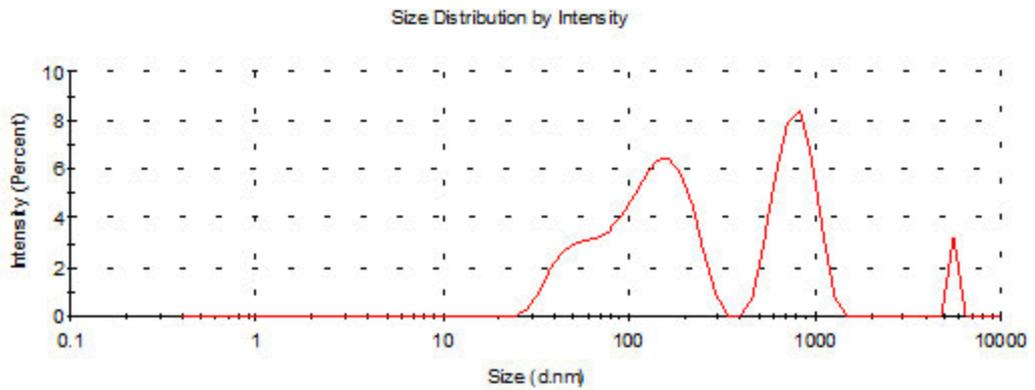**Figure 6.16 Intensity-weighted particle size distribution of Batch C1**

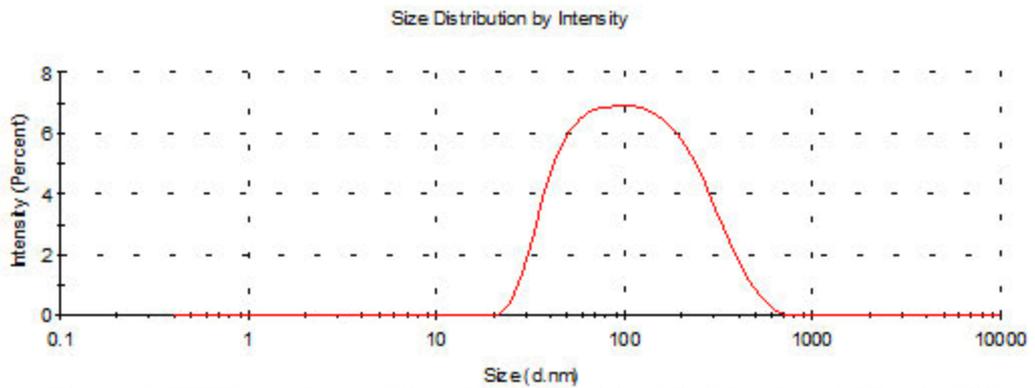**Figure 6.17 Intensity-weighted particle size distribution of Batch C2**

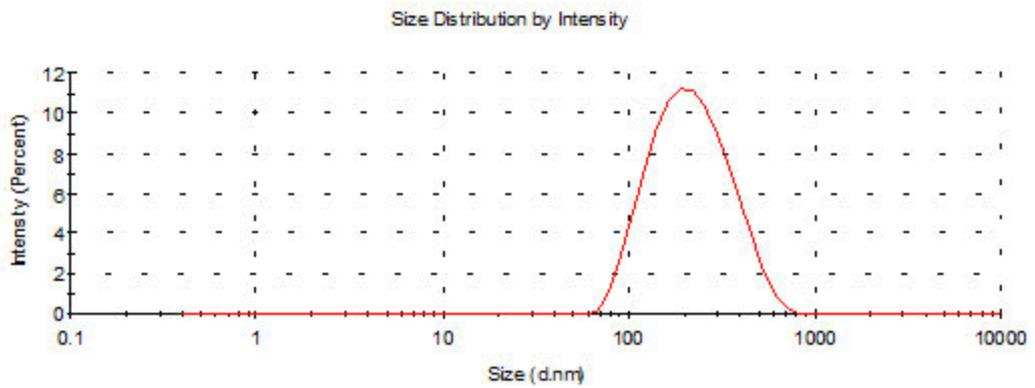**Figure 6.18 Intensity-weighted particle size distribution of Batch C3**

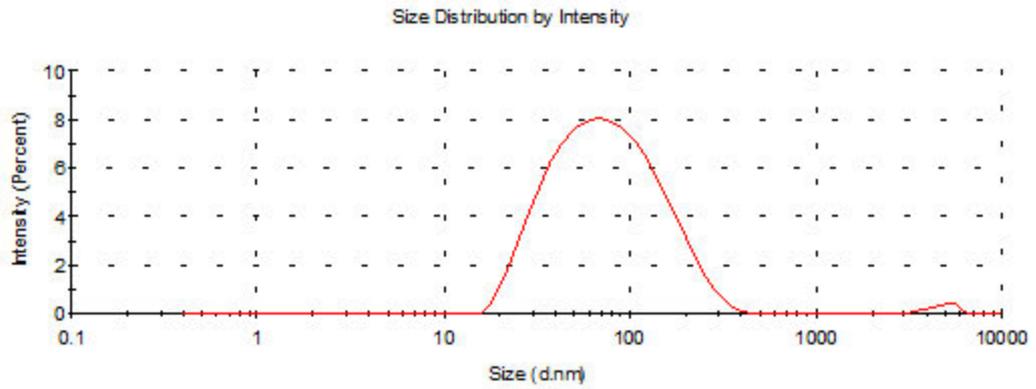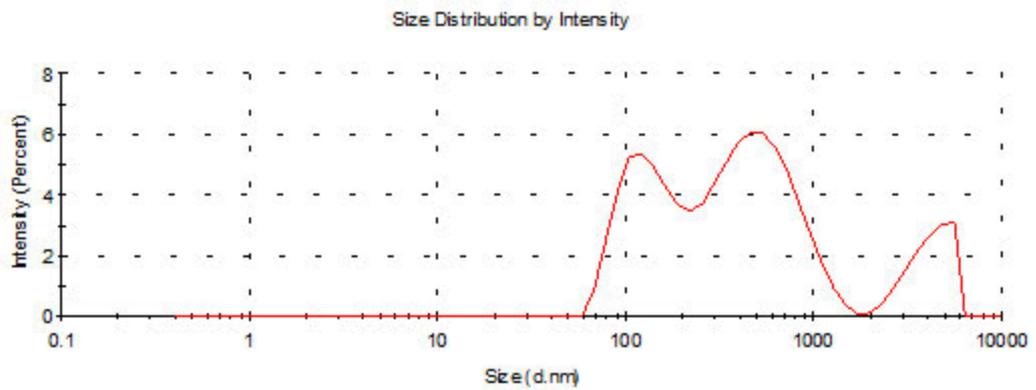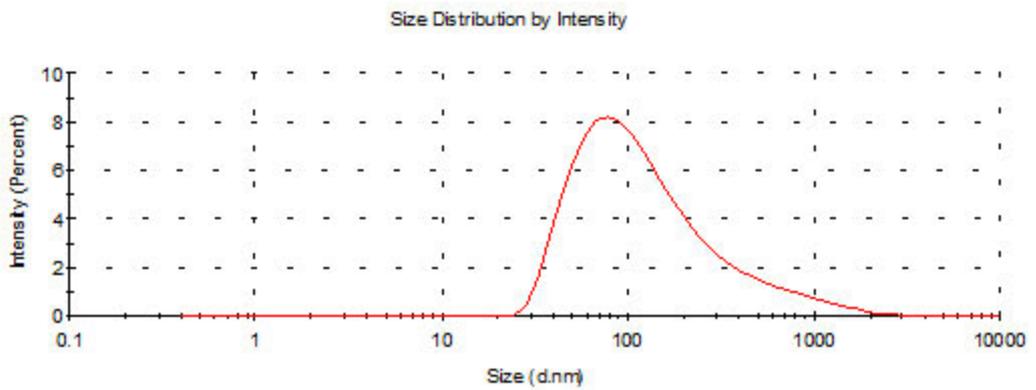**Figure 6.19 Intensity-weighted particle size distribution of Batch C4**

Size Distribution by Intensity

Figure 6.20 Intensity-weighted particle size distribution of Batch C5

Size Distribution by Intensity

Figure 6.21 Intensity-weighted particle size distribution of Batch C7
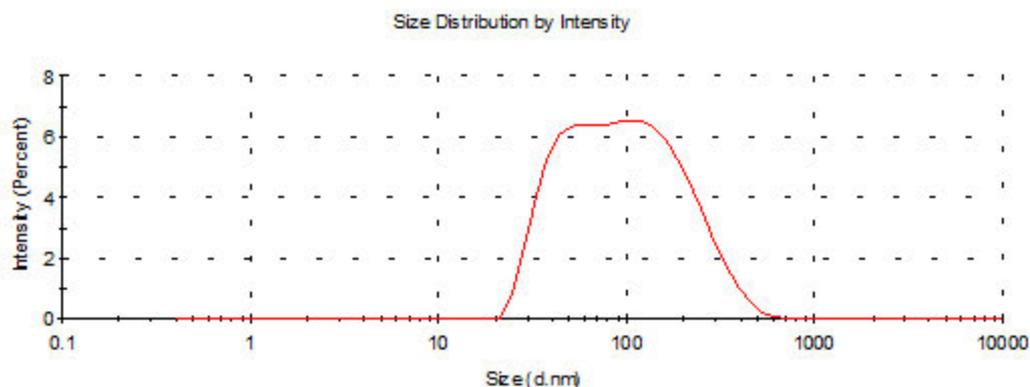
Size Distribution by Intensity

Figure 6.22 Intensity-weighted particle size distribution of Batch C8

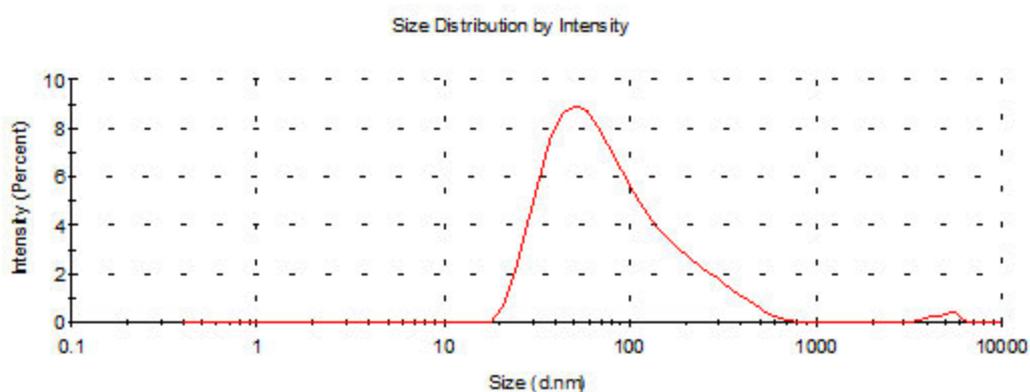Figure 6.23 Intensity-weighted particle size distribution of Batch C9

Figure 6.24 Intensity-weighted particle size distribution of Batch C10
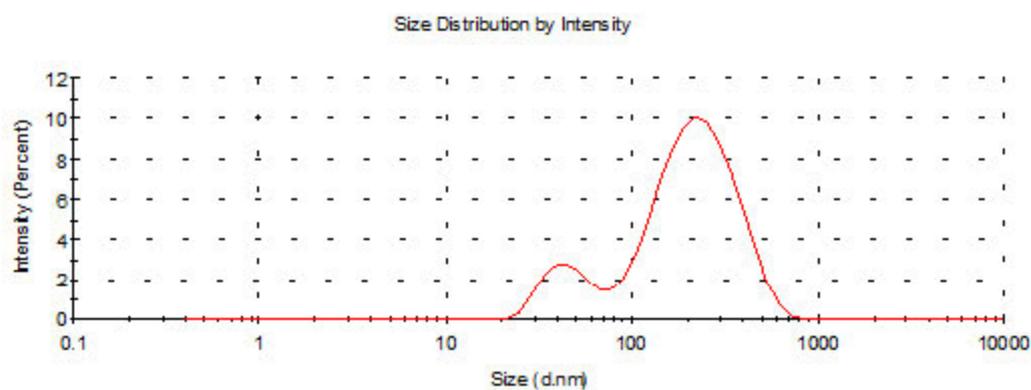

Figure 6.25 Intensity-weighted particle size distribution of Batch C11
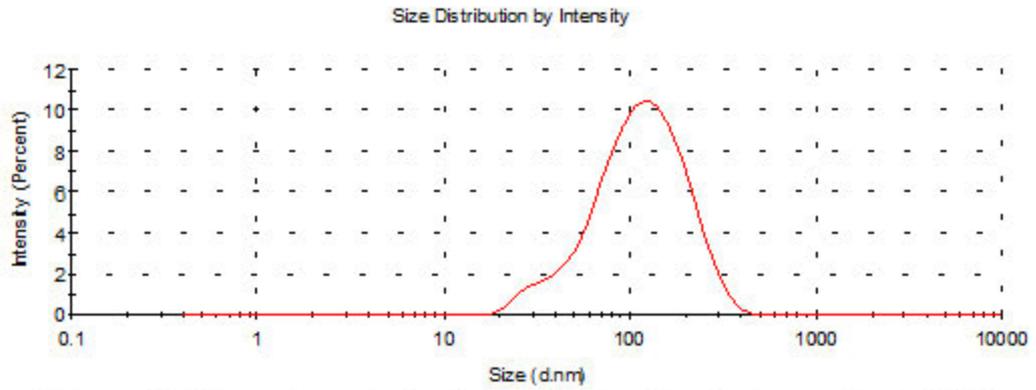
173

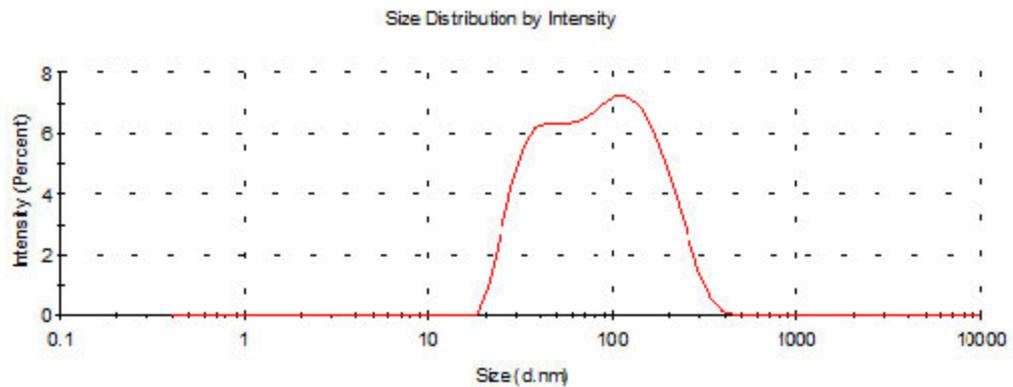Figure 6.26 Intensity-weighted particle size distribution of Batch C13

Figure 6.27 Intensity-weighted particle size distribution of Batch C14

Figure 6.28 Intensity-weighted particle size distribution of Batch C15
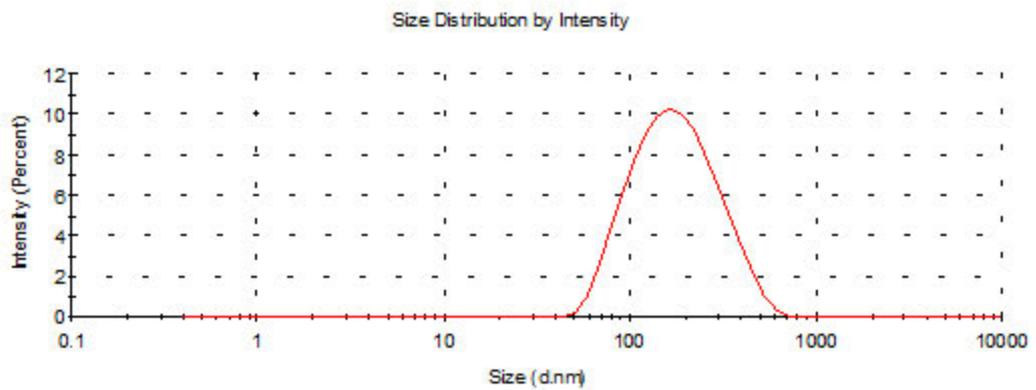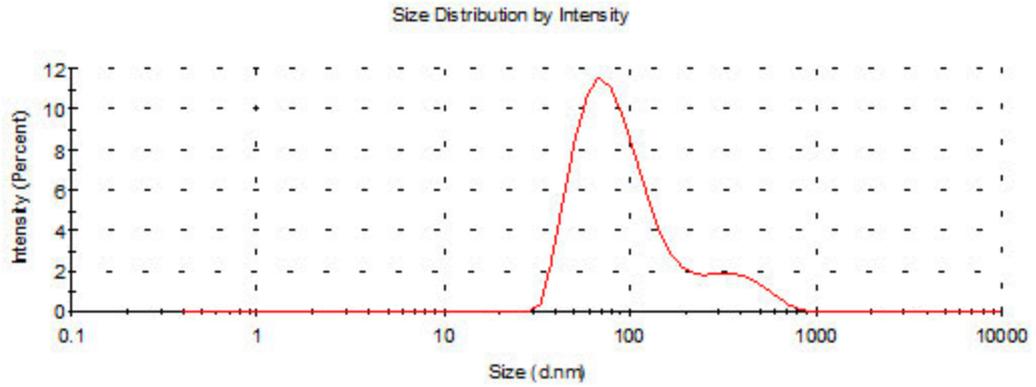
Figure 6.29 Intensity-weighted particle size distribution of Batch C16
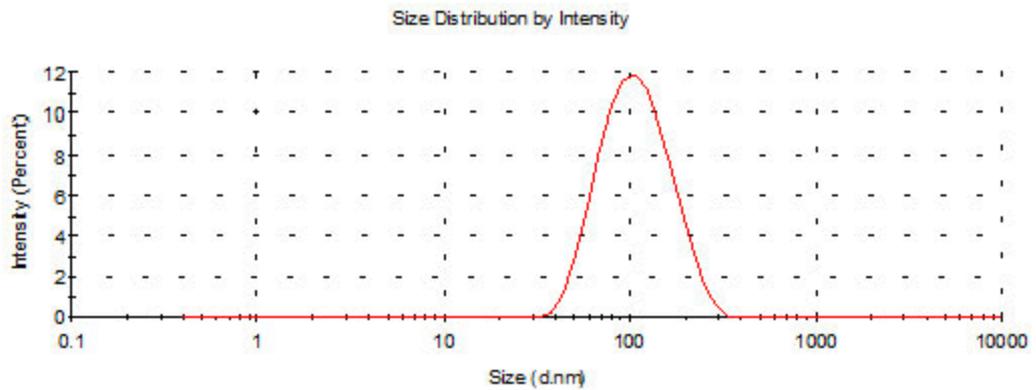
Figure 6.30 Intensity-weighted particle size distribution of Batch C17

Figure 6.31 TEM image of liposomes of Batch C10

175

Figure 6.32 TEM image of liposomes of Batch C13

Figure 6.33 TEM image of liposomes of Batch C17

Based on the preliminary screening of the liposomal components, some generalizations can be made. Increasing amounts of saturated phospholipids i.e. DSPC, HSPC, DSPE, more or less, affected the increase in the particle size with sometimes

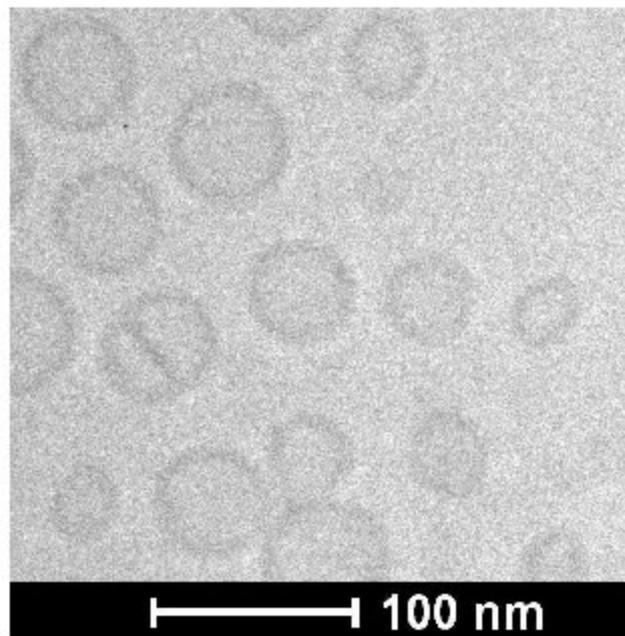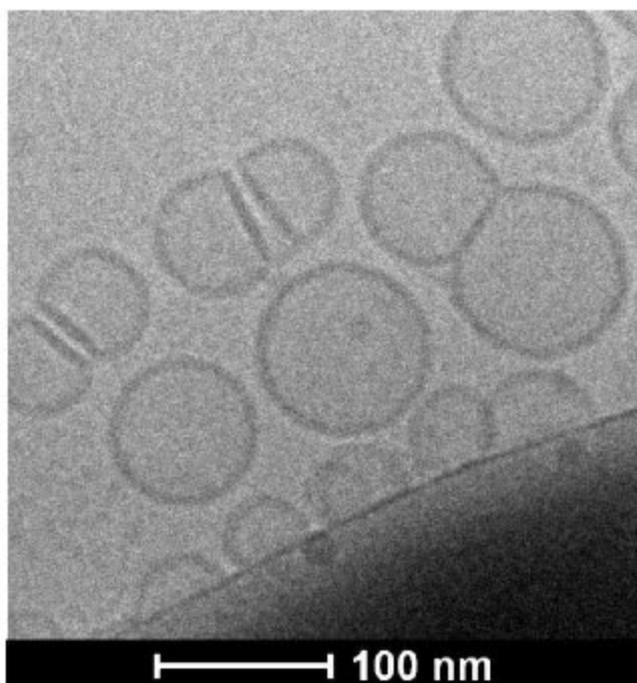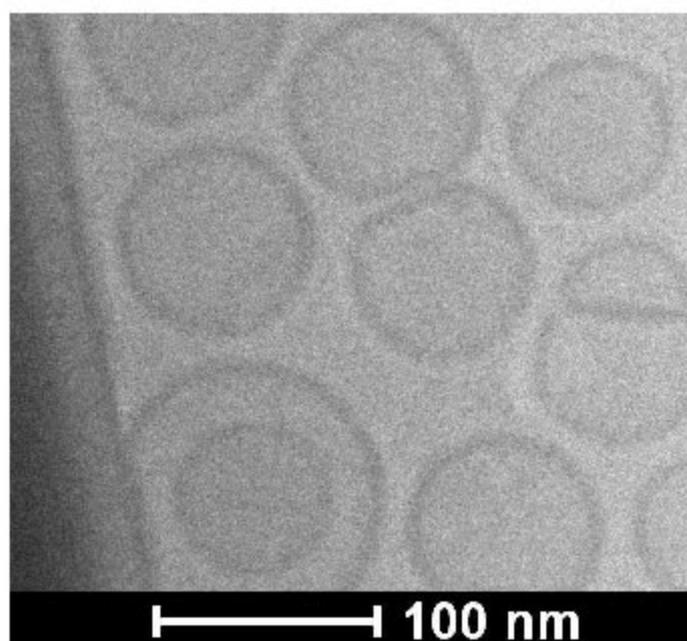formations of large lipid aggregates above the sizes of 500 nm up to $\geq 1\ \mu$ sized particles. For many batches which showed favorable particle size below 200 nm exhibited an irregular particle size distribution with bimodal distribution patterns. As it can be seen in in intensity-weighted particle size distribution curves obtained by DLS, in many formulations where the levels of EggPC were higher than 25-30 mole%, particle size showed a bimodal distribution evidenced by two peaks, one at around 20-40 nm and other at 90-110 nm size, respectively. This is due to presence of EggPC which has been reported to produce liposomal phases of particle size as low as 20 nm which will coexist with liposomes of size >90 nm formed by HSPC and EggPC (9, 10).

TEM imaging of few batches of DSPE-DOPE liposomes was carried out in order to determine the presence different lamellar phases i.e. small sized and large sized lamellar phases in the liposomes. TEM images (refer **Figure 6.31**, **Figure 6.32** and **Figure 6.33** for comparison) revealed that EggPC containing batches showed presence of liposomes with 20-50 nm particle size indicative of EggPC in higher amounts as described earlier. Additionally, it can be seen that TEM images revealed the presence of fused liposomes which is due the instability of SUVs due to their higher curvature which leads to formation of more stable LUVs in absence of any surface charge or steric polymer chains i.e. PEG-2000/PEG-5000 that would prevent their aggregation (11, 12). Moreover, during the freezing step of the cryoTEM process, the tendency of SUVs to fuse might get aggravated (11).

Based on the results obtained from the preliminary batches, batch containing SA:DSPE:DOPE:HSPC:EPC:Chol in the molar ratio of 10:10:10:35:25:10 was considered to be optimum with particle size in the range of 90-110 nm with a monomodal distribution of particles. The optimized batch of liposome was further modified with incorporation of 3 mole% of DSPE-mPEG$_{2000}$ by replacing equimolar amounts of HSPC. TEM image of the formulation presence of lamellar phases distributed around 100 nm corroborating with the results obtained with DLS. Also, the liposomes are visible as individual particles with no or negligible fusion/aggregation as compared to those prepared without DSPE-mPEG$_{2000}$. This shows the potential of mPEG chains extending over surface of liposomes to prevent the closer approach of the liposomal particles and subsequent fusion.

Further optimization of the formulation was done by employing factorial design to further fine-tune the lipid composition so as to obtain particle size of desired range with

monomodal distribution and also explore the design space where the particle size below 120 nm can be achieved with desired PDI.

6.3.2.2 Formulation Optimization using DOE

DSPE-DOPE liposomal formulations were optimized using D-optimal design with total 19 runs among which 6 model points were for preselected quadratic model, 5 points to estimate the lack of fit, 5 replicate points and additional 3 center points to evaluate for curvature and to estimate the pure error. From the results of optimum batch observed in preliminiary screening, SA:DOPE:DSPE molar ratio was kept constant i.e. 1:1:1 at concentration of 10 mole% of each and mPEG$_{2000}$-DSPE level of 3 mole% in experimental design for all batches while varying the mole% of other lipids i.e. HSPC, EPC and Chol. Variables chosen for optimization are shown in **Table 6.5**. Coded and actual values used in formulation optimization are tabulated here (**Table 6.6**) The design was also constrained so as to keep total molar concentration of three chosen lipids to be 77 mole% in every combination. Additionally, other process and formulation parameter were kept constant during optimization (thin film formation at -450 mmHg vacuum and 45°C temperature for 45 min at 100 rpm followed by hydration for 1 hr at 65°C using DFW.

Table 6.5 Various variables and responses involved in optimization

	HSPC (mole%)
Variables	EPC (mole%)
	Chol (mole%)
Response Parameter	Particle size (nm)
	PDI

Table 6.6 Coded and actual levels of HSPC, EPC and Chol used in optimization

Coded levels	Actual levels		
	A: HSPC (mole%)	B: EPC (mole%)	C: Chol (mole%)
Lower (-1)	30.0	25.0	10.0
Higher (+1)	40.0	35.0	15

Constraint	A+B+C = 77.0 mole%

Response surface modelling was applied using Design Expert 9.0.1 (Stat-Ease Inc., MN). Using multiple linear regression analysis (MLRA), different polynomial equations were evaluated for best fitting to the experimental data by determining the values of coefficients in the polynomial equations and a full and reduced model was established. Statistical soundness of the established model was checked by ANOVA statistics (13-19).

Based on the established model three-dimensional response surface plots were constructed by Design Expert Software. The 3D surface plots were useful in establishing the main effects (effect of individual variables) on the response parameter and also to have an insight to the combined effects of two variables (20-22).

Validation of the employed experimental design and chosen model for its prediction capability for the optimization of the variables was done by performing check-point analysis. Eight optimum checkpoints were selected, prepared and evaluated for response parameters. Statistical comparison between the predicted values and average of three experimental values of the response parameters was performed to derive percentage error and to evaluate significant difference between these values. Optimum formulation parameters were selected based on the specified goal i.e. particle size and particle size distribution

Optimized formulation was derived by specifying goal and importance to the formulation variables and response parameters. Results obtained from the software are further verified by actual preparation of the batches and comparing the predicted and actual results.

a) Design Matrix

19 batches of liposomes were prepared using composition depicted in the design matrix in Table. All formulations were evaluated for particle size and polydispersity index (PDI) and the results obtained are shown in **Table 6.7**. All experiments were replicated three times and mean values of experiments were fed to the design matrix for statistical evaluation.

Table 6.7 Design Matrix for Calcium Chloride Loaded Liposome Optimization

Std Run	Exp Run	Factor 1 A:HSPC mole%	Factor 2 B:EPC mole%	Factor 3 C:Chol mole%	Response 1 Mean Particle Size nm	Response 2 PDI
19	1	34.2	32.8	10.0	104.5	0.324
14	2	34.8	29.8	12.4	117.7	0.156
4	3	34.2	32.8	10.0	108.4	0.341
10	4	32.5	31.9	12.6	105.5	0.205
2	5	30.6	35.0	11.4	98.8	0.335
7	6	32.6	29.4	15.0	130.2	0.249
13	7	34.8	29.8	12.4	113.6	0.189
5	8	34.8	29.5	12.7	112.9	0.179
9	9	37.1	27.3	12.6	124.4	0.178
18	10	30.3	31.7	15.0	127.1	0.241
8	11	37.8	29.2	10.0	119.4	0.238
6	12	40.0	25.9	11.1	131.9	0.185
11	13	34.8	27.3	14.9	139.5	0.195
17	14	37.0	25.0	15.0	150.1	0.178
12	15	34.8	29.8	12.4	108.1	0.167
16	16	40.0	25.9	11.1	137.5	0.190
15	17	30.6	35.0	11.4	104.7	0.348
1	18	30.3	31.7	15.0	122.4	0.278
3	19	37.0	25.0	15.0	143.4	0.193

i. Statistical Analysis of Response 1 (Particle Size)

Selection of the prediction model:

Summary of the ANOVA results for different models as shown in **Table 6.8** which depicts sequential p-values and Lack of Fit p-values along with Adjusted and Predicted R-squared values for different models.

Table 6.8 Summary of ANOVA results for Different Models

Source	Sequential p-value	Lack of Fit p-value	Adjusted R-Squared	Predicted R-Squared	
Linear	< 0.0001	0.0758	0.8293	0.8007	

Quadratic	0.0002	0.9592	0.9498	0.9166	Suggested
Special Cubic	0.2964	0.9863	0.9506	0.9129	
Cubic	0.9416	0.8870	0.9368	0.8501	
Sp Quartic vs Quadratic	0.7137	0.9601	0.9428	0.9042	
Quartic vs Cubic	0.8870		0.9214		Aliased
Quartic vs Sp Quartic	0.9601		0.9214		Aliased

Highest polynomial showing the lowest p value (<0.05) along with highest Lack of Fit p-value (>0.1) was considered for model seleciton. Based on the criteria quadratic model was found to be best fitted to the observed responses. Special cubic and higher models were not suitable for prediction either due to low R-squared values and/or due to higher p value as compared to quadratic model (**Table 6.9**). Quartic and higher models were aliased indicating the confounding of the model terms by the other implying that the predicted response would give the wrong idea of the actual response.

Table 6.9 ANOVA Table 6.for Quadratic Mixture Model

Source	Sum of Squares	df	Mean Square	F Value	p-value Prob > F	
Model	3804.21	5	760.84	69.17	< 0.0001	significant
Linear Mixture	*3348.28*	*2*	*1674.14*	*152.19*	*< 0.0001*	
AB	*149.68*	*1*	*149.68*	*13.61*	*0.0027*	
AC	*326.07*	*1*	*326.07*	*29.64*	*0.0001*	
BC	*302.48*	*1*	*302.48*	*27.50*	*0.0002*	
Residual	143.00	13	11.00			
Lack of Fit	*22.41*	*6*	*3.74*	*0.22*	*0.9592*	*not significant*
Pure Error	*120.59*	*7*	*17.23*			
Cor Total	3947.21	18				

The Model F-value of 69.17 implies the model is significant. There is only a 0.01 % chance that a "Model F-Value" this large could occur due to noise. Values of "Prob > F" less than 0.0500 indicate model terms are significant. In this case all main effects (A, B and C as indicated by linear mixture in **Table 6.9**) are significant model terms showing that all the chosen factors have significant effect on particle size for given set of experimental conditions. Additionally, all the factors are involved in two way interactions with each other as shown by p value <0.0001 for interaction terms AB, AC and BC. Values greater than 0.1000 indicate the model terms are not significant. The "Lack of Fit F-value" of 0.22 and Lack of Fit *p* value of 0.9592 infer the Lack of Fit to be not significant relative to the pure error i.e. the selected model fits effectively to the observed experimental runs and is effective in predicting responses all over the design matrix.

Table 6.10 Summary of ANOVA results for Quadratic Mixture Model

Std. Dev.	3.32	**R-Squared**	0.9638
Mean	121.06	**Adj R-Squared**	0.9498
C.V. %	2.74	**Pred R-Squared**	0.9166
PRESS	329.26	**Adeq Precision**	25.131

Summary of ANOVA results for selected Quadratic Mixture model is shown in **Table 6.10**. The "Pred R-Squared" of 0.9166 is in reasonable agreement with the "Adj R-Squared" of 0.9498 i.e. <0.2. "Adequate precision" which is a measure of the signal to noise ratio is 25.131 indicating an adequate signal for the model to be used to nevigate the design space.
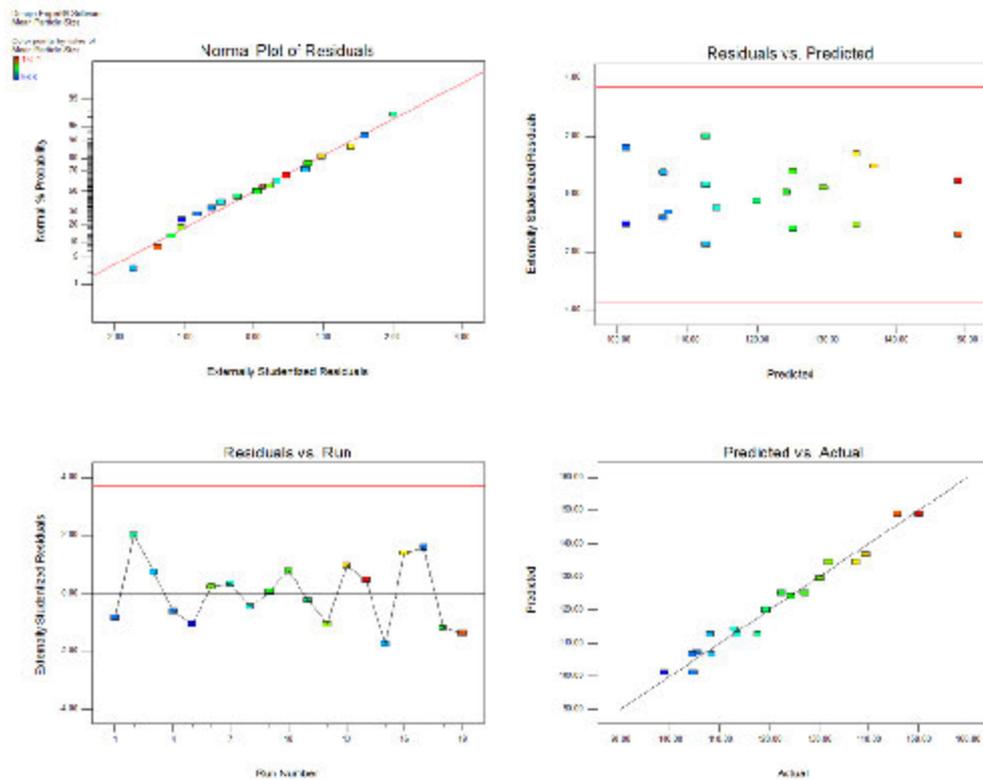
Model diagnostics

Figure 6.34 Model diagnostic plots

Various diagnostic plots for evaluation of the model are shown in **Figure 6.34**. The normal probability plot (normal plot of residuals) which shows whether the residuals follows a normal distribution or not and helps identify any specific patterns in the residuals indicative of requirement of transformations i.e. "S-shaped" curve, etc. normal plot for the current data show that data follows a straight line inferring the normal distribution of the residuals.

Residuals vs. predicted response (ascending values) plot tests if variance is distributed over the design constantly i.e. variance is not associated with the factor values as megaphone patterns (pattern like sign > or <) which indicate either decreasing or increasing residuals with increasing the factor values. This is a plot of the residuals versus the ascending predicted response values.

Residual vs. run order plots the residuals against the experimental run order i.e. order in which the experiments have been carried out. The plot with a random scatter of residuals indicate there is no time dependent changes in the residuals, i.e. there is absence of any time dependent variable among the variables selected or among the variables which

183

has been not included in the DoE. If there is such Random scattered plot of residuals in the current analysis indicate no association of residuals with time and absence of any time dependent variable.

Predicted vs. actual plot shows correlation between the observed response values and actual response values. A good correlation between the predicted and actual values (data following a straight 45° line) shows that the model chosen for analyses of data is appropriate in predicting the responses all over the design matrix. Also, this plot helps to detect a value/ values that are not easily predicted by the model. As it can be seen from the figure, plot follows a 45° straight line indicating a close estimate of predicted values with actual values.
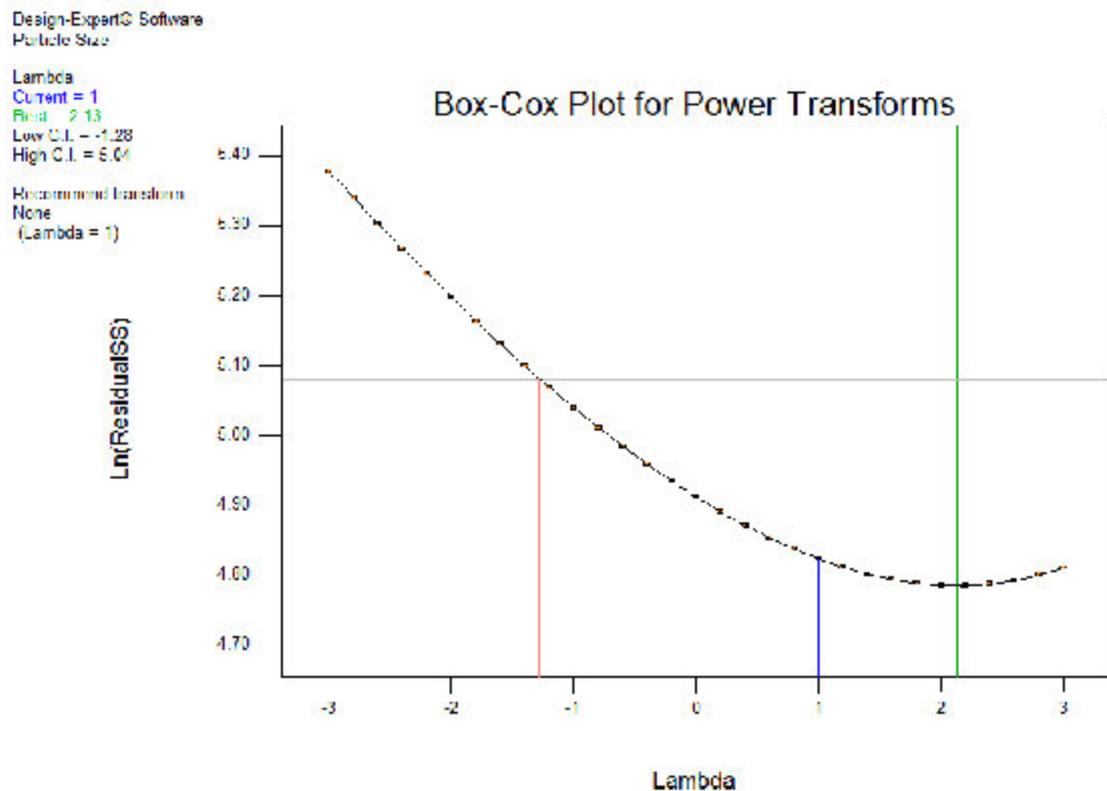

Figure 6.35 Box-Cox plot of power transformation

Box-Cox plot of Ln(residuals sum of squares) vs. λ for power transformation helps select any power transformation of observed response values required for fitting the model based on the best λ value and 95% confidence interval around it. Plot in **Figure 6.35** shows the λ value of 1, which lies near the best λ value and within 95% confidence interval of it, indicating no requirement for any power transformation.
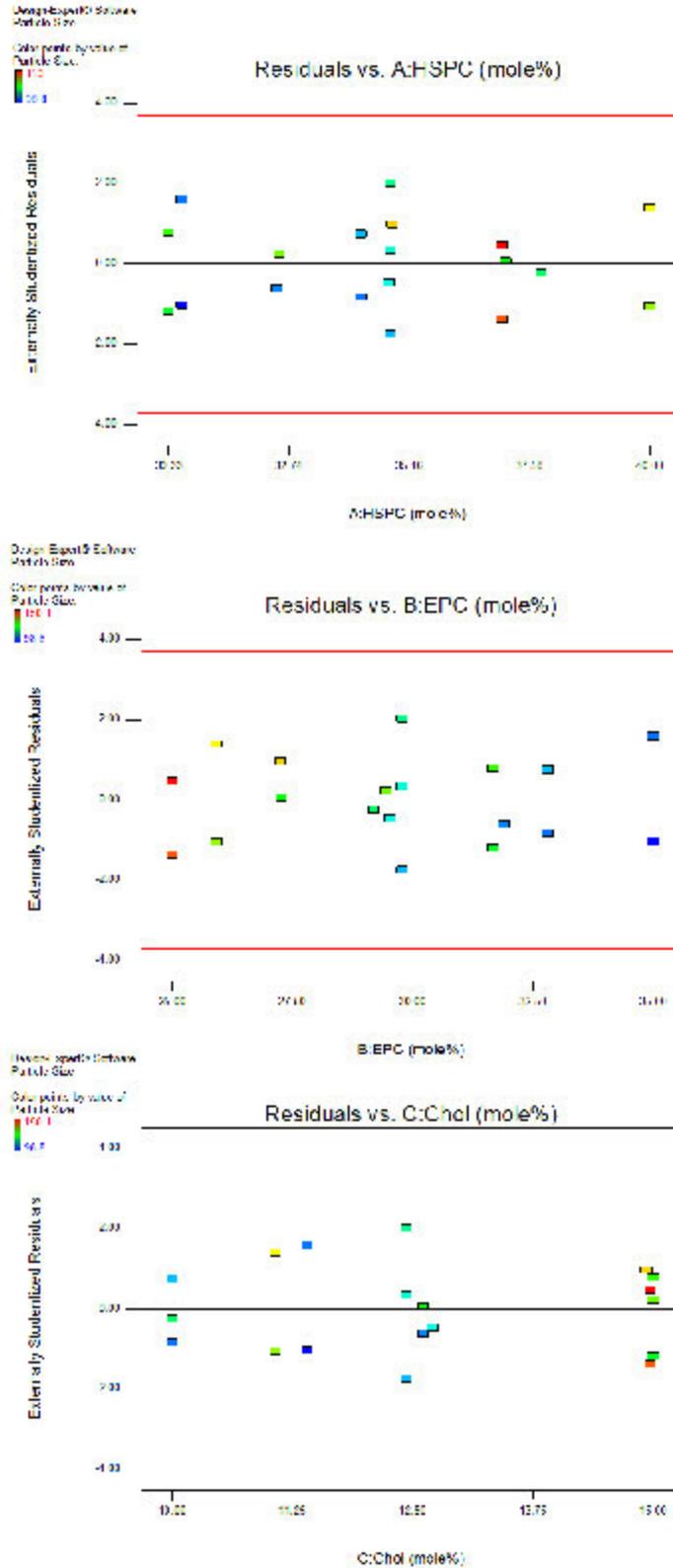
184

Figure 6.36 Residual vs. factor plots for determining the time-independence of variance

Plot of residuals vs. any factor evaluated if any association is there between the variance associated with different levels of factor i.e. any specific trends (+ve or −ve curvatures) associated with increasing level of each factor. As it can be seen from the **Figure 6.36**, plots for each factor shows a random scatter over the increasing levels of factors indicating that the model is effective in accounting for the variance for each factor.
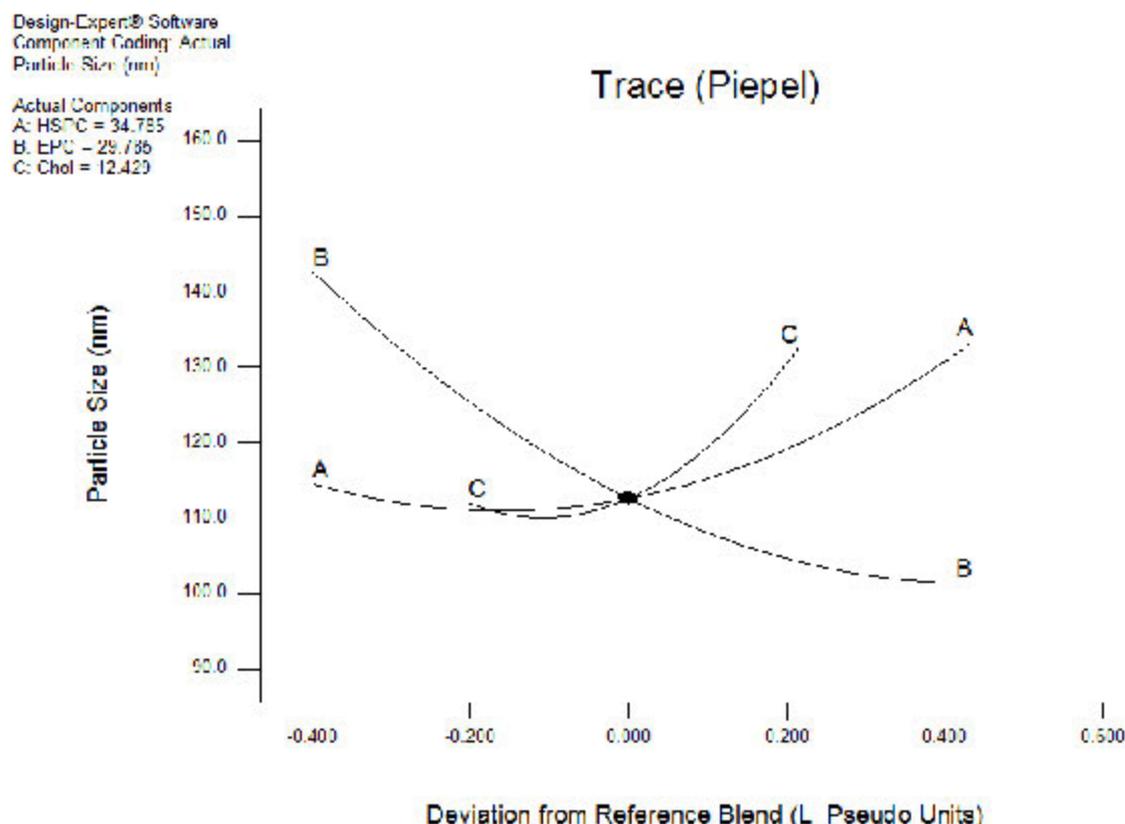
Effects of factors on response (particle size):

Figure 6.37 Piepel's plot

Piepel's plot is a trace plot showing the effect of individual factors plotting the pseudo limits of one component keeping the ratio of the changeable amounts of the each components kept constant against the response. The responses are plotted as deviations from the reference blend i.e. centroid (pseudo center point of the constrained design). As it can be seen from the plot (**Figure 6.37**), HSPC and cholesterol has positive effects on the particle size indicated by increase in the particle size along the increse in the mole% of these components. EggPC shows a negative effect on the particle size depicting steep decrese in the particle size on decreasing mole% of EggPC in the mixture.
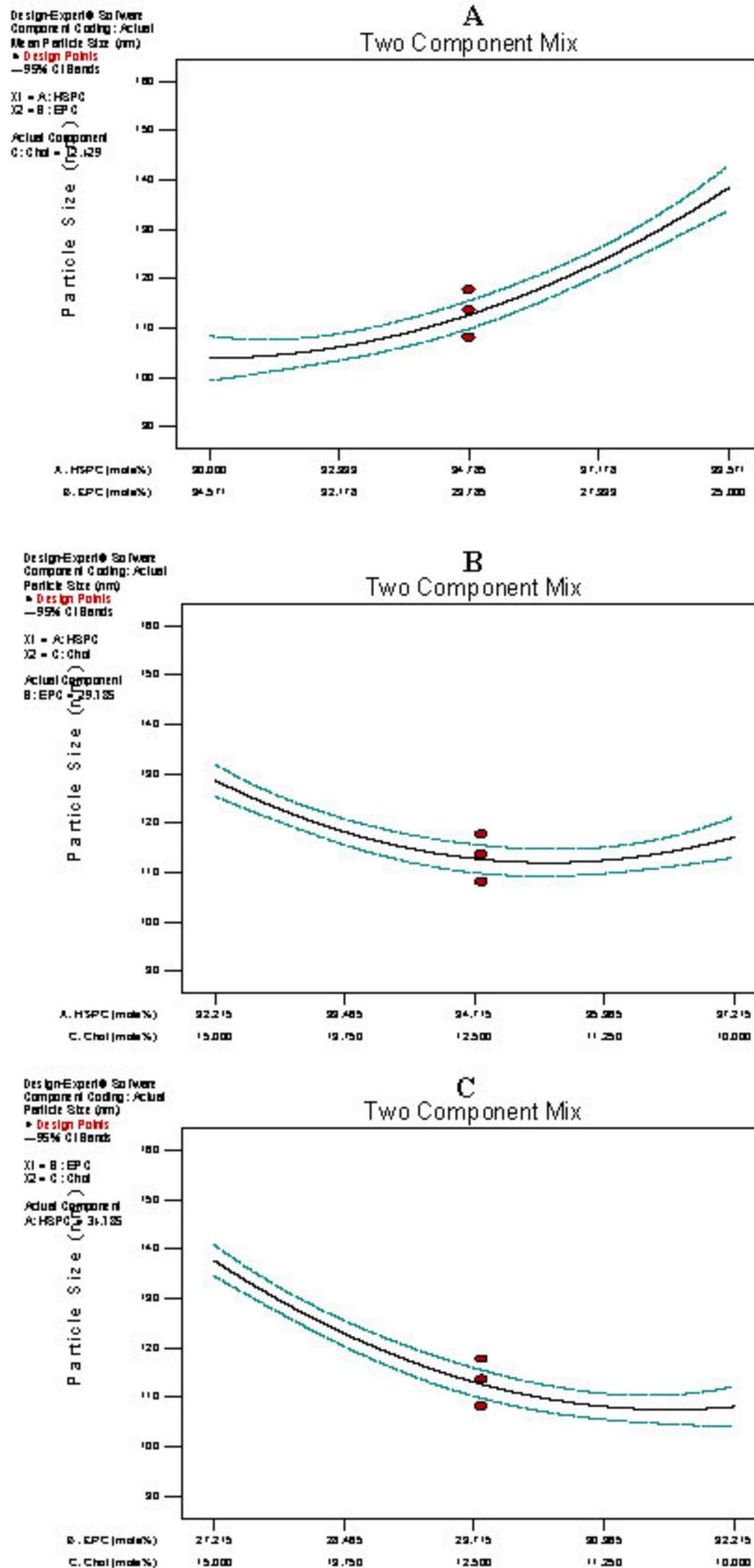
Figure 6.38 Two-component mixture plots ; A: effect of HSPC and EPC, B: effect of HSPC and Chol, C: effect of EPC and Chol

Two component mix plots shows the combined effects of two components on the response keeping the value of another component kept constant at its centroid value. As it can be seen from the **Figure 6.38** A, as the ratio of HSPC:EPC increases i.e. mole% of HSPC increases and mole% of EPC decreases, particle size increases. This can be explained by the increasing amounts of saturated long chain fatty acyl chains of phospholipids present in the HSPC (85% DSPC and 14% DPPC,) and decreasing amount of mono- and polyunsaturated phospholipids (present in the EggPC) which constitute ~49% of fatty acids in the EggPC and particularly the presence of ~40% of 1-palmitoyl-2-oleoylphosphatidylcholine (23).

Saturated long chain phospholipids are packed in the lipid bilayers in highly ordered manner (packing parameter P between 0.7-1, due to cylindrical configuration) which doesn't allow for more curvature in the lipid bilayers while cholesterol insert themselves in the lipid bilayers promoting the structure which may allow some distortion in the lipid bilayer in the form of curvature formation and increasing the stability of the bilayer. In case of the effect of HSPC:Chol, increasing ratio of HSPC:Chol show moderate effect on the particle size with a modest decrease in the particle size. This is due to the compensatory effect of EggPC which counters the effect of higher levels of HSPC as well as higher levels of cholesterol.

"Two component mix plots of effect of EggPC and Cholesterol show a steep decrease in the particle size with increasing ratio of EggPC:Chol. This effect can be attributed to the same fact that unsaturated fatty acyl chain phospholipid present in EggPC form bilayers with higher curvature i.e. unsaturated phospholipids prefer the negative curvature (inner leaflet of liposomes) more over positive curvature (outer leaflet of liposomes). This is due to their structural feature due to its packing parameter (P>1) due to the smaller headgroup than cross-sectional area of the acyl chain due to presence of unsaturation (24). Cholesterol (P<1 due to tetracyclic ring structure) which inserts between the saturated phospholipid molecules (which have P~0.8 due to cylindrical shape) allow for positive curvature by concentrating on the outer leaflet of the liposomes forming rigid bilayer structure. With increasing concentrations of EggPC, the particle size decreases which is attributed to the aforementioned justification. However, with increasing concentrations of Cholesterol, the effect of EggPC is decreasing due to subsequent decrease in the concentration of EggPC, hence, causes modest increase in the particle size. In presence of higher amounts of EggPC, the combined effect turned out to

be negative showing decreasing particle size over increasing level of EggPC. However, one thing to note here is that the effect of Egg PC, in many formulations where the levels of EggPC were higher than 30 mole%, was to give lower particle size with a bimodal distribution evidenced by two peaks in intensity weighted particle size distribution curves obtained by DLS, one at around 20-40 nm and other at 90-110 nm size, respectively. This is due to presence of EggPC which has been reported to produce liposomal phases of particle size as low as 20 nm which will coexist with liposomes of size >90 nm formed by HSPC and EggPC (9, 10).

Figure 6.39 Contour plot of effects of different components on particle size
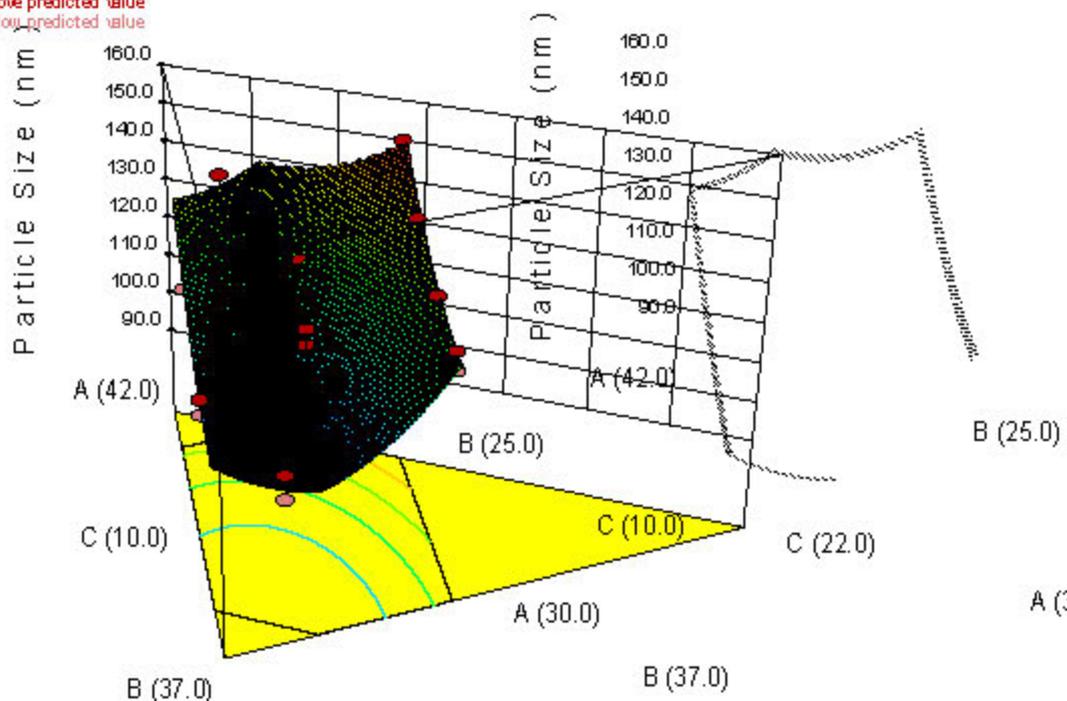
Figure 6.40 Response surface plot of effects of different components on particle size

Contour plot (**Figure 6.39**) and response surface plot (**Figure 6.40**) show effects of all three components on the particle size. To summarize, with increasing mole% of EggPC causes decrease in the particle size while increase in the mole% of HSPC and Cholesterol in the mixture brings about an increase in the particle size. The effects can be explained with similar justifications mentioned under the two component mix plots.

Equation for prediction of particle size over design matrix

Equation for prediction of particle size within the design matrix is given below.

Mean Particle Size	=
+12.01134	* HSPC
+9.64358	* EPC
+85.90405	* Chol
-0.36835	* HSPC * EPC
-1.61555	* HSPC * Chol
-1.56670	* EPC * Chol

ii. Statistical Analysis of Response 2 (Polydispersity Index-PDI)

Selection of Prediction Model:

Summary of the ANOVA results for different models as shown in **Table 6.11** depicts sequential p-values and Lack of Fit p-values along with Adjusted and Predicted R-squared values for different models.

Table 6.11 Summary of ANOVA results for Different Models

Source	Sequential p-value	Lack of Fit p-value	Adjusted R-Squared	Predicted R-Squared	
Linear	0.0004	0.0014	0.5739	0.5118	
Quadratic	< 0.0001	0.2129	0.9225	0.8865	Suggested
Special Cubic	0.1380	0.2693	0.9306	0.8851	
Cubic	0.2243	0.3391	0.9417	0.2611	
Sp Quartic vs Quadratic	0.0952	0.4516	0.9452	0.8806	
Quartic vs Cubic	0.3391		0.9450		Aliased
Quartic vs Sp Quartic	0.4516		0.9450		Aliased

Highest polynomial showing the lowest p value (<0.05) along with highest Lack of Fit p-value (>0.1) was considered for model seleciton. Based on the criteria quadratic model was found to be best fit the observed responses. Special cubic and higher models were not suitable for prediction either due to low R-squared values and/or due to higher p value as compared to quadratic model. Quartic and higher models were aliased indicating the confounding of the model terms by the other implying that the predicted response would give the wrong idea of the actual response. **Table 6.12** below shows the ANOVA analysis of the suggested quadratic model.

Table 6.12 ANOVA for Quadratic Mixture Model

Source	Sum of Squares	df	Mean Square	F Value	p-value Prob > F	
Model	0.071	5	0.014	43.85	< 0.0001	significant
Linear Mixture	*0.047*	*2*	*0.023*	*72.14*	*< 0.0001*	
AB	*5.748E-003*	*1*	*5.748E-003*	*17.82*	*0.0010*	
AC	*0.014*	*1*	*0.014*	*43.02*	*< 0.0001*	
BC	*0.020*	*1*	*0.020*	*61.37*	*< 0.0001*	
Residual	4.195E-003	13	3.227E-004			
Lack of Fit	*2.591E-003*	*6*	*4.319E-004*	*1.89*	*0.2129*	*not significant*
Pure Error	*1.603E-003*	*7*	*2.290E-004*			

Cor Total	0.075	18				

The Model F-value of 48.85 implies the model is significant. There is only a 0.01 % chance that a "Model F-Value" this large could occur due to noise. Values of "Prob > F" less than 0.0500 indicate model terms are significant. In this case all main effects (A, B and C as indicated by linear mixture in the Table) are significant model terms showing that all the chosen factors have significant effect on particle size for given set of experimental conditions. Additionally, all the factors are involved in two way interactions with each other as shown by p value <0.0001 for interaction terms AB, AC and BC. Values greater than 0.1000 indicate the model terms are not significant. The "Lack of Fit F-value" of 1.89 and Lack of Fit *p* value of 0.2129 infer the Lack of Fit to be not significant relative to the pure error i.e. the selected model fits effectively to the observed experimental results and is effective in predicting responses all over the design matrix.

Table 6.13 Summary of ANOVA results for Quadratic Mixture Model

Std. Dev.	0.018	R-Squared	0.9440
Mean	0.23	Adj R-Squared	0.9225
C.V. %	7.81	Pred R-Squared	0.8865
PRESS	8.503E-003	Adeq Precision	18.534

Summary of ANOVA results for selected Quadratic Mixture model is shown in **Table 6.13**. The "Pred R-Squared" of 0.8865 is in reasonable agreement with the "Adj R-Squared" of 0.9225 i.e. <0.2. "Adequate precision" which is a measure of the signal to noise ratio is 18.534 indicating an adequate signal for the model to be used to nevigate the design space.
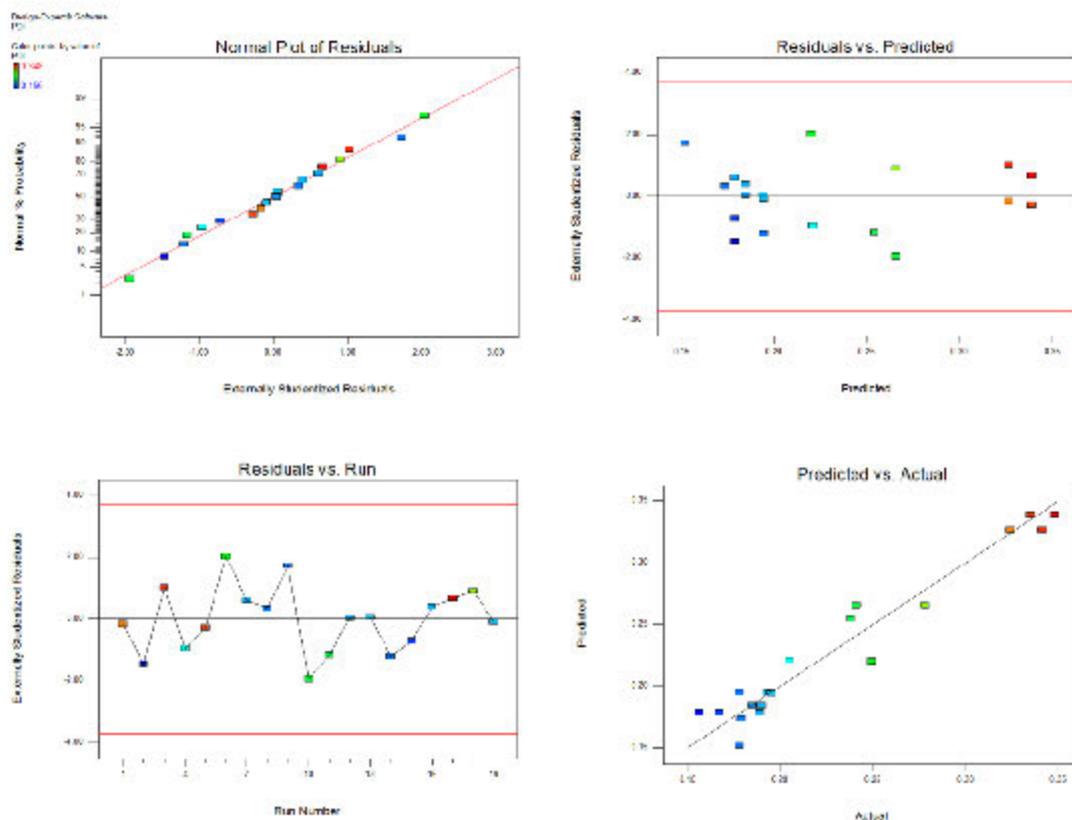
Model diagnostics

Figure 6.41 Model diagnostic plots

Various diagnostic plots for evaluation of the model are shown in **Figure 6.41**. The normal probability plot (normal plot of residuals) which shows whether the residuals follows a normal distribution or not and helps identify any specific patterns in the residuals indicative of requirement of transformations i.e. "S-shaped" curve, etc. normal plot for the current data show that data follows a straight line inferring the normal distribution of the residuals.

Residuals vs. predicted response (ascending values) plot tests if variance is distributed over the design constantly i.e. variance is not associated with the factor values as megaphone patterns (pattern like horn/ megaphone sign, <) which indicate either decreasing or increasing residuals with increasing the factor values. This is a plot of the residuals versus the ascending predicted response values.

193

Residual vs. run order plots the residuals against the experimental run order i.e. order in which the experiments have been carried out. The plot with a random scatter of residuals indicate there is no time dependent changes in the residuals, i.e. there is absence of any time dependent variable among the variables selected or among the variables which has been not included in the DoE. If there is such Random scattered plot of residuals in the current analysis indicate no association of residuals with time and absence of any time dependent variable.

Predicted vs. actual plot shows correlation between the observed response values and actual response values. A good correlation between the predicted and actual values (data following a straight 45° line) shows that the model chosen for analyses of data is appropriate in predicting the responses all over the design matrix. Also, this plot helps to detect a value/ values that are not easily predicted by the model. As it can be seen from the figure, plot follows a 45° straight line indicating close estimates of predicted values with actual values.
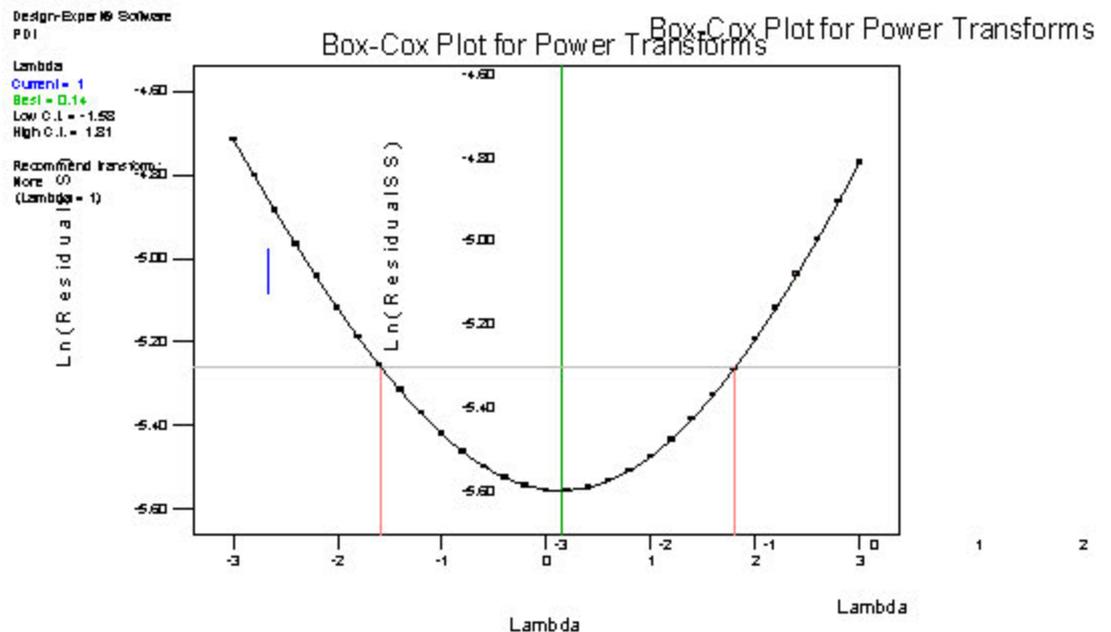

Figure 6.42 Box-Cox plot of power transformation

Box-Cox plot of Ln (residuals sum of squares) vs. λ curve for power transformation helps select any power transformation of observed response values required for fitting the model based on the best λ value and 95% confidence interval around it. Plot in **Figure 6.42** shows the λ value of 1, which lies near the best λ value and

within 95% confidence interval of it, indicating no requirement for any power transformation.
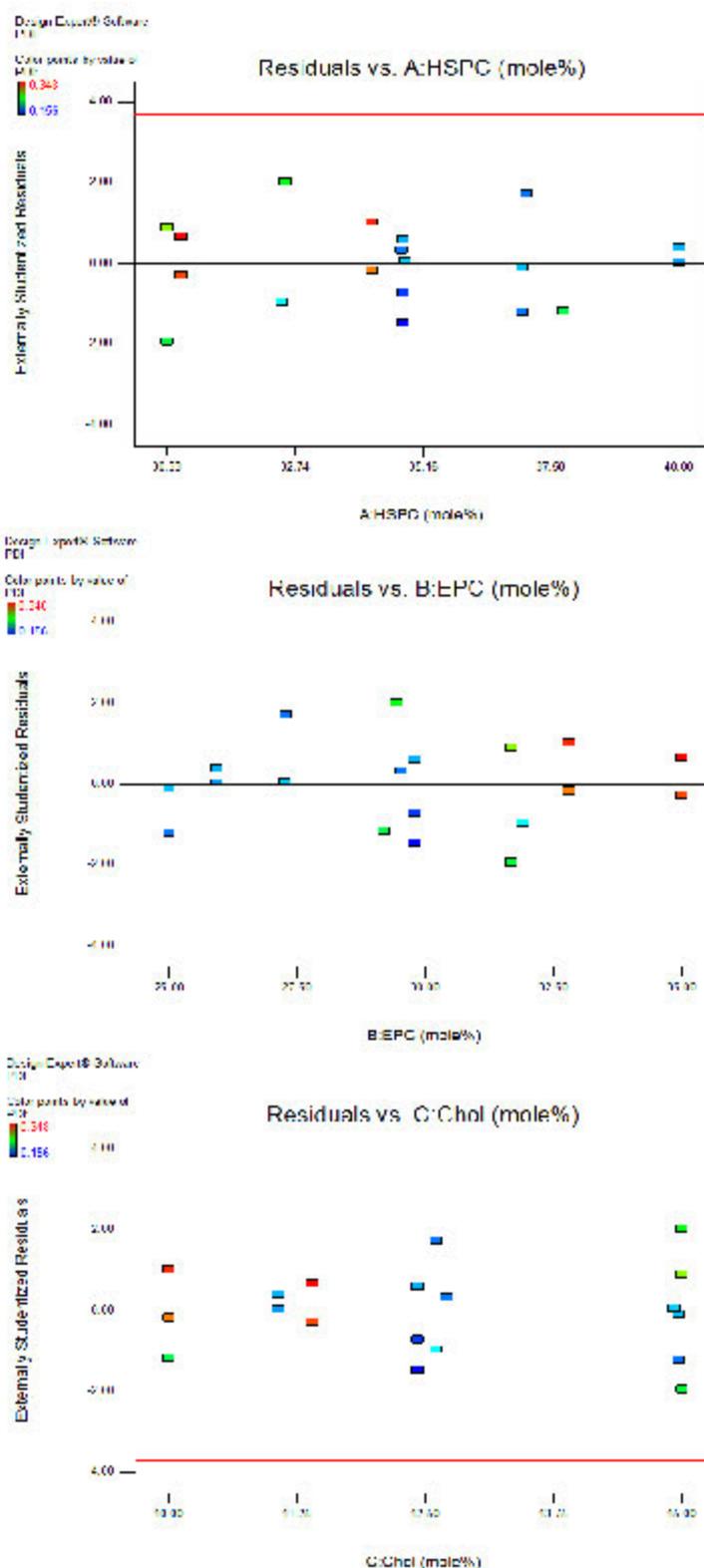

Figure 6.43 Residual vs. factor plots for determining the time-independence of variance

Plot of residuals vs. any factor evaluated if any association is there between the variance associated with different levels of factor i.e. any specific trends (+ve or −ve curvatures) associated with increasing level of each factor. As it can be seen from the **Figure 6.43**, plots for each factor shows a random scatter over the increasing levels of factors indicating that the model is effective in accounting for the variance for each factor.
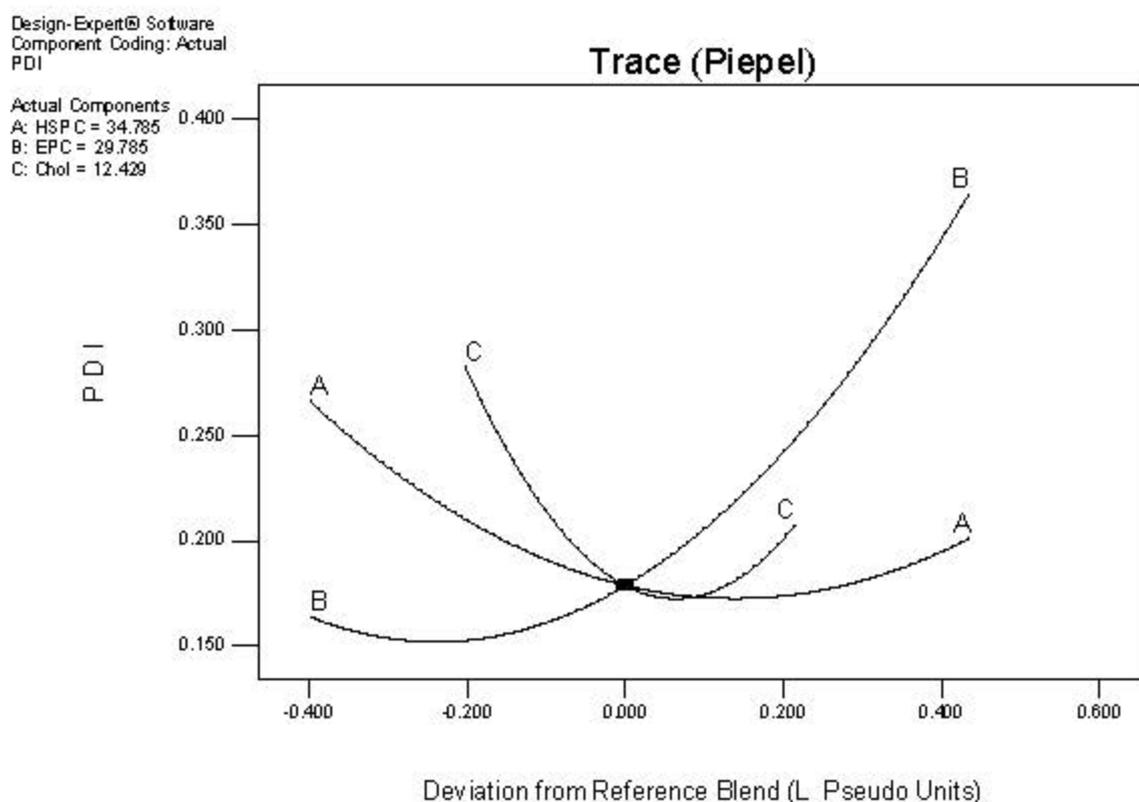
Effect of factors on response (PDI)

Figure 6.44 Piepel's plot

Piepel's plot is a trace plot showing the effect of individual factors plotting the pseudo limits of one component keeping the ratio of the changeable amounts of the each components kept constant against the response. The responses are plotted as deviations from the reference blend i.e. centroid (pseudo center point of the constrained design). As it can be seen from the **Figure 6.44**, EggPC is the factor with highest impact on PDI while HSPC and cholesterol has negative effects on the PDI producing lower values of PDI due to formation of monodisperse liposomes.
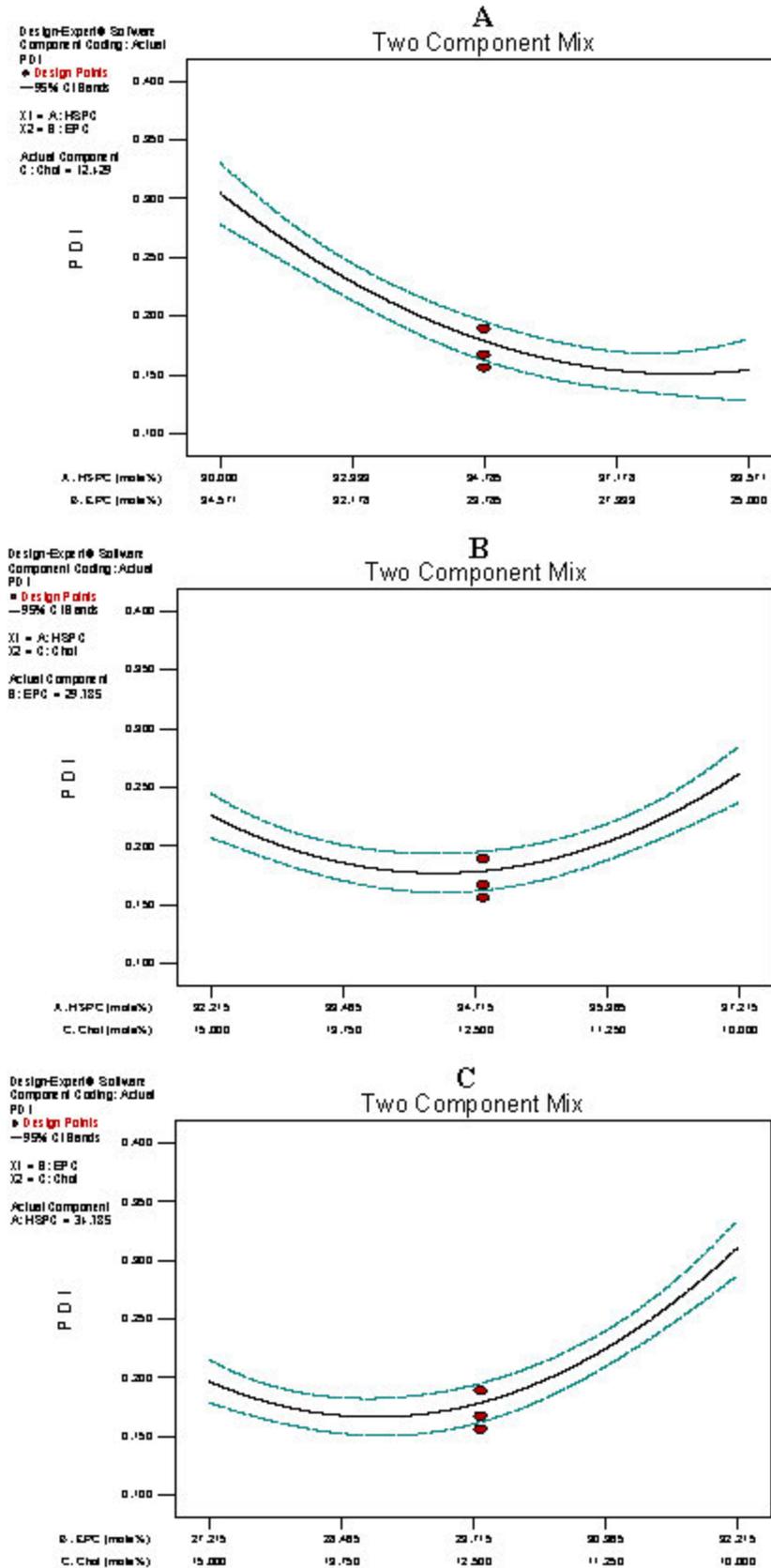
Figure 6.45 Two-component mixture plots; A: effect of HSPC and EPC, B: effect of HSPC and Chol, C: effect of EPC and Chol

Two component mix plots shows the combined effects of two components on the response keeping the value of another component constant at its centroid value. As it can be seen from the **Figure 6.45** A, as the ratio of HSPC:EPC increases i.e. mole% of HSPC increases and mole% of EPC decreases, PDI decreases. The same trend is seen with two component mix plots of EggPC and cholesterol where increasing mole% of EggPC leads to higher PDI. This can be explained by the formation of two liposomal species below 40 nm and above 90 nm due to presence of EggPC as described earlier. Figure 6.8 B shows effect of cholesterol and HSPC on PDI. What is noteworthy here is that, at a given level of EggPC, increasing the content of HSPC and/or decreasing content of cholesterol in liposomes has a moderate curvilinear effect shown by a moderate decrease initially followed by a slight rise in PDI. This is due to the presence of bilayer promoting effect of HSPC which compensates for the low amount of Cholesterol at high HSPC:Chol ratios and bilayer stabilizing property of cholesterol that compensates for relatively low amount of HSPC through promoting bilayer rigidity even in presence of higher levels of unsaturated phospholipids (EggPC and DOPE) as compared to saturated phospholipids (HSPC).

Additionally, considering the effect of HSPC and cholesterol separately in presence of EggPC, increasing mole% of HSPC as well as cholesterol leads to decrease in PDI values of liposomes which infer the presence of uniform sized liposomes with monomodal distribution. Noteworthy observation in the experimental results was that all the formulations with PDI values below 0.200 were having monomodal distribution while others with PDI above 0.200 represented a mix of monomodal, bimodal and sometimes trimodal distribution of particles. Hence, the primary aim of the optimization was to obtain a region in the design space where the particle size is as low as possible due to their desirability for the gene delivery and PDI value of <0.200 to have uniform monodisperse system of liposomes to confer a similar distribution kinetics in vivo.
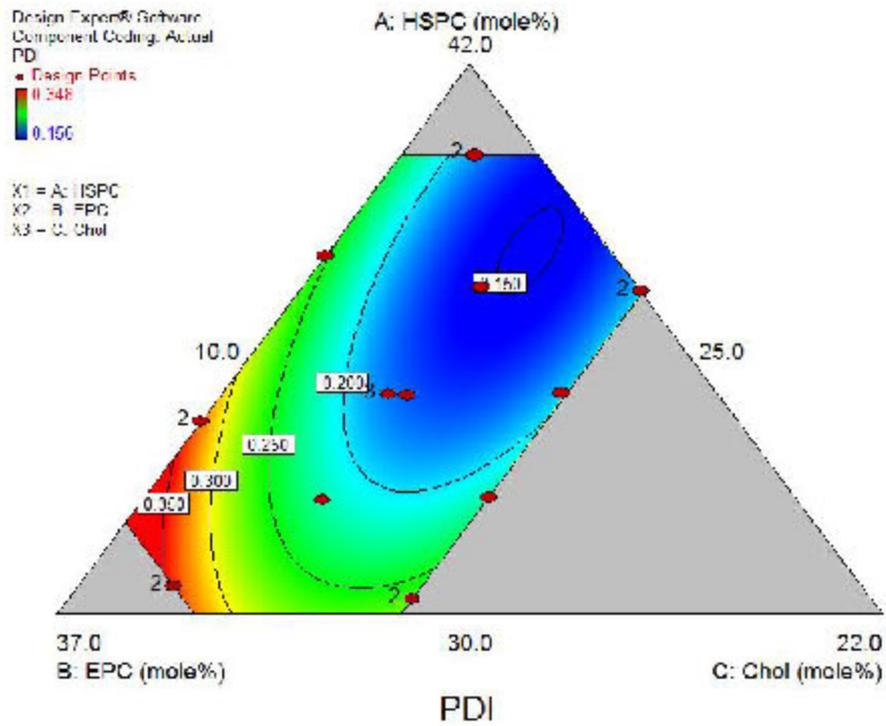
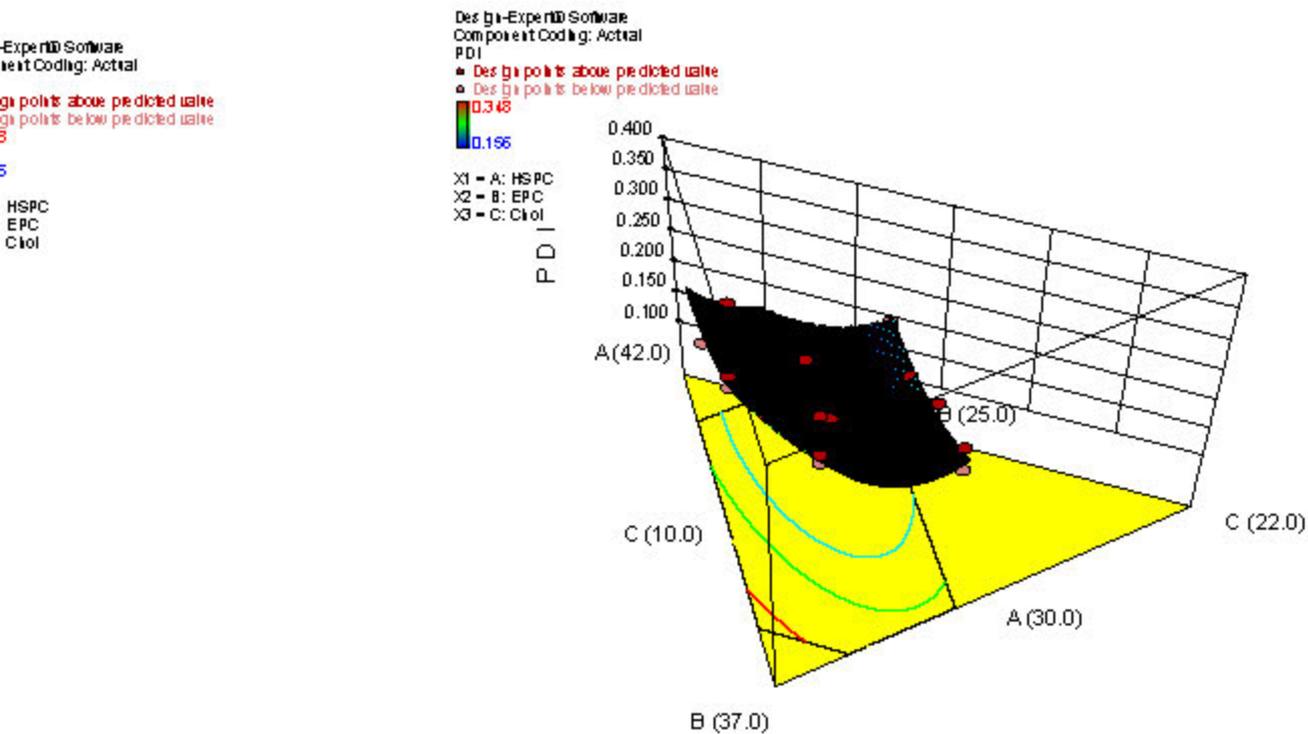**Figure 6.46 Contour plot of effects of different components on PDI**

Figure 6.47 Response surface plot of effects of different components on PDI

Contour plot (**Figure 6.46**) and response surface plot (**Figure 6.47**) show effects of all three components on the particle size. To summarize, with increasing mole% of EggPC causes decrease in the particle size while increase in the mole% of HSPC and Cholesterol in the mixture brings about an increase in the particle size. The effects can be explained with similar justifications mentioned under the two component mix plots.

Equation for prediction of particle size over design matrix

Equation for prediction of particle size within the design matrix is given below.

PDI=	
+0.046305	* HSPC
+0.095257	* EPC
+0.57145	* Chol
-2.21570E-003	* HSPC * EPC
-0.010488	* HSPC * Chol
-0.012268	* EPC * Chol

iii. Selection of Formulation Parameters

Constraints applied to select the best formulation parameters based on the desired particle size and polydispersity index (**Table 6.14**).

Table 6.14 Constraints Applied for Selection of Optimized Batch

Name	Goal (to be optimized)	Lower Limit	Upper Limit
HSPC (mole%)	in range	30.0	40.0
EPC (mole%)	in range	25.0	35.0
Chol (mole%)	in range	10.0	15.0
Particle size (nm)	to minimize	98.8	150.1
PDI	to minimize	0.156	0.348

All the affecting factors were to be optimized within the range choosen for design matrix. Particle size was to be optimized at the minimum value possible in the range observed experimentally (98.8-150.1 nm) and PDI was to be optimized at the minimum value possible in the experimentally observed range of 0.156-0.348. Surface plots (**Figure 6.48** A and B) show that the region with the lowest particle size doesn't coincide with the region with the lowest PDI which requiers a trade-off between the selected parameters for selection of an optimized batch. The optimization was based on the desirability criteria which makes the best trade-off between the constrains and selecting a combination which satisfies the criteria the best for optimizaiton and weighs the prediction based on a desirability index which ranges from 0 (for the least suited combination) to 1 (the best suited combination). The desirability plot which depicts the desirability index over the design is shown in **Figure 6.49** showing a flag where the optimized batch lies.
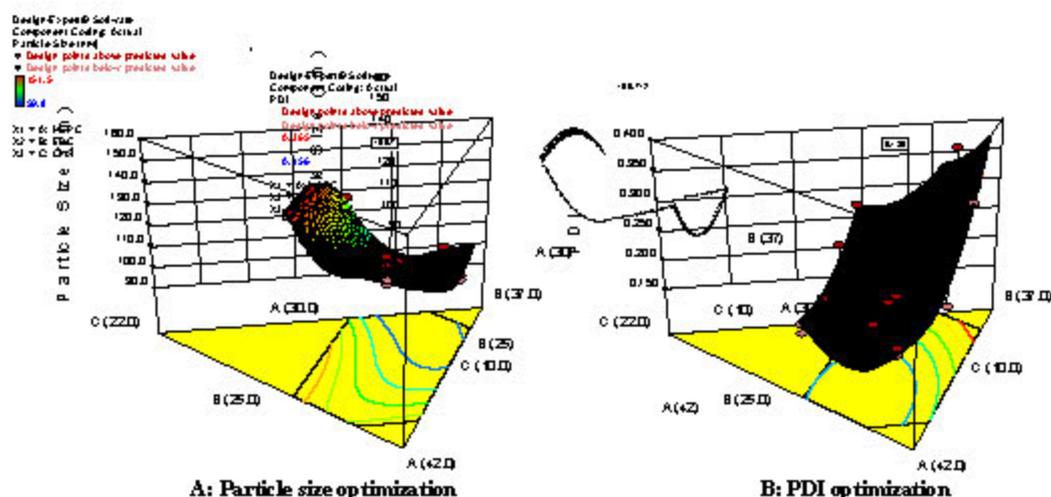

A: Particle size optimization   **B: PDI optimization**

Figure 6.48 Surface plots showing optimum particle size and PDI at best trade-off for the constraints
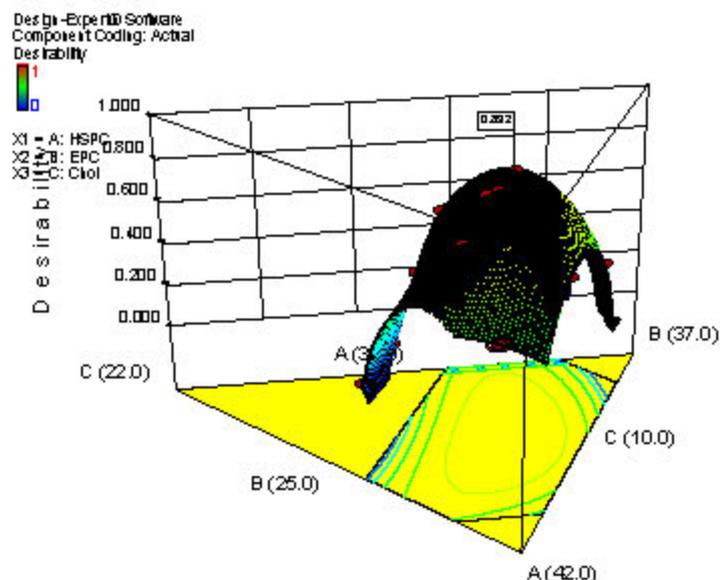
Figure 6.49 Desirability Plot for Selection of Optimized Batch

Based on the maximum desirability, one formulation (desirability 0.832) was found to best fit the selection constraints. Predicted responses of this batch were 109. 7 nm particle size and 0.186 PDI (**Table 6.15**).

Table 6.15 Optimized Batch Parameters Based on Desirability

HSPC	EPC	Chol	Particle Size	PDI	Desirability
35	28	14	106.7	0.206	0.892

Additionally, selection criteria was also applied in order to select the design space within the design matrix where desired formulation responses can be observed. The selection criteria were particle size range of 100-125 nm and PDI of 0.150-0.200 and based on these criteria, following design space was found (**Figure 6.50**).
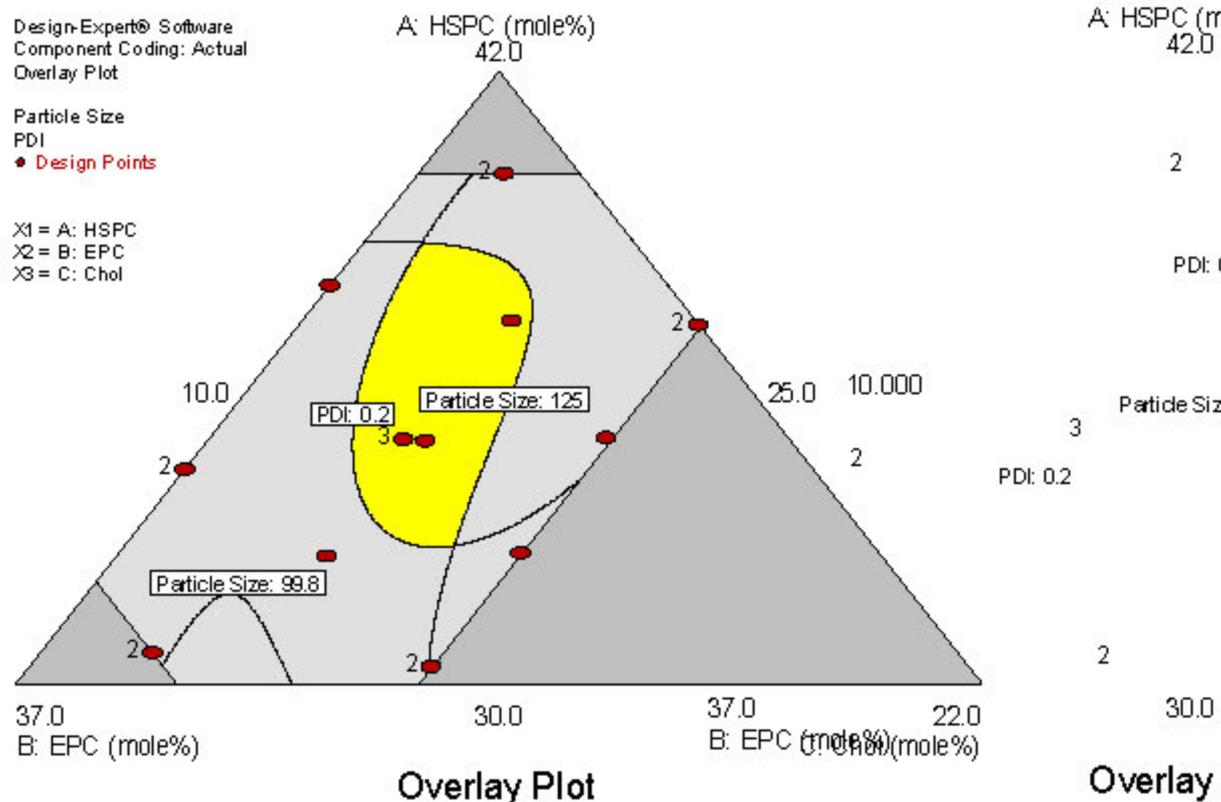
Figure 6.50 Design space with optimum response parameters

iv. Point Prediction and Confirmation:

Table 6.16 below shaows predicted response for the solution selected above along with the Stndard deviatoin, 95 % confidence interval and 95% tolerance interval of the response. Confirmation of the response was done by carrying out the experiment using the selected factor values in triplicate.

Table 6.17 shows and confirms that experimental and predicted values are in good agreement concluding the suitablity of the selected model for optimization.

Table 6.16 Predicted Responses of the Optimized Batch

Response	Predicted	Std Dev	95% CI* low	95% CI high	95% TI# low	95% TI high
Particle Size (nm)	106.7	3.8	104.2	113.3	92.0	127.4
PDI	0.206	0.022	0.166	0.206	0.084	0.288

* CI indicates Confidence Interval

\# TI indicates Tolerance Interval (99% of the population will be within this range for all future batches)

Table 6.17 Experimental Confirmation of the Predicted Responses

Response	Predicted	Std Dev	Experiental Mean	Std Dev
Particle Size (nm)	106.7	3.8	111.4	4.2
PDI	0.206	0.022	0.178	0.015

*Experiments were performed in triplicate.

Optimized batch obtained through DoE was further used for preparation of the liposomes of cationic DOPE with modified DSPE.

6.3.2.3 Preparation of liposomes of different modified lipids

Optimized formulation of stearyl amine and DSPE was used further for preparation of liposomes with modified lipids synthesized from DSPE. All formulations were prepared such as to have molar level of SA and modified lipids same in the lipid composition of bilayer i.e. 10 mole% and 20 mole% respectively. Prepared liposomes were evaluated for particle size distribution and zeta potential analyses. **Figure 6.51, Figure 6.52, Figure 6.53** and **Figure 6.54** show particle size distribution characteristics of the different optimized liposomes. The results are showed in Error! Reference source not f ound..

It was observed that all formulations demonstrated similar particle size characteristics. No significant differences in particle size were observed between the liposomes of SA-DSPE over liposomes prepared with modified lipids. However, the zeta potential distribution was different for all formulations which might be attributed to the differences in head-group size which extends over the surface of liposomes. In SA-DSPE liposomes, small head-group ($-NH_3^+$) of stearyl amine would be placed inside the liposome bilayer such that the it lies near to the phosphate group of DOPE where a partial local loss of surface charge would take place which would give zeta potential of 42.8±4.6 mV (8). Effect would also be there for the liposomes prepared of modified stearyl amines and zeta potentials shown would be due to the overall effect of modified head-group and DOPE in the liposomes.

Table 6.18 Particle size and Zeta potential characteristics of optimized liposomes and liposomes of modified DSPE

Liposomes/ Lipoplexes	Parameters		
	Particle size (z-average	PDI	Zeta potential

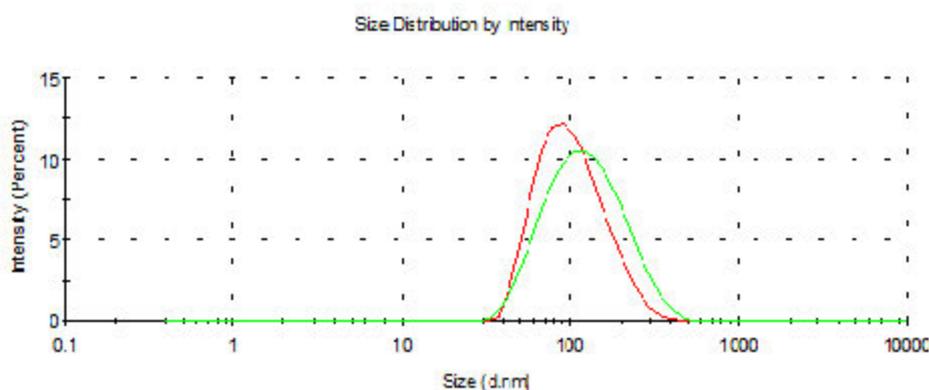|	diameter, nm)		(mV)
NSA-DSPE	93.7±9.7	0.245±0.036	50.6±3.7
DOPE/DSPE	111.4±4.2	0.178±0.015	-2.5±6.4
SA-DSPE	101.5±5.8	0.196±0.039	42.8±4.6
BHDSPE	106.5±12.2	0.216±0.020	39.2±3.8
HDSPE	101.4±16.2	0.200±0.052	36.7±3.5
BCDSPE	109.9±8.5	0.214±0.031	40.7±3.8
CDSPE	105.3±10.4	0.227±0.061	38.4±4.2
BADSPE	106.0±16.2	0.243±0.038	36.5±2.2
ADSPE	99.48±13.6	0.210±0.056	32.6±4.3
DOTAP	96.4±7.9	0.235±0.039	63.2±6.6

Figure 6.51 Intensity-weighted particle size distribution of non-PEGylated (Red) and PEGylated (Green) liposomes
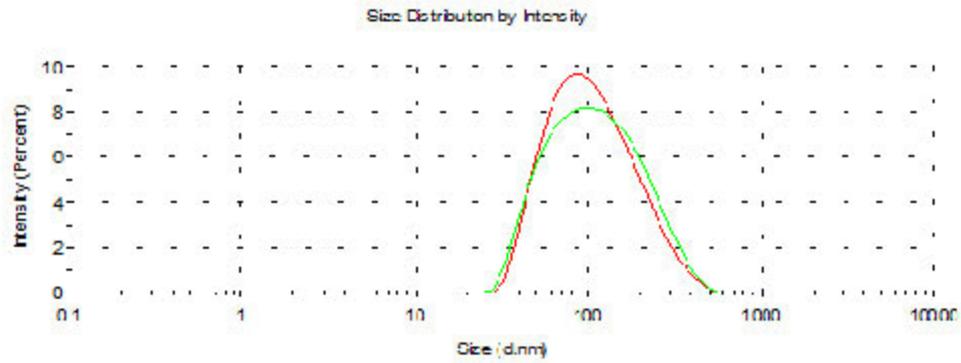
Figure 6.52 Intensity-weighted particle size distribution of HDS liposomes (Red) and BHDS liposomes (Green)
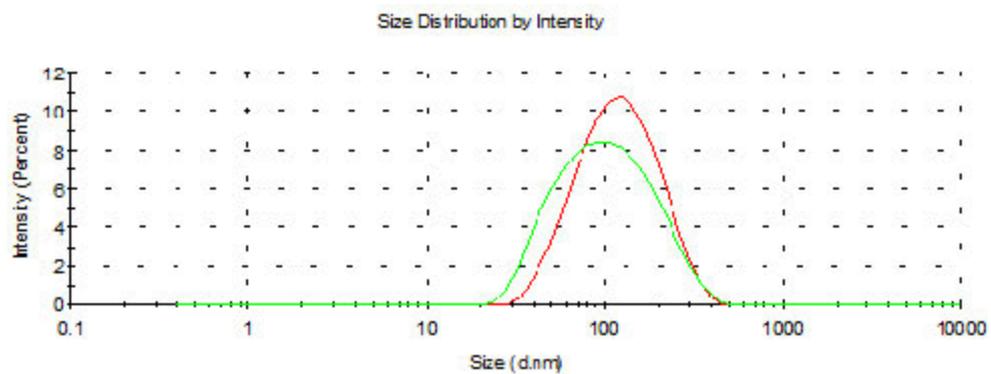

Figure 6.53 Intensity-weighted particle size distribution of BCDS liposomes (Red) and CDS liposomes (Green)
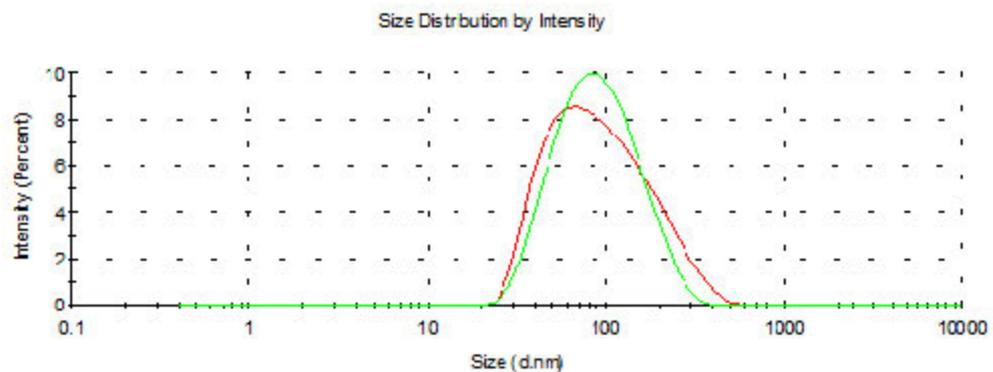

Figure 6.54 Intensity-weighted particle size distribution of ADS liposomes (Red) and BADS liposomes (Green)

6.3.3 Preparation of lipoplexes

Formulation and process parameters involved in the complexation of pDNA with cationic liposomes were also optimized. Process parameters were optimized for complexation of pDNA with DSPE liposomes. Optimization of formulation was done based on the complexation efficiency of lipoplexes. Liposomes with and without PEG$_{2000}$-DSPE were prepared and complexation efficiencies were evaluated. Liposomes were incubated with pDNA at different L/P molar ratios (ratio of moles of cationic lipid to moles of phosphates of pDNA) to optimize the complexation efficiency of lipoplexes.

6.3.3.1 Optimization of Process Parameters

Different process parameters involved in the preparation of lipoplexes were optimized initially. These process parameters included incubation temperature and incubation time. Complete retardation of pDNA on gel by lipoplexes was considered desired output parameter for selection of optimum process parameter. While keeping one factor constant, effect of another variable was observed on desired output parameters.

a) Incubation Time

Incubation time plays an important role in complete complexation of pDNA with liposomes. As the formulation was PEGylated, effect of incubation time needed to be evaluated initially for non-PEGylated liposomes mined to determine the L/P ratio that can completely retard pDNA on gel and also to have an idea of interference of PEG chains on time for complete complexation and complexation efficiency. Many reports suggest that incubation should be between 30 min at ambient temperature (25-27). On incubation period of 30 min and 45 minutes were chosen as a primary parameter to determine the complexation ratio of L/P ratio. It was observed that at both incubation temperatures, there were no differences in complexation efficiencies of lipoplexes and the complete retardation was observed at L/P ratio of 1.5 and higher (**Figure 6.55** and **Figure 6.56**).

Ratios of ≥1.5 was required for complete retardation of the pDNA which indicates that all the cationic amino groups are not available for the complexation of the pDNA. This might be attributed to the differential distribution of stearyl amine in the liposomal bilayer with some molecules being in the outer leaflet of the liposomes (which are actually available for the complexation) and some on the inner leaflet. The view is supported by the similar results explained in the literature (28). However, liposomes of monocationic lipids such as DOTAP, DSTAP etc. have been demonstrated in literature to show

complete retardation at even higher charge ratio i.e. N/P ratio of 2 which corresponds to L/P ratio of 2.0 for stearyl amine. The low L/P ratio (1.5) for stearyl amine liposomes can be justified by the reason that stearyl amine being a cationic lipid having a cone shaped structure (due to its critical packing parameter <0.5) would prefer the self-assembled structures which show positive curvature. Hence, it would show higher tendency to redistribute in the outer leaflet of the liposome which shows a positive curvature as compared to the negative curvature of the inner leaflet. Secondly, the complexation taking place between all the cationic amines of stearyl amines and incubated pDNA phosphates is not necessary to retard DNA on gel; rather, strong interactions among the few cationic charges separated effectively over the surface of liposomes and the pDNA molecule would be sufficient to retain strongly the pDNA in the lipoplex structure. This in turn indicates that low complexation efficiency at N/P ratio of 1.00 or even higher of the conventionally prepared lipoplexes which usually use liposomes prepared with 1:1 ratio of cationic lipid and supporting lipid is due to overlapped DNA molecules on the liposomes which has been clearly demonstrated by extensive increase in the size of the liposomes after complexation (27, 28). This is due to closely arranged cationic charges making the interaction between the DNA close to the charges stronger but distantly located pDNA phosphate groups having less strong ionic interaction.
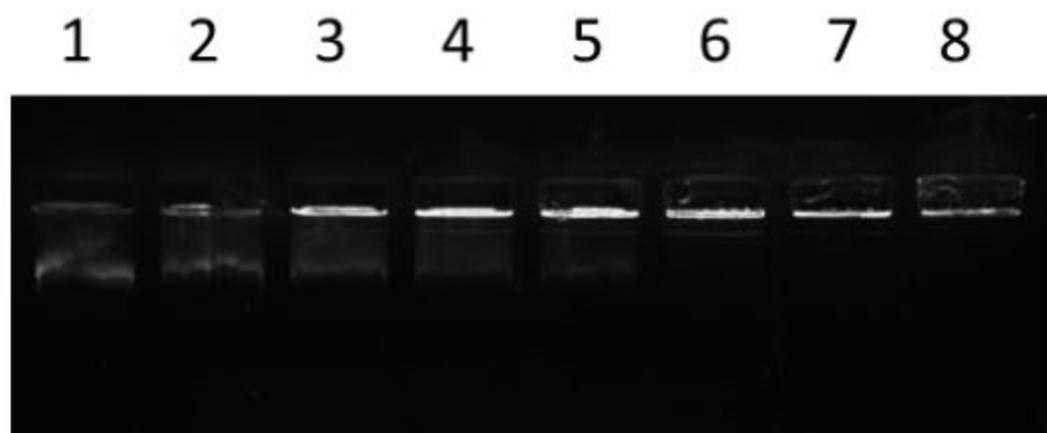

Figure 6.55 Complexation efficiency of non-PEGylated lipoplexes – 30 min incubation
(200 ng pDNA/well, SA/P ratio: Lane 1-naked, lane 2-0.25, lane 3-0.5, lane 4-0.75, lane 5-1, lane 6-1.5, lane 7-2, lane 8-4)
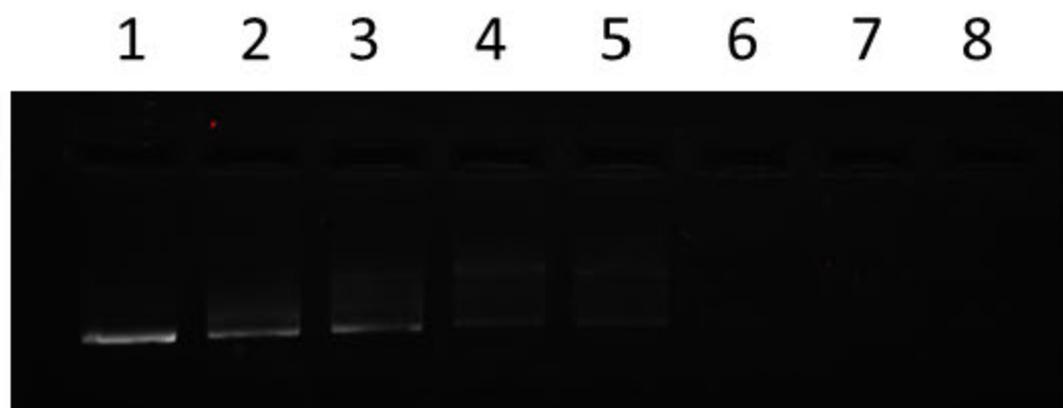
Figure 6.56 Complexation efficiency of non-PEGylated lipoplexes – 45 min incubation
(200 ng pDNA/well, SA/P ratio: Lane 1-naked, lane 2-0.25, lane 3-0.5, lane 4-0.75, lane 5-1, lane 6-1.5, lane 7-2, lane 8-4)

Based on the results obtained with non-PEGylated liposomes, PEGylated liposomes were incubated with pDNA at different L/P ratios for different incubation periods. It was observed that PEGylation affected the complexation efficiencies of liposomes (refer **Figure 6.57**, **Figure 6.58** and **Figure 6.59**). Results are tabulated in **Table 6.19** and as it can be seen with incubation period of 30 min which showed bands of pDNA even at L/P ratios of 1.5 and 2.0 and complete retardation was observed at L/P ratio of 4.0. With increasing incubation period, L/P ratio for complete retardation decreased i.e. L/P ratio of 2.0 at 45 min incubation and L/P ratio of 1.5-2.0 at 60 min incubation period. From this observation, L/P ratio required for complete complexation of pDNA was considered to be >1.5 and complete complexation at L/P ratio of 2.0 required 30 minutes for non-PEGylated liposomes and 60 minutes for PEGylated liposomes. The decreased complexation efficiency of pDNA with liposomes at lower incubation times might be due to hindrance of PEG chains on the surface of liposomes which would mask the cationic charge, however, the higher charge density of pDNA will force the pDNA molecule towards the liposome surface and allow it to overcome the barrier of the PEG chains to closely associate with the cationic amine groups of the SA.

Figure 6.57 Complexation efficiency of PEGylated lipoplexes 30 min incubation at 25°C
(200 ng pDNA/well, SA/P ratio: Lane 1-naked, lane 2-0.25, lane 3-0.5, lane 4-0.75, lane 5-1, lane 6-1.5, lane 7-2, lane 8-4)

Figure 6.58 Complexation efficiency of PEGylated lipoplexes 45 min incubation at 25°C
(200 ng pDNA/well, SA/P ratio: Lane 1-naked, lane 2-0.25, lane 3-0.5, lane 4-0.75, lane 5-1, lane 6-1.5, lane 7-2, lane 8-4)
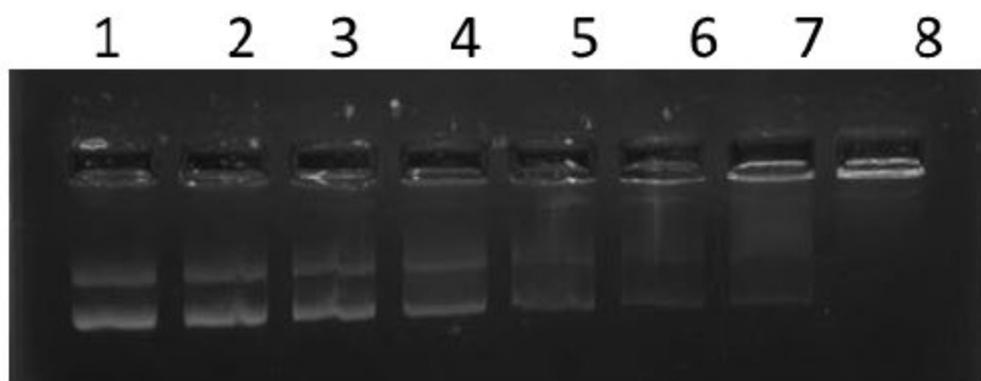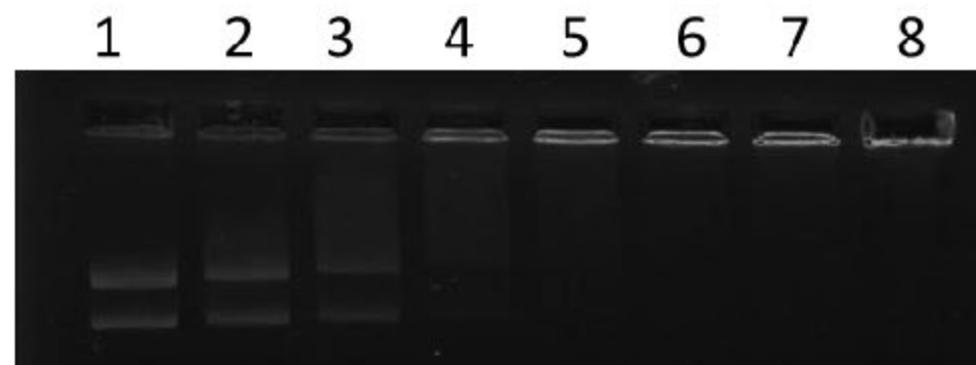

Figure 6.59 Complexation efficiency of PEGylated lipoplexes 60 min incubation at 25°C
(200 ng pDNA/well, SA/P ratio: Lane 1-naked, lane 2-0.25, lane 3-0.5, lane 4-0.75, lane 5-1, lane 6-1.5, lane 7-2, lane 8-4)
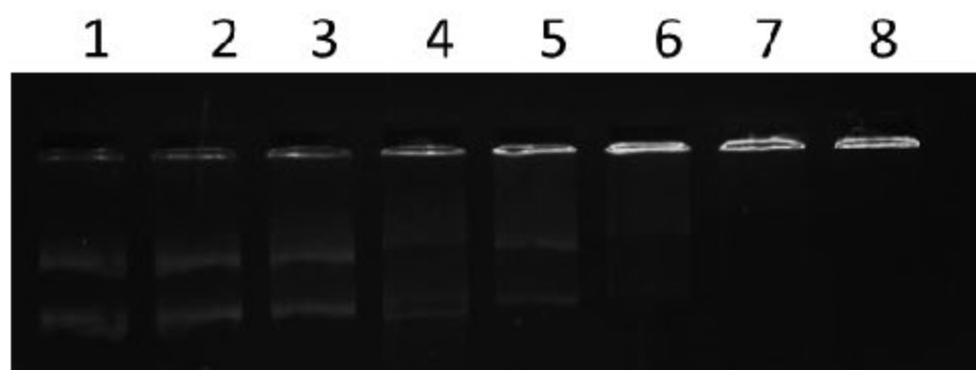
Table 6.17 Experimental Confirmation of the Predicted Responses

Formulation	Incubation Time (min)	L/P ratio	% pDNA complexed#
Effect of Incubation Time (at 25°C)			
Non-PEGylated liposomes	30 min	0.5	48.63±8.24
		0.75	66.72±5.36
		1	91.34±6.42
		1.5	95.3±4.63
		2,4	>98.8%
	45 min	0.5	44.55±6.72
		0.75	71.53±2.39
		1	96.45±4.23
		1.5	>98.8%
		2,4	>98.8%
PEGylated liposomes	30 min	0.5	19.52±9.50
		1	47.63±8.61
		1.5	66.51±5.18
		2	86.58±4.71
		4	98.47±2.48
	45 min	0.5	30.25±5.65
		1	54.41±4.18
		1.5	68.25±5.60
		2	98.88±2.39
		4	99.70±2.00
	60 min	0.5	38.80±4.16
		1	75.12±4.45
		1.5	95.20±2.10
		2	98.50±2.73

Formulation	Incubation temperature (°C)	L/P ratio	% pDNA complexed
		4	99.29±2.08
Effect of incubation temperature (at 30 min incubation period)			
PEGylated liposomes	25°C	0.5	20.56±7.41
		1	51.63±7.05
		1.5	66.55±5.26
		2	86.52±4.79
		4	98.20±2.50
	37°C	0.5	28.52±6.40
		1	66.26±5.16
		1.5	82.10±3.70
		2	95.71±4.60
		4	98.79±2.45
	45°C	0.5	36.65±8.95
		1	76.92±8.60
		1.5	93.15±6.80
		2	98.41±3.42
		4	99.60±1.90

[#]All Experiments were performed in triplicate.

b) Incubation temperature

In order to investigate the effect of temperature on complexation efficiency of lipoplexes, PEGylated lipoplexes were incubated with pDNA at different temperatures i.e. at room temperature 25°C±2°C and 37°C±2°C temperature and 45°C±2°C temperature for 30 min period. It was observed that for a particular incubation period, temperature affected the complexation efficiency of liposome (**Figure 6.57**, **Figure 6.60** and **Figure 6.61**; refer **Table 6.19** for complexation efficiencies). For 30 min incubation, the complexation efficiency at any L/P ratio was decreasing in the order of incubation temperature of

45°C>37°C>25°C. This might be attributed to the increased mobility of pDNA molecules rendering the flexibility in the pDNA structure to approach the cationic surface. Also, increasing temperature will increase the movement of PEG chains extending on the surface of liposomes which will allow closer approach of the pDNA nearer to the cationic charge bypassing the PEG chains. Secondly, it can be concluded from the study that at lower temperatures and lower incubation times, the drags of pDNA seen in the gel even at higher L/P ratios would be due to the pDNA located over the surface of liposomes at outer end of the PEG chains which will get delodged from the surfaces on application of voltage. However, as it can be seen from the images of gel incubated at 37°C and 45°C, even naked DNA is not showing clearly demarcated bands rather bands with drags indicating that the structure of DNA is changed on exposure to temperature."

Figure 6.60 Complexation efficiency of PEGylated lipoplexes – 30 min incubation at 37°C
(200 ng pDNA/well, SA/P ratio: Lane 1-naked, lane 2-0.25, lane 3-0.5, lane 4-0.75, lane 5-1, lane 6-1.5, lane 7-2, lane 8-4)
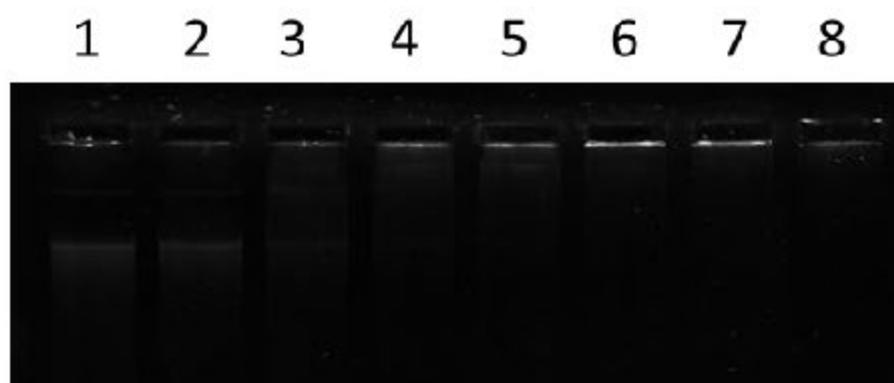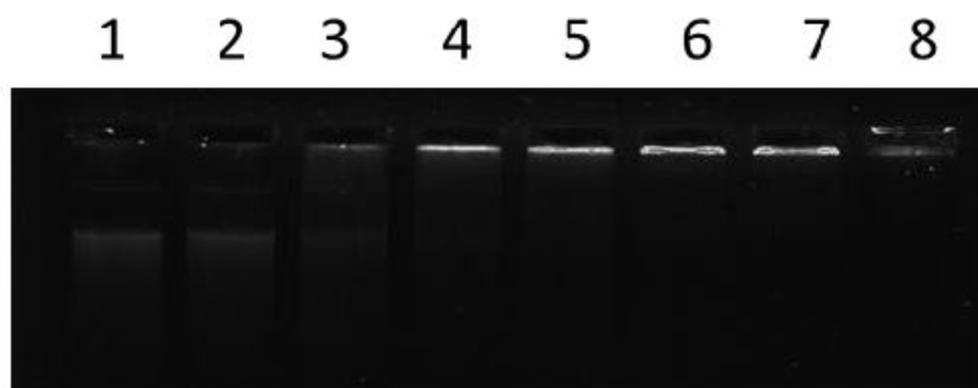

Figure 6.61 Complexation efficiency of PEGylated lipoplexes – 30 min incubation at 45°C
(200 ng pDNA/well, SA/P ratio: Lane 1-naked, lane 2-0.25, lane 3-0.5, lane 4-0.75, lane 5-1, lane 6-1.5, lane 7-2, lane 8-4)

Based on the observations of effect of temperature and incubation period on complexation efficiencies, temperature of 25°C was considered for further development in order to avoid high temperature exposure of pDNA as well as formulation and incubation period of ≥60 minutes was considered to allow for the maximum complexation at 25°C temperature.

6.3.3.2 Optimization of Formulation Parameters

Optimization of the formulation parameters was done by determining the complexation efficiency in terms of ratio of moles of stearyl amine-DSPE to moles of phosphate of pDNA (L/P ratio). Complexation efficiencies of liposomes prepared with different lipids synthesized from DSPE were determined at different L/P ratios. To have a comparative evaluation of complexation efficiency of synthesized lipids against stearyl amine and DOTAP based liposomes, complexation efficiencies of lipoplexes prepared at different L/P ratios were also investigated. DOTAP and DOPE were taken in 1:1 mole ratios at concentration equivalent to the concentration of SA-DSPE or lipids synthesized from DSPE on molar basis so as to have equimolar concentration of cationic lipids in the formulation i.e. 0.0011132 mmoles of cationic lipids in 2 mL of formulation. DOTAP/DOPE lipoplexes were prepared by the same procedure as employed in preparation of DSPE lipoplexes. Briefly, DOTAP and DOPE were taken in a RBF followed by preparation of thin film by solvent evaporation using chloroform and methanol (3:1) as solvent at 45°C on rotary evaporator under vacuum, followed by hydration to form liposomes at 55°C and subsequent size reduction by extrusion.

All prepared lipoplexes were prepared at L/P ratio of 0.25, 0.50, 0.75, 1.00, 1.5, 2.00 and 4.00. Complexation efficiencies were determined at each N/P ratio by gel electrophoresis, UV spectrophotometric assay and QuantiFlour fluorimetric assay. Gel electrophoresis images obtained with different lipoplex formulations are shown from **Figure 6.62** to **Figure 6.69** and complexation efficiencies are reported in the **table 6.20.**

Table 6.20 Optimization of formulation parameters – L/P ratio optimization for different PEGylated liposomes

Liposomes	L/P ratio	Complexation efficiency (% pDNA complexed)		
		Gel electrophoresis	UV-spectrophotometry	QuantiFlour assay
SA-DSPE	0.25	18.32±5.91		
	0.50	37.85±4.96	40.25±3.52	40.25±4.15
	0.75	60.14±3.48		
	1.00	76.15±2.45	78.74±2.52	77.55±2.75
	1.50	98.12±2.10		
	2.00	99.12±2.75	99.45±1.23	99.62±1.05
	4.00	99.20±2.98		
BHDSPE	0.25	21.01±4.25		
	0.50	45.36±5.81	48.85±2.45	48.24±2.15
	0.75	78.25±4.51		
	1.00	97.75±2.96	98.41±2.15	98.80±1.02
	1.50	98.42±3.58		
	2.00	98.98±1.29	99.15±2.14	99.14±0.91
	4.00	100.01±2.12		
HDSPE	0.25	45.35±5.14		
	0.50	96.88±3.65	98.44±3.25	98.42±1.25
	0.75	98.75±3.14		
	1.00	98.64±1.58	98.52±2.21	98.75±2.10
	1.50	98.25±2.56		
	2.00	101.02±2.19	98.59±1.52	99.41±1.11
	4.00	99.91±2.12		

Liposomes	L/P ratio	Complexation efficiency (% pDNA complexed)		
		Gel electrophoresis	UV-spectrophotometry	QuantiFlour assay
BCDSPE	0.25	19.52±4.52		
	0.50	43.58±5.45	48.25±3.14	45.58±2.85
	0.75	74.52±3.75		
	1.00	96.74±3.16	98.45±2.41	99.25±1.40
	1.50	98.20±2.91		
	2.00	98.35±1.85	100.29±1.03	99.15±1.32
	4.00	99.41±2.01		
CDSPE	0.25	49.25±4.20		
	0.50	97.52±1.85	99.65±2.15	98.65±3.54
	0.75	99.24±2.52		
	1.00	99.08±1.81	100.51±0.93	99.45±1.36
	1.50	98.94±2.09		
	2.00	99.12±2.85	99.56±2.18	99.11±2.45
	4.00	100.91±2.36		
BADSPE	0.25	24.56±2.95		
	0.50	56.45±4.85	53.26±2.58	52.95±1.52
	0.75	75.36±6.42		
	1.00	96.48±3.25	98.45±1.58	97.92±1.19
	1.50	98.85±3.21		
	2.00	99.76±1.98	98.79±1.90	99.19±2.01
	4.00	99.49±2.24		
ADSPE	0.25	52.14±4.21		
	0.50	99.12±3.10	99.10±2.51	98.75±1.49

Liposomes	L/P ratio	Complexation efficiency (% pDNA complexed)		
		Gel electrophoresis	UV-spectrophotometry	QuantiFlour assay
	0.75	98.45±2.95		
	1.00	99.15±3.14	100.09±1.59	99.02±1.19
	1.50	100.14±1.52		
	2.00	99.52±3.68	100.10±2.08	99.16±0.97
	4.00	100.62±2.58		
	0.50	32.75±3.85		
	0.75	62.14±4.01		
	1.00	78.05±3.36	76.81±2.95	79.25±2.18
DOTAP/DOPE	1.25	91.86±4.75		
	1.50	96.56±2.85	81.74±1.29	79.21±2.07
	2.00	98.79±3.10	99.45±1.09	98.91±1.23
	4.00	99.20±1.71		

Experiments were performed in triplicate

In case of DOTAP/DOPE lipoplexes, complete retardation required L/P ratio higher than 1.50. This view is consistent with the results reported in literature which showed complete retardation on gel of DNA at L/P ratio of 1.50 and higher (which corresponds to their N/P ratios of 1.50 and higher). The results corroborate with the results cited in the literature (28, 29). This is due to the electrostatic interaction of pDNA with the external surface of the liposomes and hence, as supported by the external model of DNA binding to cationic liposomes, cationic lipid molecules located on the outer layer of the bilayer are involved in the complexation with DNA (30). In case of cationic liposomes of stearyl amine-DSPE the same hypothesis would apply and can be justified by the explanation given in optimization of process.

For modified DSPE molecules, BHDSPE, BCDSPE and BADSPE are singly charged cationic molecules while HDSPE, CDSPE and ADSPE are doubly charged

molecules, with histidine, guanidine and arginine being the cationic groups. BHDSPE is having an imidazole ring which bears a positive charge at physiological pH due to its pKa between 6-7. However, considering the effect of pH of 6.5-7.0 which is observed for autoclaved double distilled water, ionization range of 25.3-51.7% can be considered for the lipid having imidazole ring of histidine. This indicated that, at physiological pH, %ionization will become even lower for the lipids having pKa of 6-6.5. According to the anticipated %ionization, complexation efficiency was expected to be lower for lipids with Boc protected 1° amine groups. However, as it can be seen from the gel electrophoresis results, complexation efficiency were similar for lipoplexes with HDSPE liposomes which are having a free 1° amine group and one ionizable imidazole nitrogen with respect to their N/P ratio i.e. L/P ratio of 0.5 corresponds to the N/P ratio 1.0 for HDSPE liposomes and L/P ratio of 1 corresponds to the N/P ratio of 1.0 for BHDSPE liposomes. This is due to the induction of ionization of histidine moieties by pDNA which causes local microenvironmental pH reduction due to it highly ionization phosphate groups with pKa of 1.569 (for internucleotide phosphate groups) and 1.5 and 6.5 (for terminal phosphate groups). This means DNA phosphate groups are essentially completely ionized at pH above 4.5 (3 pH units above pKa, >99.9% ionized) (31). The ionization potential of pDNA is so strong the pH around the DNA molecule is 3 pH units lower than the bulk of the pH (32). This would induce complete ionization of the histidine rings of the BHDSPE molecules as well as and HDSPE molecules. However, in case of HDSPE lipoplexes availability of equimolar quantity of 1° amine for complexation will neutralize the DNA charge rendering the remaining histidine residues retain their pH dependent ionization characteristic. Additionally, the results also explain the availability of all the cationic charges for complexation which can be explained by the relative distribution of the cationic lipid in the outer leaflet of the liposomes. As explained earlier for stearyl amine, lowered packing parameter for the modified DSPE can be expected due to increase in the head-group size which would be more favoured for their localization in the outer leaflet of the lipid bilayer. This in turn would account for more availability of cationic charge on the outer surface of the liposomes. Combined effect of pDNA induced ionization as well as more availability of cationic charge on the outer leaflet support the complexation efficiency results of the liposomes.

Nevertheless, in order to have a strong ionic interaction and stability in vivo, N/P ratio of 2 i.e. L/P ratio of 2 for BHDSPE lipoplexes and L/P ratio of 1 for HDSPE

lipoplexes have been used for further in vivo studies. Same fundamentals explain the complexation of the BCDSPE and CDSPE lipoplexes which are similar to BHDSPE and HDSPE lipoplexes except for the difference in the head-group which is larger for carnosine based lipoplexes as compared to histidine based lipoplexes. As anticipated from the structures, large head-group was anticipated to provide better complexation as compared to small head-group, however, no differences in the complexation efficiencies were observed.

In case of BADSPE and ADSPE lipoplexes, the complexation efficiencies followed similar trends as that of BHDSPE and HDSPE lipoplexes, respectively. The guanidinium group of the arginine which has ionization pKa of 12.2 and primary amine group which has pKa of 8.6 show that, for both lipoplexes, guanidinium group will be completely ionized at pH below 9 and >97% of primary amine will be ionized at the pH used for complexation. This was extrapolated to the experimental complexation values as well which showed complete complexation of pDNA at L/P ratio of 1 for BADSPE lipoplexes and L/P ratio of 0.5 for ADSPE lipoplexes. One generalization is made is for the amine of stearyl amine playing role in complexation of pDNA. Though, its molar amount is calculated for considering the moles of lipid being complexed to moles of pDNA, its contribution in the ratio L/P or N/P is taken as constant and not taken into account.
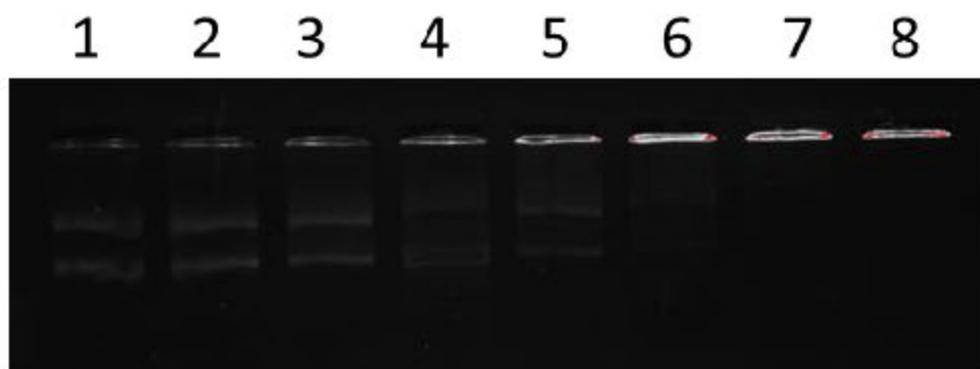

Figure 6.62 Complexation efficiency of Non-PEGylated lipoplexes
(200 ng pDNA/well, L/P ratio: Lane 1-naked, lane 2-0.25, lane 3-0.5, lane 4-0.75, lane 5-1, lane 6-1.5, lane 7-2, lane 8-4)

Figure 6.63 Complexation efficiency of PEGylated lipoplexes – 60 min incubation (200 ng pDNA/well, SA/P ratio: Lane 1-naked, lane 2-0.25, lane 3-0.5, lane 4-0.75, lane 5-1, lane 6-1.5, lane 7-2, lane 8-4)
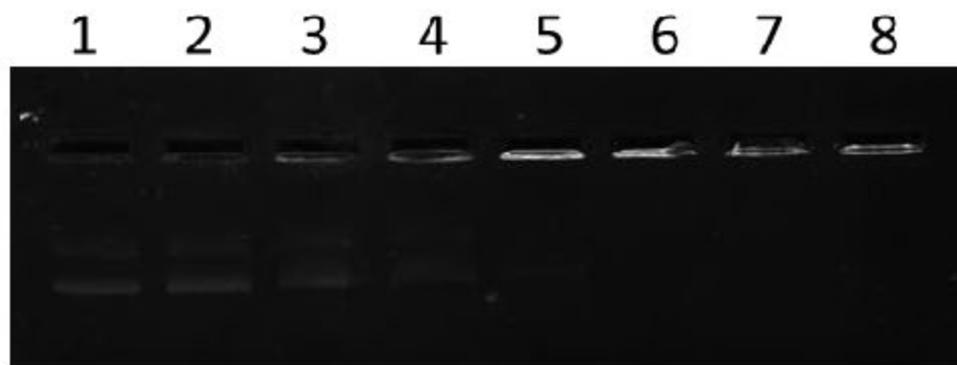

Figure 6.64 Complexation efficiency of BHDSPE lipoplexes (200 ng pDNA/well, L/P ratio: Lane 1-naked, lane 2-0.25, lane 3-0.5, lane 4-0.75, lane 5-1, lane 6-1.5, lane 7-2, lane 8-4)

Figure 6.65 Complexation efficiency of HDSPE lipoplexes (200 ng pDNA/well, L/P ratio: Lane 1-naked, lane 2-0.25, lane 3-0.5, lane 4-0.75, lane 5-1, lane 6-1.5, lane 7-2, lane 8-4)

Figure 6.66 Complexation efficiency of BCDSPE lipoplexes
(200 ng pDNA/well, L/P ratio: Lane 1-naked, lane 2-0.25, lane 3-0.5, lane 4-0.75, lane 5-1, lane 6-1.5, lane 7-2, lane 8-4)

Figure 6.67 Complexation efficiency of CDSPE lipoplexes
(200 ng pDNA/well, L/P ratio: Lane 1-naked, lane 2-0.25, lane 3-0.5, lane 4-0.75, lane 5-1, lane 6-1.5, lane 7-2, lane 8-4)
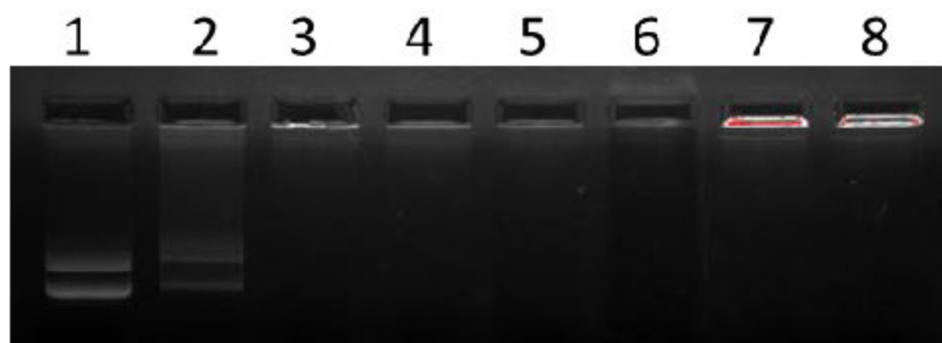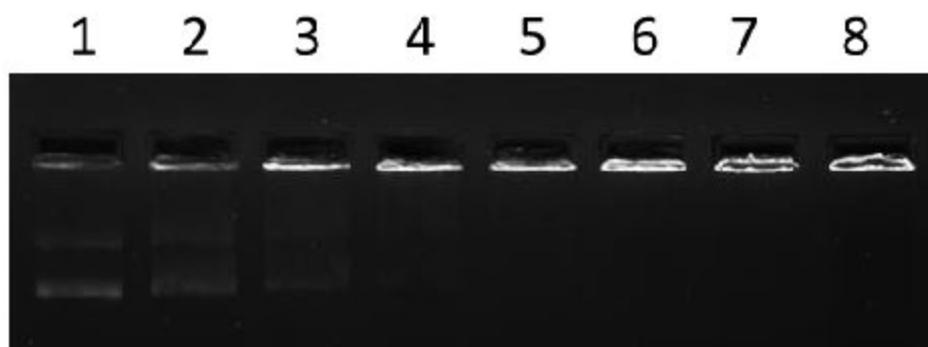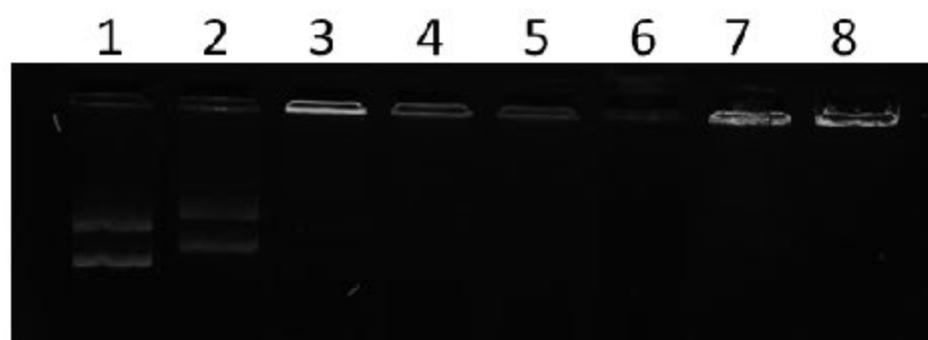

Figure 6.68 Complexation efficiency of BADSPE lipoplexes
(200 ng pDNA/well, L/P ratio: Lane 1-naked, lane 2-0.25, lane 3-0.5, lane 4-0.75, lane 5-1, lane 6-1.5, lane 7-2, lane 8-4)
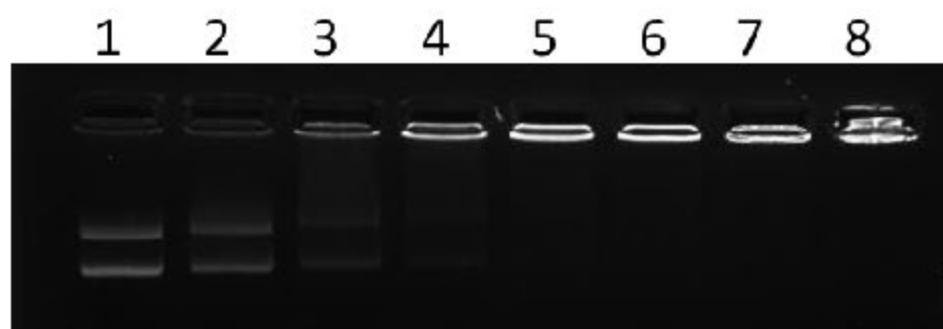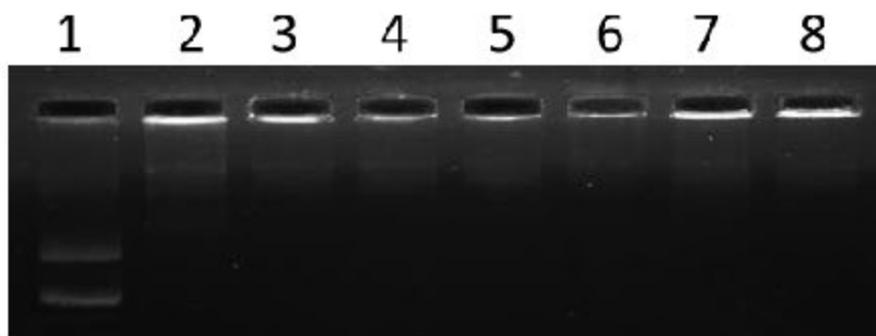
Figure 6.69 Complexation efficiency of ADSPE lipoplexes
(200 ng pDNA/well, L/P ratio: Lane 1-naked, lane 2-0.25, lane 3-0.5, lane 4-0.75, lane 5-1, lane 6-1.5, lane 7-2, lane 8-4)

6.3.3.3 Physicochemical characterization of the lipoplexes

Lipoplex formulations prepared at L/P ratio of 2.00 for SA-DSPE, BHDSPE, BCDSPE, BADSPE and DOTAP lipoplexes and at L/P ratio of 1.00 for HDSPE, CDSPE and ADSPE lipoplexes were evaluated further for physicochemical properties. L/P ratios were chosen to attain the N/P ratio of 2.00 which helps in making comparisons of the physicochemical properties of the lipoplexes as well as in vitro and in vivo outcomes of the lipoplexes.

a) Assay of the pDNA content of the lipoplex preparation

Lipoplexes were assayed for pDNA content to see if any loss of pDNA occurs during the preparation steps. Assay was performed by UV spectrophotometry and spectrofluorometric assay. Results are shown in Table. Results demonstrate that there is no loss of pDNA during the processing of the formulation. All formulations showed pDNA content within 5% boundary of pDNA content i.e. within 95.00-105.00%. Additionally, results of both the analysis method corroborate with each other (**Table 6.21**).

Table 6.21 Assay of different liposomal formulations

Lipoplex formulation	Assay (%pDNA)	
	UV spectrophotometry	QuantiFluor® Assay
SA-DSPE	99.80±2.78	99.95±1.29
BHDSPE	98.60±3.16	99.41±2.09
HDSPE	99.79±3.62	100.11±0.85

BCDSPE	100.21±1.99	100.85±1.95
CDSPE	100.05±3.01	99.87±1.65
BADSPE	99.86±3.58	101.01±2.13
ADSPE	99.45±2.15	100.36±1.54
DOTAP	99.31±4.00	100.69±2.41

b) Complexation efficiencies of lipoplexes

Complexation efficiencies of lyophilized lipoplexes were determined by UV spectrophotometry and spectrofluorometry after ultracentrifugation of the samples. Complexation efficiencies of lipoplexes prepared at L/P ratio of 2.00 are given in the **Table 6.22**. There was no significant change in the complexation efficiencies of lipoplexes after lyophilization indicating that the cryoprotectant-bulking agent (sucrose), the freezing process and the drying cycles did not affect the electrostatic interaction between the liposomes and pDNA.

Table 6.22 Effect of lyophilization on complexation efficiencies of lipoplexes

Lipoplex formulation	Complexation efficiency (%) Before lyophilization	
	UV spectrophotometry	QuantiFluor® Assay
SA-DSPE	99.40±1.31	99.74±1.29
BHDSPE	99.05±2.20	99.26±0.87
HDSPE	98.74±1.58	99.40±1.26
BCDSPE	100.30±1.15	99.26±1.35
CDSPE	99.41±2.20	99.18±2.40
BADSPE	98.87±1.95	99.27±2.41
ADSPE	100.23±2.22	99.12±0.90
DOTAP	99.48±1.12	98.90±1.21

c) Particle size and zeta potential of lipoplexes

Particle size and zeta potential results of lipoplexes are shown in the **Table 6.23** below. The results show that all lipoplexes maintained their particle size during the lyophilization and were strongly cationic charged with positive zeta potential values. Particle size was affected at a minimal extent by the freeze-drying process. Additionally, no effect on the zeta potential values indicates the maintenance of the electrostatic characteristic of the lipoplexes during the lyophilization process.

Table 6.23 Particle size and Zeta potential characteristics of optimized liposomes and their lipoplexes

Liposomes/ Lipoplexes	Liposomes			Lipoplexes (N/P ratio of 2)		
	Particle size (z-average diameter, nm)	PDI	Zeta potential (mV)	Particle size (z-average diameter, nm)	PDI	Zeta potential (mV)
NSA-DSPE	93.7±9.7	0.245±0.036	50.6±3.7	192.5±46.5	0.475±0.154	34.8±6.9
SA-DSPE	101.5±5.8	0.196±0.039	42.8±4.6	105.3±6.5	0.235±0.038	29.6±3.6
BHDSPE	106.5±12.2	0.216±0.020	39.2±3.8	113.5±8.1	0.259±0.029	31.3±4.9
HDSPE	101.4±16.2	0.200±0.052	36.7±3.5	112.6±6.5	0.238±0.038	23.5±3.1
BCDSPE	109.9±8.5	0.214±0.031	40.7±3.8	121.5±8.8	0.251±0.041	32.6±2.8
CDSPE	105.3±10.4	0.227±0.061	38.4±4.2	119.4±9.1	0.272±0.019	25.9±3.5
BADSPE	106.0±16.2	0.243±0.038	36.5±2.2	115.4±10.5	0.272±0.049	33.5±3.6
ADSPE	99.48±13.6	0.210±0.056	32.6±4.3	109.2±9.6	0.275±0.042	26.0±5.9
DOTAP	96.4±7.9	0.235±0.039	63.2±6.6	487.9±62.8	0.432±0.048	45.65±5.8

d) Cryo-TEM of lipoplexes

Cryo-TEM image of different lipoplexes is shown through **Figure 6.75** to **Figure 6.75**. As it can be seen in the micrographs, all lipoplex formulations were of unilamellar nature with spherical shape. Thickness of the lamella and diameter were determined using ImageJ software ver. 1.50c (National Institute of Health, USA). Diameter of the lipoplexes ranged from 90 nm to 110 nm which is congruous with the dynamic light scattering data based on the intensity based particle size distribution. Lamellar thickness of lipoplexes were also similar for all liposomal formulations which was around 5-10 nm range.

Additionally, TEM images support the view of 'external model' of lipoplex formation in which the DNA is located on the outer surface of the liposomes in contrast to the 'internal model' which denotes the DNA coated by cationic lipid layer (30).
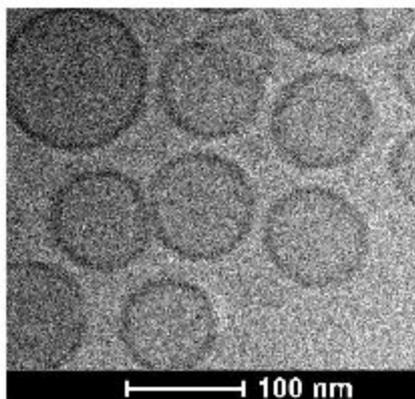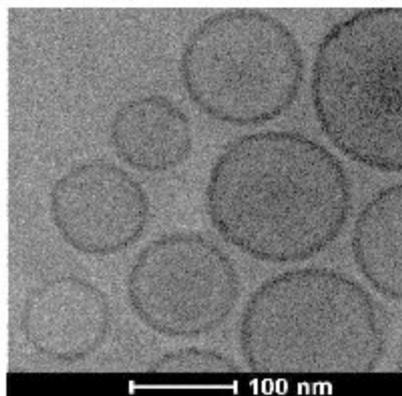

Figure 6.70 TEM image of liposomes of BHDSPE lipoplexes
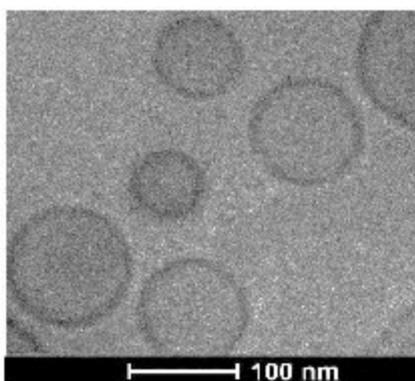

Figure 6.71 TEM image of liposomes of HDSPE lipoplexes

Figure 6.72 TEM image of liposomes of BCDSPE lipoplexes
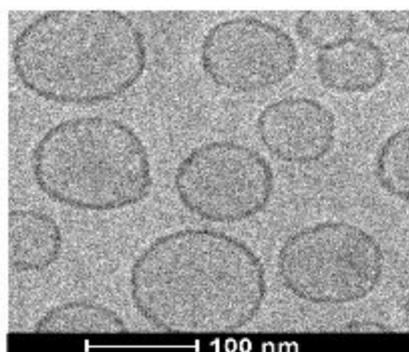
Figure 6.73 TEM image of liposomes of CDSPE lipoplexes
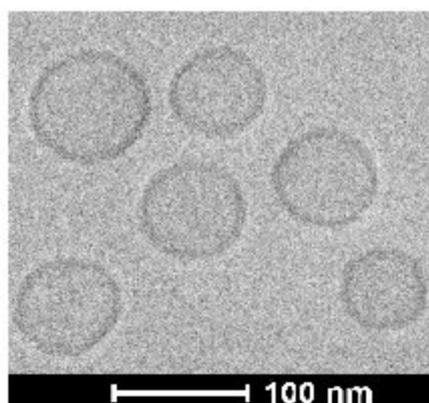
Figure 6.74 TEM image of liposomes of BADSPE lipoplexes
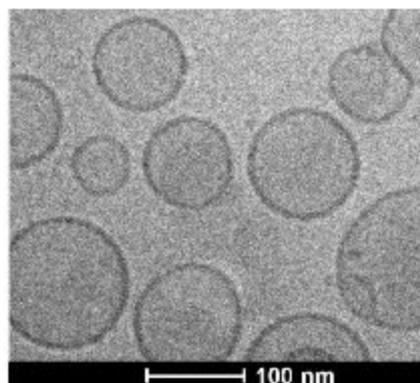
Figure 6.75 TEM image of liposomes of ADSPE lipoplexes

6.3.4 Lyophilization of lipoplexes

Lyophilization of lipoplexes was done in order to provide stability to the lipoplexes as the solid-state stability is higher than the liquid state stability. Lipoplexes were prepared at L/P ratio of 2.00 (i.e. N/P ratio of 2.0) for SA, BHDSPE, BCDSPE, BADSPE liposomes and at L/P ratio of 1.00 (i.e. N/P ratio of 2) for HDSPE, CDSPE and ADSPE liposomes. Lyophilization would preserve the pDNA activity for longer period of time.

Sucrose has been used as a cryoprotectant for lyophilization to prevent any detrimental effect of freezing on the lipoplexes and to maintain their physical integrity (33-36). Particle movement in unfrozen portion during lyophilization is significantly suppressed by sucrose rendering the particles to be isolated enough to prevent aggregation (35, 36). Sucrose was chosen based on our previous experience with the liposomal formulations (37, 38).

Sucrose was tried at three different concentrations (i.e. 10% w/v, 20% w/v and 25% w/v) to evaluate its effectiveness as cryoprotectant as well as a bulking agent. Concentrations were chosen so as to provide the bulking effect i.e. to provide a porous cake with high bulk volume and physical integrity along with the cryoprotective effect. i.e. to prevent fusion of lipoplexes and to prevent effect of growth of ice crystal which can rupture the morphology of the lipoplexes. These effects collectively preserve the particle size of the lipoplexes during freezing steps by preventing local concentration of lipoplexes during freezing. Optimization of the sucrose concentration was done with HDSPE lipoplexes and optimized concentration was extrapolated to other lipoplexes for lyophilization.

Results for the lyophilization optimization are summarized in **Table 6.24**. It was observed that sucrose concentrations of 20% and above were able to form porous cake while at lower concentrations; cakes obtained were collapsed/shrinked. Additionally, the formulations were able to reconstitute within 2 minutes at all concentrations. Sucrose concentrations of ≥20 were also efficient in preserving the lipoplex characteristics in terms of the particle size distribution and zeta potential.

Table 6.24 Effect of lyophilization on particle size and zeta potential of HDSPE lipoplexes

Lipoplexes	Sucrose concentration (%w/v)	Particle Size* (nm)	PDI* (Polydispersity index)	Zeta Potential (mV)
HDSPE	Before lyophilization	113.5±8.1	0.259±0.029	31.3±4.9
	10%	162.5±6.6	0.385±0.075	20.3±2.8
	20%	118.2±5.9	0.274±0.049	26.4±2.5
	30%	145.6±5.8	0.261±0.039	28.9±1.9

*Experiments were performed in triplicate.

Lyophilization cycle and sucrose concentration of 20% as bulking/cryoprotecting agent were further used for lyophilization of other lipoplex formulations. Lyophilized cakes were evaluated for reconstitution time, particle size, zeta potential as well as moisture content. The reconstitution time gives idea of time taken for formulation to return to its original dispersion state and moisture content gives the effectiveness of lyophilization cycle to reduce the moisture content of all formulations as the moisture content may affect the stability of the formulation on long term storage. Results of the reconstitution time and moisture content are given in **Table 6.25**. All the formulations were able to restore to uniform liposomal dispersion within 2 minutes of reconstitution. Additionally, the lyophilized cakes showed <3% w/w of moisture content for all lipoplexes indicating higher stability on storage.

Table 6.25 Reconstitution time and water content of lyophilized lipoplexes

Lipoplexes	Reconstitution time	Water Content (%w/w)
NSADSPE	2 min	1.25±0.18
SADSPE	2 min	1.19±0.21
BHDSPE	2 min	1.39±0.35
HDSPE	2 min	1.25±0.22
BCDSPE	2 min	1.20±0.85
CDSPE	2 min	1.45±0.25
BADSPE	2 min	1.25±0.19
ADSPE	2 min	1.26±0.32

*Experiments were performed in triplicate.

Table 6.26 Effect of lyophilization on complexation efficiencies of lipoplexes

Lipoplex formulation	Complexation efficiency (%) Before lyophilization		Complexation efficiency (%) After lyophilization	
	UV spectrophotometry	QuantiFluor ® Assay	UV spectrophotometry	QuantiFluor ® Assay
SADSPE	99.45±1.23	99.62±1.05	99.75±2.09	98.79±2.10
BHDSPE	99.15±2.14	99.14±0.91	98.78±1.85	99.03±1.58
HDSPE	98.59±1.52	99.41±1.11	100.05±2.19	98.15±2.01
BCDSPE	100.29±1.03	99.15±1.32	99.45±2.40	99.79±1.59

CDSPE	99.56±2.18	99.11±2.45	98.59±2.04	99.58±1.65
BADSPE	98.79±1.90	99.19±2.01	99.19±2.32	99.65±1.85
ADSPE	100.10±2.08	99.16±0.97	99.52±1.49	100.25±1.59
DOTAP	99.45±1.09	98.91±1.23	100.32±1.85	98.59±2.05

*Experiments were performed in triplicate.

Table 6.27 Particle size and Zeta potential characteristics of optimized lipoplexes and lipoplexes of modified DSPE

Formulation	Before lyophilization			After lyophilization		
	Particle size (z-average diameter)	PDI	Zeta potential	Particle size (z-average diameter)	PDI	Zeta potential
SADSPE	105.3±6.5	0.235±0.038	29.6±3.6	108.6±12.2	0.241±0.035	26.5±4.2
BHDSPE	113.5±8.1	0.259±0.029	31.3±4.9	118.2±5.9	0.274±0.049	28.4±2.5
HDSPE	112.6±6.5	0.238±0.038	23.5±3.1	120.2±15.9	0.245±0.028	22.3±4.4
BCDSPE	121.5±8.8	0.251±0.041	32.6±2.8	133.4±10.5	0.256±0.041	29.6±3.9
CDSPE	119.4±9.1	0.272±0.019	25.9±3.5	128.5±13.5	0.279±0.029	24.2±2.8
BADSPE	115.4±10.5	0.272±0.049	33.5±3.6	126.4±13.6	0.282±0.021	30.7±3.0
ADSPE	109.2±9.6	0.275±0.042	26.0±5.9	115.4±14.8	0.284±0.031	23.6±4.1
DOTAP	487.9±62.8	0.432±0.048	45.65±5.8	-	-	-

*Experiments were performed in triplicate.

The process of lyophilization includes steps of freezing followed by drying at reduced pressure. Freezing process may lead to fusion of lipoplexes and may cause increase in particle size as well as polydispersity of the lipoplexes which can ultimately affect the zeta potential and complexation efficiency. Hence, lipoplexes were evaluated for the changes in particle size and PDI as well as zeta potential and complexation efficiency. Upon lyophilization. Results (

Table 6.26 and **Table 6.27**) indicate only marginal increase in the mean z-averaged particle size for all lipoplexes along with a slight non-significant increase in the mean PDI values indicating a slight upward shift of the polydispersity of the dispersions indicating negligible fusion during the freeze-drying process. Lyophilized formulation ensures a good shelf stability of the pDNA lipoplexes.

6.4 References

1.   Leventis R, Silvius JR. Interactions of mammalian cells with lipid dispersions containing novel metabolizable cationic amphiphiles. Biochimica et biophysica acta. 1990;1023(1):124-32.
2.   Zuidam NJ, Barenholz Y. Electrostatic and structural properties of complexes involving plasmid DNA and cationic lipids commonly used for gene delivery. Biochimica et biophysica acta. 1998;1368(1):115-28.
3.   Zabner J, Fasbender AJ, Moninger T, Poellinger KA, Welsh MJ. Cellular and molecular barriers to gene transfer by a cationic lipid. The Journal of biological chemistry. 1995;270(32):18997-9007.
4.   Yang JP, Huang L. Time-dependent maturation of cationic liposome-DNA complex for serum resistance. Gene therapy. 1998;5(3):380-7.
5.   van Winden ECA, Crommelin DJA. Long term stability of freeze-dried, lyoprotected doxorubicin liposomes. E J Pharm Bio. 1997;43(3):295-307.
6.   Raffournier C, Ollivon M, Couvreur P, Dubernet C. Solubility of triacylglycerols or stearylamine in phospholipid vesicles. Trends in Colloid and Interface Science XVII. Progress in Colloid and Polymer Science. 126: Springer Berlin Heidelberg; 2004. p. 6-13.
7.   Israelachvili J. The science and applications of emulsions — an overview. Colloids and Surfaces A: Physicochemical and Engineering Aspects. 1994;91:1-8.
8.   Hirsch-Lerner D, Zhang M, Eliyahu H, Ferrari ME, Wheeler CJ, Barenholz Y. Effect of "helper lipid" on lipoplex electrostatics. Biochimica et biophysica acta. 2005;1714(2):71-84.
9.   Hupfeld S, Holsaeter AM, Skar M, Frantzen CB, Brandl M. Liposome size analysis by dynamic/static light scattering upon size exclusion-/field flow-fractionation. Journal of nanoscience and nanotechnology. 2006;6(9-10):3025-31.
10.   Ingebrigtsen L, Brandl M. Determination of the size distribution of liposomes by SEC fractionation, and PCS analysis and enzymatic assay of lipid content. AAPS PharmSciTech. 2002;3(2):9-15.
11.   Ye Q, Biltonen R. Differential Scanning and Dynamic Calorimetric Studies of Cooperative Phase Transitions in Phospholipid Bilayer Membranes. In: Hilderson H, Ralston G, editors. Physicochemical Methods in the Study of Biomembranes. Subcellular Biochemistry. 23: Springer US; 1994. p. 121-60.
12.   Palankar R, Ramaye Y, Fournier D, Winterhalter M. Functionalized liposomes. Advances in Planar Lipid Bilayers and Liposomes. 2008;7:39-58.
13.   Ducat E, Brion M, Lecomte F, Evrard B, Piel G. The experimental design as practical approach to develop and optimize a formulation of peptide-loaded liposomes. AAPS PharmSciTech. 2010;11(2):966-75.
14.   Naik S, Patel D, Surti N, Misra A. Preparation of PEGylated liposomes of docetaxel using supercritical fluid technology. The Journal of Supercritical Fluids. 2010;54(1):110-9.

15.   Singh B, Dahiya M, Saharan V, Ahuja N. Optimizing drug delivery systems using systematic "design of experiments." Part II: retrospect and prospects. Critical reviews in therapeutic drug carrier systems. 2005;22(3):215-94.

16.   Xiong Y, Guo D, Wang L, Zheng X, Zhang Y, Chen J. Development of nobiliside A loaded liposomal formulation using response surface methodology. International journal of pharmaceutics. 2009;371(1-2):197-203.

17.   Stensrud G, Sande SA, Kristensen S, Smistad G. Formulation and characterisation of primaquine loaded liposomes prepared by a pH gradient using experimental design. International journal of pharmaceutics. 2000;198(2):213-28.

18.   Singh B, Mehta G, Kumar R, Bhatia A, Ahuja N, Katare OP. Design, development and optimization of nimesulide-loaded liposomal systems for topical application. Current drug delivery. 2005;2(2):143-53.

19.   Armstrong NA, James KC. Understanding Experimental Designs and Interpretation in Pharmaceutics. London: Ellis Horwood; 1990.

20.   Box GEP, Hunter WG, Hunger JS. Statistics for Experimenters. New York: Wiley; 1978.

21.   Mak KWY, Yap MGS, Teo WK. Formulation and optimization of two culture media for the production of tumour necrosis factor-β in Escherichia coli. Journal of Chemical Technology & Biotechnology. 1995;62(3):289-94.

22.   Box GEP, Wilson KB. On the Experimental Attainment of Optimum Conditions. Journal of the Royal Statistical Society Series B (Methodological). 1951;13(1):1-45.

23.   van Hoogevest P, Wendel A. The use of natural and synthetic phospholipids as pharmaceutical excipients. European Journal of Lipid Science and Technology. 2014;116(9):1088-107.

24.   Mouritsen OG. Lipids, curvature, and nano-medicine. European Journal of Lipid Science and Technology. 2011;113(10):1174-87.

25.   Moghaddam B, McNeil SE, Zheng Q, Mohammed AR, Perrie Y. Exploring the correlation between lipid packaging in lipoplexes and their transfection efficacy. Pharmaceutics. 2011;3(4):848-64.

26.   Eliyahu H, Servel N, Domb AJ, Barenholz Y. Lipoplex-induced hemagglutination: potential involvement in intravenous gene delivery. Gene therapy. 2002;9(13):850-8.

27.   Barichello J, Ishida T, Kiwada H. Complexation of siRNA and pDNA with Cationic Liposomes: The Important Aspects in Lipoplex Preparation. In: Weissig V, editor. Liposomes. Methods in Molecular Biology. 605: Humana Press; 2010. p. 461-72.

28.   Ciani L, Ristori S, Salvati A, Calamai L, Martini G. DOTAP/DOPE and DC-Chol/DOPE lipoplexes for gene delivery: zeta potential measurements and electron spin resonance spectra. Biochimica et Biophysica Acta (BBA) - Biomembranes. 2004;1664(1):70-9.

29.   Cao A, Briane D, Coudert R. Chapter 5: Cationic Liposomes as Transmembrane Carriers of Nucleic Acids. In: Liu AL, editor. Advances in Planar Lipid Bilayers and Liposomes. Volume 4: Academic Press; 2006. p. 135-90.

30.   Ma B, Zhang S, Jiang H, Zhao B, Lv H. Lipoplex morphologies and their influences on transfection efficiency in gene delivery. Journal of controlled release : official journal of the Controlled Release Society. 2007;123(3):184-94.

31.   Chamberlin SI, Merino EJ, Weeks KM. Catalysis of amide synthesis by RNA phosphodiester and hydroxyl groups. Proceedings of the National Academy of Sciences of the United States of America. 2002;99(23):14688-93.

32.   Lamm G, Pack GR. Acidic domains around nucleic acids. Proceedings of the National Academy of Sciences of the United States of America. 1990;87(22):9033-6.

33.   Molina MC, Allison SD, Anchordoquy TJ. Maintenance of nonviral vector particle size during the freezing step of the lyophilization process is insufficient for preservation of activity: insight from other structural indicators. J Pharm Sci. 2001;90(10):1445-55.

34.   Allison SD, Anchordoquy TJ. Mechanisms of protection of cationic lipid-DNA complexes during lyophilization. Journal of Pharmaceutical Sciences. 2000;89(5):682-91.

35.   Armstrong TK, Anchordoquy TJ. Immobilization of nonviral vectors during the freezing step of lyophilization. Journal of Pharmaceutical Sciences. 2004;93(11):2698-709.

36.   Allison SD, Molina MC, Anchordoquy TJ. Stabilization of lipid/DNA complexes during the freezing step of the lyophilization process: the particle isolation hypothesis. Biochimica et biophysica acta. 2000;1468(1-2):127-38.

37.   Vhora I, Khatri N, Desai J, Thakkar HP. Caprylate-conjugated Cisplatin for the development of novel liposomal formulation. AAPS PharmSciTech. 2014;15(4):845-57.

38.   Khatri N, Baradia D, Vhora I, Rathi M, Misra A. Development and characterization of siRNA lipoplexes: Effect of different lipids, in vitro evaluation in cancerous cell lines and in vivo toxicity study. AAPS PharmSciTech. 2014;15(6):1630-43.